DOCTOR OF PHILOSOPHY

High capacity optical fibre transmission systems.

Blank, Lutz Christian

Award date:
1992

Awarding institution:
Bangor University

A Thesis submitted to the University of Wales

in candidature for the degree of

Doctor of Philosophy.

HIGH CAPACITY OPTICAL FIBRE TRANSMISSION SYSTEMS

by

Lutz Christian Blank Dipl.-Ing.

August 1992

School of Electronic Engineering Science

University of Wales

Bangor, Gwyned.

Acknowledgements

This research work has been carried out on a part-time basis whilst I have been employed at BT Laboratories (formerly British Telecom Research Laboratories), and I am grateful to BT for having provided me with the opportunity to pursue this work. As the studies are to some extent aligned with my project activities for BT, much inspiration has been drawn from the numerous stimulating discussions and joint experimental investigations with my colleagues throughout the years, in particular within the Future Systems Studies Group and the Optical Transport and Processing Group in the Main Optical Networks Division. Where my colleagues have provided a "tangible" contribution to this work by helping to demonstrate experimentally some of the ideas developed for this thesis, references to our joint publications of the results are provided.

My thanks go to Prof.M.J.O'Mahony, who was my industrial supervisor when he was working at BT Laboratories and who provided guidance and encouragement, and to my academic supervisor Prof.J.J.O'Reilly who first introduced me to the field of Optical Communications, and who after providing much inspiration throughout the years now has carried out the thankless task of proof reading this thesis.

CONTENTS

SUMMARY

In this thesis a number of system design options are studied for the generation and processing of ultra-high speed optical data, based on the technique of Optical Time Division Multiplexing. The limits are investigated with regard to maximum unregenerated transmission distances for linear propagation over single mode fibre with large chromatic dispersion. Overall, the aim is to minimise the bandwidth requirements of electronic and opto-electronic system components for a given optical line capacity whilst at the same time maximising the chromatic dispersion limited propagation distances, thus exploring the potential for future system and network operating speeds of several tens of Gbit/s.

A summary of standard system designs and their performance in terms of maximum system speed and dispersive fibre propagation provides an introduction into the field of high performance fibre optic data communication systems. Particular examples are used to introduce the device models subsequently employed in the analysis of new system configurations. This includes a description of the system performance measurements which are the basis for the performance analyses of the proposed ultra-high speed systems.

In the field of fibre transmission research a variety of electrical interface and optical line signal formats are being investigated, each being appropriate for particular application areas and offering varying compromises between performance, complexity and user friendliness. In the context of this thesis the investigations are limited to high capacity time division multiplexed configurations, which represent a medium to longer term alternative as well as a complementary approach to the currently widely pursued system capacity upgrades by means of optical wavelength or frequency division multiplexing. Moreover, ultra-high speed time division multiplexed transmission is fundamentally compatible with WDM system operation, providing a future upgrade path for multi-wavelength systems being developed at the present time.

The vehicle for these investigations is a set of computer models. Optical signal generation, pulse propagation in single-mode fibre, optical time domain processing, amplification and optical receiver detection are all included in the models to allow end-to-end system performance studies. Experimental results are presented at various stages to validate the models employed.

CHAPTER I

INTRODUCTION

I.1 HIGH CAPACITY FIBRE OPTIC TRANSMISSION SYSTEMS

Since the first installation of optical fibre transmission systems at the end of the 1970's, today's telecommunication systems rely almost entirely on fibre for high capacity core network transmission with local networks, and recently also the final drop to the customer, being considered for conversion to optical transmission. However, the original promise of optical fibre transmission, namely that it would provide practically unlimited capacity, is still to be fulfilled. Although the installed fibre provides in principle transmission capacity many orders of magnitude larger than is utilised so far, it has proved far more difficult to access this potential capacity.

Early transmission systems were based on multimode fibres and ≈ 800 nm transmitter wavelength operation, whilst more recent systems employ 1.3 μm lasers to make use of the reduction in fibre attenuation at longer wavelengths. The relatively large core diameter of multimode fibres (≈ 50 μm) allows for ease of optical coupling in and out of the fibre. However, the large number of spatial modes propagating in the fibre results in modal dispersion, i.e. differential propagation delays between modes, and leads to a fibre length dependent bandwidth limitation. Consequently the advent of high performance semiconductor lasers at 1.3 and 1.55 μm prompted a general move away from multimode and towards the use of monomode fibre for the majority of telecommunications applications. With a core diameter of approximately 10 μm, it supports propagation of only one spatial mode (consisting of two orthogonal polarisations), and provides low attenuation of ≈ 0.35 dB/km at 1.3 μm and ≈ 0.2 dB/km at 1.55 μm. Low values of fibre chromatic dispersion in the 1.3 μm wavelength window in standard step-index monomode fibre and in the 1.55 μm window of the subsequently developed

dispersion-shifted monomode fibre have resulted in system configurations which were limited in performance solely by device speed limitations and system power budgets.

Improvements in semiconductor devices, such as increased operating speed of electronic multiplexing equipment, improved laser designs and photodetector/receiver developments allowed a steady increase in the achievable line-rates and unrepeatered transmission distances. Due to the large fibre bandwidth mainly binary digital signalling is employed, in the format of on-off intensity modulation. Most of the development effort was aimed at improving the power budget capability at the signalling line-rates of interest, i.e. to maximise the difference between available transmitter output power and minimum acceptable receiver input signal level, with special emphasis on receiver optimisation. However, increases in line-rates, from 2 and 34 Mbit/s to 140 and 565 Mbit/s and beyond, meant that for practical tolerances on the mean emission wavelength of Fabry-Perot lasers, coupled with variations in the wavelengh of zero chromatic dispersion of the installed fibre, pulse dispersion once again began to limit the achievable line-rate and distances, even when operating in the 1.3 μm wavelength window near the chromatic dispersion zero of standard step-index monomode fibres. Making use of the lower attenuation of the 1.55 μm wavelength window was not possible with step-index fibres for line-rates beyond approximately 34 Mbit/s due to the interactions between the laser source spectrum and the fibre chromatic dispersion.

The problem of chromatic dispersion seemed to be solved with the introduction of Distributed Feedback Lasers (DFB) in 1983/84: a semiconductor laser with built-in wavelength selective grating to provide a single line in the wavelength emission spectrum. Thus system efforts once again were geared towards improving power budgets, such that especially for transmission at 1.55 μm, impressive transmission distances became possible, allowing unrepeaterd transmission over more than 100 km at line-rates of up to several hundred Mbit/s.

However, as a consequence of further developments in device technology, and especially with the advent of high performance optical amplification techniques, power budget constraints can now be removed relatively easily, and signal distortion due to

transmission path pulse dispersion presents once more the limiting factor in system designs for next generation line-rates of several Gbit/s and beyond.

Today, digital optical fibre transmission systems are operational at line-rates mainly between 2 Mbit/s and 565 Mbit/s, with 1.7 and 2.5 Gbit/s trunk transmission on selected routes. For further substantial capacity increases Wavelength Division Multiplexing (WDM) techniques are being envisaged in the near to medium term future, by employing signal transmission in the 1.3 μm and 1.55 μm wavelength windows simultaneously (capacity doubling) or through multi-wavelength operation within one of the two low loss fibre windows. Channel numbers in excess of ten per window have been demonstrated experimentally, and practical systems employing four to six channels are currently under consideration. By utilising both transmission windows, a total capacity increase of more than an order of magnitude will be realisable. In addition to straight capacity increases, WDM techniques are also aimed at providing flexibility for networking applications, i.e. to combine capacity increases with channel routing, capacity switching and protection switching. The advent of high performance optical amplification devices allows multiple cascades of transmission spans as well as cascades of wavelength selective components in a networking environment. The use of fibre amplifiers together with grating based WDM components may result in negligible crosstalk between adjacent channels, and since the individual channels remain independent, this technique represents a relatively straight forward upgrade path from single channel optical transmission to multi-channel high capacity networking and routing. In this context however it is vital that the limits are known for maximum transmission line-rate and distance achievable in each of the wavelength channels, since with optical amplification optical paths in the long haul transmission network may reach lengths of several hundred kilometers.

An alternative approach to channel management is offered by coherent modulation and detection techniques, originally mainly aimed at extending the power budget of point-to-point transmission systems, due to an improved receiver sensitivity compared with standard on-off amplitude modulated direct detection systems. However, recent advances in optical amplification techniques have allowed direct detection systems to operate with span

capabilities similar to those of coherent systems, at substantially reduced system complexity. Coherent detection techniques may still offer advantages in the area of all–optical networks, where the coherent detection process can be employed to selectively detect one channel amongst a set of closely spaced signals, which together may occupy one channel of a WDM transmission and distribution network. The added complexity of coherent detection is thus used to achieve a higher channel packing density. Fundamentally, however, it represents a similar approach to transmission capacity increase and networking as provided by standard WDM techniques described above. Consequently WDM techniques are envisaged to be employed first, with coherent techniques to follow later, if and when required.

Another signal modulation and channel management approach of interest is subcarrier multiplexing [Darcie, Dixon, Kasper and Burrus] in which traditional electrical carrier modulation schemes are employed, with the combined carriers then applied directly to a laser or external modulator for conversion to optical signals and transmission on fibre. After opto–electronic signal detection in a wideband receiver, traditional electrical demultiplexing of the individual channels is carried out. This approach has only become possible due to advances in semiconductor laser linearity, resulting in sufficiently low intermodulation distortion, even with a reasonably large index of modulation on the laser. For highest performance systems, external modulation may be employed as an alternative to the simpler direct laser modulation approach. From an overall networking viewpoint, subcarrier modulation falls into the same category as WDM and coherent FDM systems, namely the individual channels are independent, and frequency domain operations are required to transfer information between different electrical and optical carrier frequencies or wavelengths.

Whilst optical frequency or wavelength domain multiplexing will almost certainly provide for substantial capacity and flexibility increases in the transmission networks of the near future, the option of time division multiplexing is at the same time being pursued for further substantial increases in achievable transmission capacity. In 1985, 2.5 Gbit/s operation was first demonstrated under field conditions [Blank, Garnham and Walker], with

laboratory systems based on electronic multiplexing and opto-electronic signal conversion at the full line-rate having now been operated at line-rates upto 17 Gbit/s [Hagimoto, Miyamoto, Kataoka, Kawano and Ohhata]. In order to achieve further substantial capacity increases of a factor of ten or more, as in the case of WDM operation, the basic speed of semiconductor electronic and opto-electronic devices provides a limiting factor.

However, leaving these constraints aside, the question arises as to the advantages of the time domain approach in comparison with wavelength multiplexing techniques. In the time multiplexing configuration all incoming data channels have to be synchronised, i.e. the channels cannot remain independent as in WDM, FDM or subcarrier systems. On the other hand, a worldwide move away from plesiochronous network operation towards synchronised networking (SDH - Synchronous Digital Hirarchy, and SONET - Synchronous Optical Networks) will ease the difficulties of channel synchronisation greatly. Furthermore, once individual channels are synchronised, networking options emerge which provide either alternative or complementary functionality to the WDM networking scenario. Specifically, time domain multiplexing facilitates the exchange of data between different transmission channels, by means of 'drop-and-insert' operations, thus providing dramatically increased networking flexibility. Especially in conjunction with 'over-capacity' provided in the transmission network, and the potential use of packet transmission at the optical level, large simplification of the overall network structure and the associated management and control functions may become possible. In addition, such higher line-rate TDM signals may still be routed through WDM channels, i.e. the development of one approach does not compromise the pursuit of the alternative options.

By increasing the time division multiplexed line-rates substantially, however, the limits of device technologies will be reached relatively quickly, as mentioned above. Latest production devices (electronic multiplexers, lasers, receivers) are suitable for the implementation of 2.5 Gbit/s systems, with research devices and first prototype system demonstrators promising practical system operation to $\approx$ 10 Gbit/s. Further substantial increases in capacity, however, are likely to require the addition of optical processing techniques in order to overcome fundamental device speed limitations. Such an approach

would rely on traditional system designs to be employed to optical line-rates up to maybe 10 Gbit/s, with subsequent optical time division multiplexing leading to optical signals at tens of Gbit/s and capable of exceeding 100 Gbit/s (O)TDM in the longer term.

In order to investigate the prospects for such systems, two areas have to be addressed. Firstly, the limits of practical standard system configurations need to be identified, with regard to maximum achievable speeds and transmission distances, and secondly, suitable system configurations are required for the implementation of appropriate optical processing, based on available optical or opto-electronic devices. In this way, any future improvements in device technologies will benefit both the speed capability of traditional systems and the maximum capacity of OTDM systems based on the same or similar devices. Finally, the achievement of ultra-high speed optical data generation and processing will be of little benefit unless fibre propagation of the thus assembled ultra-high speed data streams is possible over distances of practical interest.

I.2 SCOPE OF THIS THESIS

In this work the limitations are analysed for transmission data-rates and achievable propagation distances of high performance optical fibre transmission systems, employing electrical as well as optical time division multiplexing. The aim is to identify limits for ultra-high capacity digital pulse transmission based on linear propagation in monomode silica fibre. A range of system configurations of practical interest have been studied, based on transmitter laser sources such as directly modulated Fabry-Perot lasers (widely employed in current systems), DFB lasers (mainly used in latest higher capacity links), and externally modulated signal sources. Computer models of the overall systems have been developed to investigate performance limits, and experimental results have been obtained to demonstrate the validity of the models. New proposals are made for the generation of ultra-high speed optical data for transmission and networking, mainly assuming low speed opto-electronic devices for the implementation of ultra-high speed OTDM system configurations. Apart

from techniques for the generation of ultra-high speed binary digital optical pulse streams, multi-level signalling has been analysed as a means of combining the optimisation of the optical signal generation process with improvements in the transmission span capability at very high digital line-rates.

I.3 CONTRIBUTIONS

The main contributions of this thesis are as follows :

(i) Techniques have been identified and analysed for the generation of ultra-short optical pulses, based on external modulation of a CW optical source and suitable for use in ultra-high speed optical transmission systems operating at line speeds well beyond the electrical bandwidth of the modulators employed. In addition to their application to optical pulse generation, the techniques are also suitable for optical processing in Optical Time Division Multiplexing systems.

(ii) External data modulation of a CW or pulsed optical carrier signal has been optimised with regard to the required modulator bandwidth for a given data rate. As a result, standard modulators may be employed for the generation of a number of optical signal formats with minimum modulator bandwidth requirements.

(iii) Application of the above findings to OTDM system operation has allowed conclusions to be drawn regarding the maximum OTDM system speed for a given set of devices and the trade-offs between system capacity and simplicity of operation.

(iv) A comparison has been carried out of the optical propagation characteristics of a variety of optical pulse shapes, allowing conclusions to be drawn as to the suitability of commonly employed analytical estimations of system performance for both NRZ and RZ signals.

(v) Duobinary detection of binary optical transmitter signals has been identified as permitting large increases in chromatic dispersion limited maximum system lengths, applicable both to NRZ and RZ transmitter formats.

(vi) Optical three-level data generation followed by three-level receiver detection has been found to also provide large increases in the maximum chromatic dispersion limited fibre propagation distances.

(vii) Optical time domain processing of dispersed optical data has been analysed and found to enable improvements in system performance to be obtained.

(viii) For transmission distances beyond the fibre chromatic dispersion limits identified above, 2-R optical regeneration (Retiming and Reshaping) has been analysed. The optical pulse generation and OTDM processing functions developed in this work are directly applicable to this task, and it is shown that substantial increases are possible in transmission distances without full 3-R regeneration, especially in an OTDM networking context with system speeds beyond the capability of standard electro-optic 3-R regenerators.

I.4 ORGANISATION OF THE THESIS

In Chapter II the characteristics of the main components of high capacity TDM optical transmission systems are summarised, and an outline is given of the approach taken for modelling the end-to-end system performance for particular system configurations of interest. Example system models are compared with experimental results in order to validate the models. In particular, suitable models are introduced for Fabry-Perot lasers, single-line DFB lasers and external modulation by means of Mach-Zehnder devices, for implementation of electrical-to-optical data conversion in the transmitter. A discussion of opto-electronic data amplification and regeneration as well as all-optical signal amplification is included, covering the available approaches for combatting transmission path attenuation. After a brief description of the fundamental characteristics of the

transmission fibre, the model assumed for optical receivers is outlined, together with a discussion of the question of overall system performance measurements.

In Chapter III several 'standard' system configurations are analysed in order to identify the limits to maximum achievable transmission line-rates and distances.

Chapter IV introduces alternative data modulation techniques, aimed at facilitating the generation of ultra-high speed optical TDM data streams, both for standard electrically multiplexed system designs and for optically multiplexed systems at substantially higher line-rates.

Optimisation of high speed pulse generation for extended pulse propagation may result in substantial increases in the allowable transmission distance, before fibre dispersion leads to unacceptable system penalties. Chapter V begins with an analysis of the propagation performance of a range of optical pulse shapes, followed by detailed end-to-end system modelling in order to establish the applicability of analytical estimates on system dispersion limits for a range of binary signal shapes. This is followed by an analysis of optical three-level transmission as a practical means to increasing chromatic dispersion limited fibre transmission distances. The chapter is concluded with a discussion of optical processing techniques in an optical networking environment, not only for the generation and manipulation of data at high speeds, but also for the extension of the fibre chromatic dispersion limitations identified earlier.

Finally, in Chapter VI the thesis is concluded with a summary of the main findings followed by a discussion of issues which would benefit from further study.

CHAPTER II

MODELING FIBRE OPTIC TRANSMISSION SYSTEMS

II.1 INTRODUCTION

In this chapter the models are presented which will be employed lateron for subsequent system performance analyses. Semiconductor laser diodes, optical amplifiers, monomode fibre and optical receivers are the main components of current high performance transmission systems, with fast optical switches operated as amplitude modulators or channel switching elements providing additional functionality which will find applications in system configurations of enhanced performance.

In order to be able to model the performance of a fibre optic transmission system, suitable descriptions of the system components are required, covering all devices in the transmission path from the electrical data applied to the system through to the recovered electrical output signal. Transmission systems operating at high line-rates employ laser sources of various types. At the current operating speeds of a few hundred Mbit/s upto a few Gbit/s direct laser modulation may be employed. For particular high performance system applications the laser may be operated continuous wave (CW) with binary digital data impressed onto the optical carrier via an external modulator. Consequently a transmitter model is required which incorporates all the relevant device characteristics and which can then be included in an overall system model for evaluating complete system capabilities and limitations. In the context of this work suitable models have been chosen for (multi-longitudinal mode) Fabry-Perot lasers, single-longitudinal mode Distributed FeedBack (DFB) lasers, and Mach-Zehnder (MZ) external modulators.

After a brief overview over the relevant characteristics of high performance semiconductor laser diodes, the operating characteristics of Mach-Zehnder external modulators will be summarised, followed by a brief discussion of data regeneration and optical amplification techniques. A description of the propagation characteristics of silica

monomode optical fibre is then followed by a brief summary of optical receiver issues and of the method employed in the context of this work for the evaluation of overall system performance.

II.2 SEMICONDUCTOR LASERS

In todays high capacity optical fibre transmission systems semiconductor lasers are employed almost exclusively as transmitter sources, due to their small size, power efficient operation, high speed capability and suitable optical wavelength domain emission characteristics. With both standard Fabry–Perot and single–line DFB (or Distributed Bragg Reflector, DBR) lasers in use, the following descriptions of their dynamic characteristics summarise the basis for the device models as employed in subsequent system performance analyses. Models applicable for steady–state laser operation and optimisation may be found in for example [Thompson]. The requirement here is for a dynamic model able to adequately describe the transient behaviour of directly modulated lasers. After a presentation of the laser dynamics as modelled by the laser rate equations, the emission spectrum of Fabry–Perot and single–frequency lasers will be discussed, thus completing the description of laser modelling in both the time domain and the optical wavelength domain.

II.2.1 Laser Rate Equations

In order to be able to model the dynamic behaviour of the semiconductor laser, descriptions of the gains and losses of both electronic carriers and photons are required, i.e. the rates at which carriers enter and leave the lasing cavity need to be established. Appendix A2–1 summarises the rate equations as usually given in relevant text books, together with an analysis of the intrinsic small signal laser frequency response. An example time domain laser response to a drive current pulse of suitable bias and level is shown in Fig.2.1, for laser parameters appropriate for a 1.55 μm ridge waveguide laser made at BT

Laboratories (carrier life time τ = 2 nsec, photon life time τ_{ph} = 3 psec, transparency carrier density $n_t = 1.1 \cdot 10^{23}$, damping factor $\beta_{sp} = 2 \cdot 10^{-5}$).

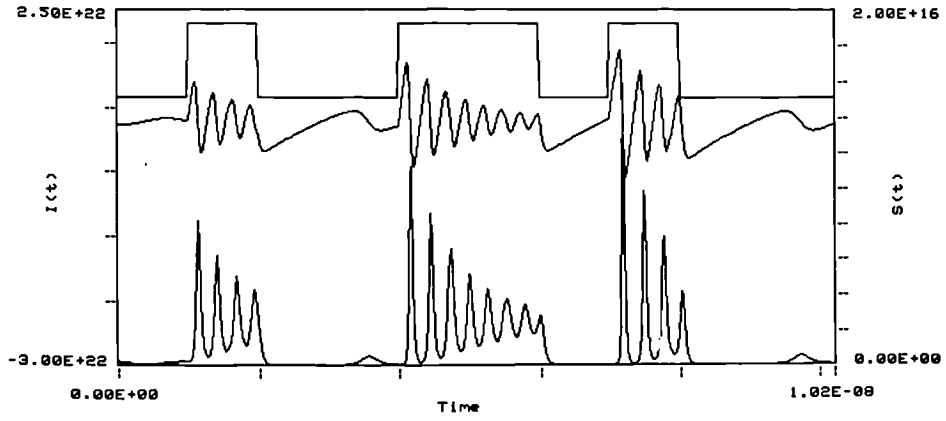

Fig. 2.1 Basic Rate Equation Model

The traces represent from top to bottom: injection current, carrier density and photon density or optical output. The injection current is taken to vary from approximately lasing threshold to twice threshold, the electrical driving waveform being ideal rectangular pulses as shown. Whilst the optical output waveform of Fig.2.1 shows some aspects of the expected behaviour, such as a distinct turn–on delay as well as a slow turn–off, the pulse shapes themselves bear little resemblance to the actually observed laser behaviour: a weakly damped oscillatory behaviour is shown on laser turn–on, in contrast to the far more damped transient behaviour of real devices.

The problem lies in the assumption of uniform carrier and photon distributions within the laser cavity, whilst in practice carrier diffusion effects lead to a dramatic increase in the damping of the transient laser behaviour. Non–uniform photon and carrier distributions across the laser have been discussed in for example [Thompson], [Buus] and [Tucker and Pope]. Details are given in Appendix A2–2. Solving the resulting new set of rate equations for the same laser drive conditions as above and with the carrier diffusion parameter D_c taking the value $5 \cdot 10^8$ results in a laser output waveform as shown in Fig.2.2.

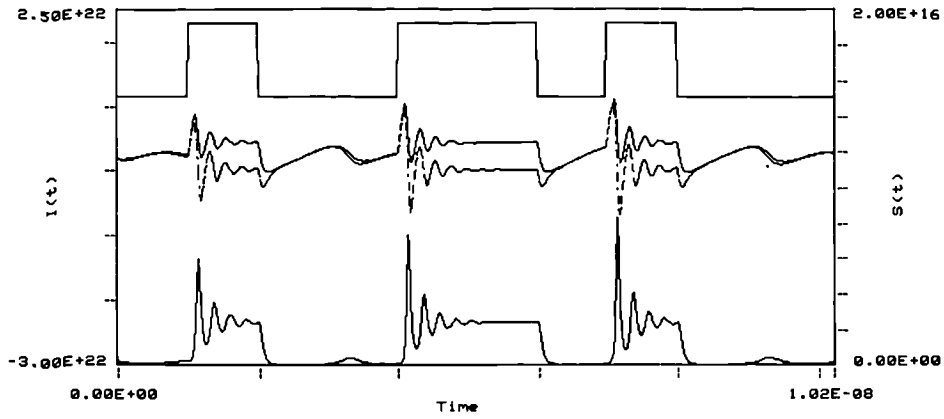

Fig. 2.2 Rate Equation Laser Model including Carrier Diffusion

The carrier density is now represented by two traces for the two components as defined in the model of Appendix A2-2. The graph shows clearly how carrier diffusion plays an important role in damping the laser response, and the resulting waveforms now agree well with measured laser characteristics. How the laser bias level influences the shape of the emitted optical pulses is shown in Fig.2.3. Each of the four graphs depicts the laser injection current, carrier density levels and the optical power output waveform. The first graph is for a laser bias of approximately 85% of its threshold value, showing exponential carrier density level recovery after turn-off which leads to data patterning such that the shape of subsequent pulses depends on the previous data sequence. The second result is for modulation from threshold, resulting in a substantially reduced amount of data patterning, hardly visible on the time scale employed here although the large transient overshoot in the optical output during laser turn-on is still maintained. In the third graph the bias level is increased to 15 % above threshold, giving rise to a poor optical extinction ratio while providing a more damped laser switch-on behaviour. However, slow relaxation oscillations now occur also in the optical 'off' level, thus still allowing substantial patterning to take place. Finally, in the fourth graph a bias level of twice threshold results in a data pattern independent transformation of the electrical input signal into an optical power waveform, with the residual relaxation oscillations differing between the two signal levels as a result of the difference in the injection current and the resulting difference in the dynamic laser behaviour at the two operating levels.

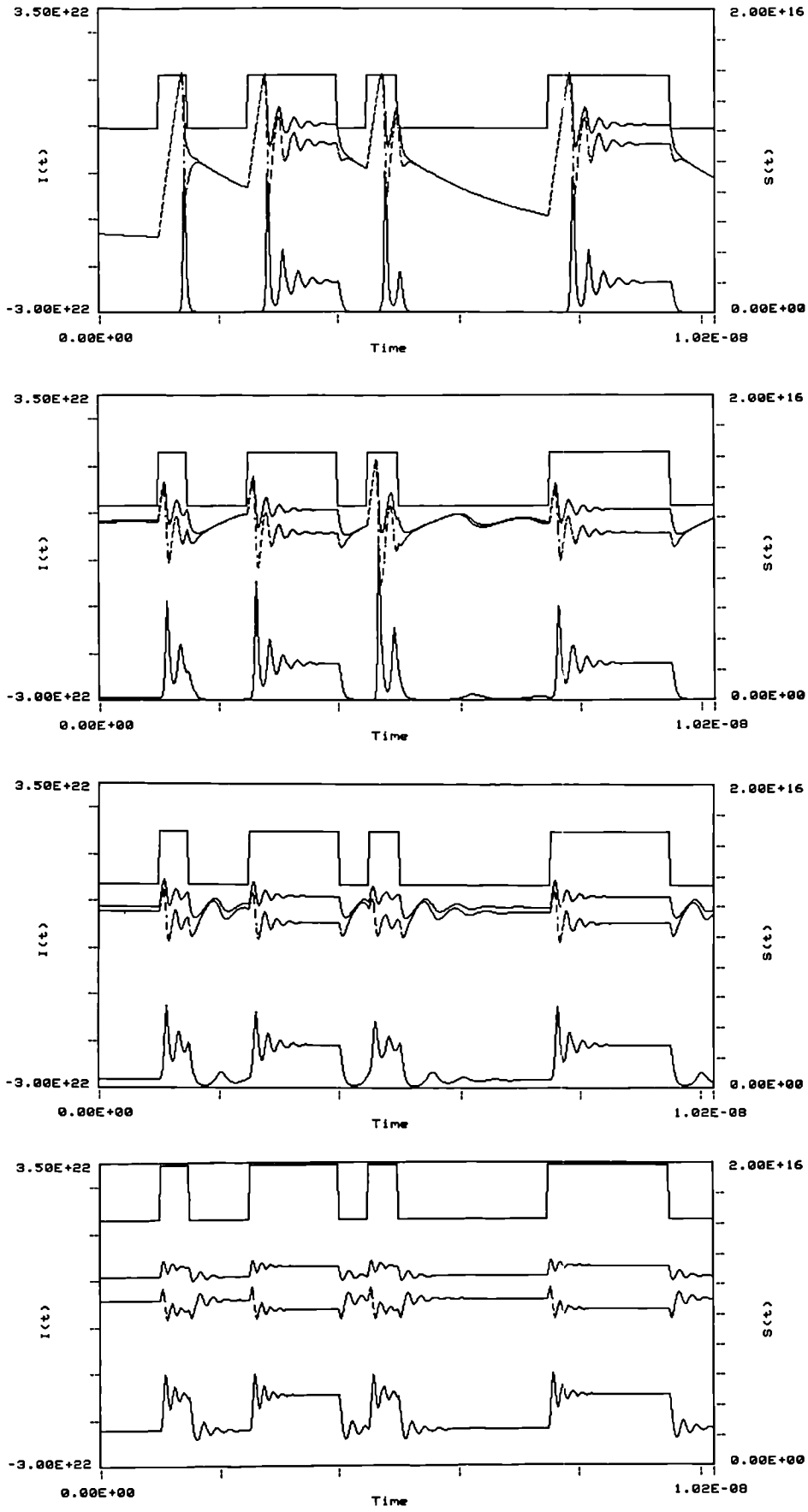

Fig.2.3 Laser Behaviour for different Bias Levels: 15 % below threshold, at threshold, 15 % above and 100 % above.

The system damping provided by carrier diffusion can alternatively be approximated through the introduction of a non-linear gain compression term $1/(1+\varepsilon S)$ in the rate equation for the electron carrier density, resulting in a modified version of the original two rate equations [Tucker and Pope].

Optimisation of laser designs for ultra-high speed direct injection current modulation have led to small signal bandwidths well beyond 20 GHz [Bowers, Hemenway, Bridges and Burkhardt], [Bowers], and large signal digital data modulation capability to 10 Gbit/s and beyond [Tucker, Wiesenfeld, Gnauck and Bowers], [Fujita, Kitamura, Torikai, Henmi, Yamada, Suzaki, Takano and Shikada], [Gnauck, Burrus, Wang and Dutta]. With current semiconductor laser designs, however, the laser photon and carrier life times, which to a large extent determine the intrinsic speed, are unlikely to be improved sufficiently to allow further significant increases in laser performance. Therefore, direct modulation of semiconductor lasers is unlikely to be extended to ultra-high speed system operation due to the limitations in both the electronic signal processing capability of semiconductor devices and the intrinsic speed limitations in the laser.

II.2.2 Fabry-Perot Laser

The rate equations described in the previous section detail the relationship between electronic carriers and optical intensity (photons) in the laser cavity, without taking into account wavelength characteristics of the laser material gain or wavelength dependent transmission characteristics of the optical cavity. In 1.3 μm and 1.55 μm wavelength Fabry-Perot lasers the cavity resonances are spaced by typically 1 nm, which in conjunction with a material gain bandwidth of several nm leads to a multi-wavelength Fabry-Perot (or 'multi-mode') spectrum, even for continous wave, steady-state operation. Comprehensive modeling in this case would require one photon rate equation for each mode, with the gain coefficient being wavelength dependent as given by the material gain profile. In addition to this multi-wavelength spectrum, changes in the laser active layer carrier concentration during transients lead to changes in refractive index, and thus

transients in the absolute wavelength (frequency) of each mode. For digital optical fibre transmission systems, however, this effect may usually be neglected, since the spectral width is determined by the overall Fabry–Perot emission spectrum, such that dynamic variations within each wavelength mode are of little consequence.

Additionally, however, variations occur in the instantaneous power of each lasing mode for constant total optical output power, known as mode partitioning. The consequences of this behaviour on the performance of optical transmission systems will be discussed in Chapter III.

II.2.3 Distributed Feedback Laser

For high speed, long–distance digital optical fibre transmission systems the width of the optical emission spectrum of Fabry–Perot lasers limits severely the maximum capacity and span achievable. Consequently modified laser structures have been devised to achieve single wavelength operation, and currently the most widely employed laser is the Distributed Feedback or DFB laser, with alternative designs such as Disributed Bragg Lasers (DBR) and External Cavity Lasers being investigated for coherent systems use and applications requiring laser wavelength tunability.

In the DFB laser a refractive index grating is added to the structure above the laser active layer, with the device design optimised for good coupling of the propagating optical wave to the grating. The grating fulfills two functions, firstly it provides the feedback to allow lasing to be achieved (normally provided by the facet reflectivities in a Fabry–Perot laser), and secondly it performs the wavelength filtering operation which leads to single longitudinal mode laser operation. Discussions of device design and analyses of the main issues for transmission system applications such as small signal modulation bandwidth, large signal laser response, and static and dynamic optical linewidth may be found in for example [Thompson], [Tucker], [Nelson, Westbrook and Fiddyment], [Ogita, Yano and Imai]. In the context of this work, stable single–longitudinal mode operation is assumed for the DFB laser, with typical CW laser linewidths of the order of a few MHZ to a few

tens of MHz (power dependent), thus sufficiently small compared with the signal modulation bandwidth of several GHz not to be of importance in the digital pulse transmission applications under consideration here.

The DFB grating determines the laser operating wavelength by means of the grating pitch and the material refractive index. The refractive index in turn, however, depends on the active layer carrier density. Although the carrier density is notionally clamped at its threshold value for device operation above threshold, small variations occur for changes in operating conditions, as well as larger transients during high speed direct laser injection current modulation, as was shown in Fig.2.2. Consequently, the instantaneous laser wavelength is directly linked to the instantaneous laser carrier density, resulting in laser wavelength variations as shown in Fig.2.4 for an example laser output signal waveform, with peak-to-peak wavelength variations of the order of several Angstrom.

Fig.2.4 DFB Laser Current, Instantaneous Wavelength and Optical Power (top to bottom)

From a device and overall system modelling point of view it is convenient that the rate equation model may be employed to calculate from a given electrical laser drive waveform the resulting time-domain optical power waveform as well as the instantaneous laser output wavelength, allowing the construction of a full electrical field description of the laser output signal.

For laser operation above threshold, an analysis of the laser behaviour indicates that the instantaneous laser frequency deviation can be derived directly from the output power waveform as calculated from the rate-equations, without reference to the time-resolved

laser carrrier density [Koch and Bowers], [Koch and Linke]. The relationship is given in Equation 2.1, with α representing the laser line-width enhancement factor, the value of which depends on the exact laser type and device operating conditions [Westbrook (1)], [Westbrook (2)], [Ogita, Yano, Ishikawa and Imai] but is typically in the range 4 to 8.

$$\Delta f(t) = \frac{\alpha}{4\pi} \cdot \frac{d}{dt} (\ln(P(t)) + \frac{\alpha}{4\pi} \cdot \text{const} \cdot P(t) \qquad (2.1)$$

Comparison with the calculated wavelength chirp for the same laser drive signal and bias conditions as in the 3-rate-equation model (Fig.2.4) confirms that identical results are obtained for operation above threshold. However, around and below threshold (low optical output power) the carrier density induced wavelength changes are not reproduced correctly with the simplified model. In the following the full three rate equations will be used throughout to model the laser dynamic wavelength behaviour.

II.3 EXTERNAL MODULATORS

Due to the wavelength chirp of standard semiconductor DFB lasers alternative devices may be required for the implementation of pure optical data modulation. Whilst research is ongoing into methods for achieving pure intensity laser modulation with direct current injection, an alternative approach of practical interest is based on external modulation of a CW optical beam, thus allowing the separation of the two functions of optical signal generation (laser diode) and data modulation (external modulator). For applications in high capacity or ultra-long range intensity modulated systems the use of an external intensity modulator thus permits the avoidance of the laser wavelength chirp of directly modulated DFB lasers. The most widely employed design is the balanced Mach-Zehnder interferometer configuration, which will be the basis for system studies in the following chapters.

In addition to enabling optical signal generation with sufficient control over both the

optical intensity and its frequency and phase, external modulators can also find applications in areas of optical signal processing such as optical pulse shaping, data multiplexing and demultiplexing. In the past mainly Lithium Niobate ($LiNbO_3$) waveguide modulators and switches were available in the 1.3μm and 1.55μm signal wavelength windows, however, semiconductor devices research is aiming to implement the same functionality in III–V materials, allowing subsequent integration of the laser, the modulator and further active and passive devices. In the following a brief description of the main characteristics of external modulators will be given, in preparation for their use as system components in Chapters III, IV and V.

For the implementation of intensity modulation the Mach–Zehnder (MZ) interferometric configuration is currently the most widely used design since it requires only a maximum differential optical phase shift of π between the two arms of the interferometer during the modulation process in order to change from complete signal extinction to transparency, thus minimising the potential for the re–introduction of wavelength chirp as for example in semiconductor absorption modulators [Koyama and Iga], [Suzuki, Noda, Kushiro and Akiba]. A device input optical waveguide is followed by a Y–junction which divides the input optical power into two parallel waveguides, followed by a further Y–junction for recombining the signals at the output of the device. By means of electrodes over one or both of the Mach–Zehnder arms optical phase shifts are introduced via the electro–optic effect, leading at the output Y–junction to constructive, partially destructive or destructive interference between the two signals. Since the optical phase shift introduced in the waveguide(s) is linear with applied voltage, the device transfer function, defined as the ratio of optical output power to optical input power, is a function of the applied electrical voltage as given in Eq.2.2 where V_π represents the voltage required to achieve a π phase shift of the optical signal, resulting in complete signal extinction at the modulator output.

$$\frac{P_{out}}{P_{in}} = \frac{1}{2} \cdot \left(1 + \cos\left(\pi \frac{V}{V_\pi}\right)\right) \qquad (2.2)$$

For use as on–off intensity modulator the electrical data would normally be applied with a peak–to–peak amplitude equal to V_π, operating around a bias point $V_\pi/2$. However, alternative drive levels and bias points will be explored later in this work for the implementation of data modulation and signal processing at increased system speeds and with minimum electrical drive requirements. Whilst the electro–optic transfer function given above may be obtained with either a single ended or a balanced modulator configuration, only the balanced design (both interferometer arms being modulated in anti–phase) has the potential for ideal intensity modulation without additional wavelength chirp. In the following, balanced modulators will be assumed.

In the optical wavelength domain the MZ modulator may show a large optical bandwidth such that a good device extinction ratio (e.g. better than 20 dB optical) is achievable over a signal wavelength range of several tens of nanometers. In the electrical domain however, the effective modulator bandwidth is limited by the electrical bandwidth of the electrodes as well as by the difference in propagation speed between the optical signal in the optical waveguides and the electrical drive signal in the electrodes [Alferness]. To maximise the electrical bandwidth, travelling wave electrode structures are employed for high speed modulators above 3 GHz bandwidth, and in order to limit the walk–off between the electrical and optical signal, short devices are required, resulting in increased values for the switching voltage V_π, or alternatively device designs need to be employed which intrinsically minimise the difference in propagation delay between the electrical and optical waves. However, for narrow band electrical drive signals or in applications in which the amplitude frequency response but not the phase response is of importance, special electrode structures have been developed, which allow operation to substantially higher frequencies than is currently achievable with broadband designs [Alferness], [Jungerman, Johnson, Dolfi and Nazarathy], [Morris, Legg, Ford and Rosher]. In the system modeling below, the electrical bandwidth of the modulators will be assumed to be unlimited, with its actual frequency response or bandwidth included in the characteristics of the electrical drive signal.

The non-linear transfer function of the MZ modulator makes it well suited to operations with bandwidth limited digital data drive signals. As an example, Fig.2.5 shows the modulator output signal 'eye' diagram for the case of a bandwidth limited electrical input signal of sinusoidal electrical pulse shape, for CW modulator optical input.

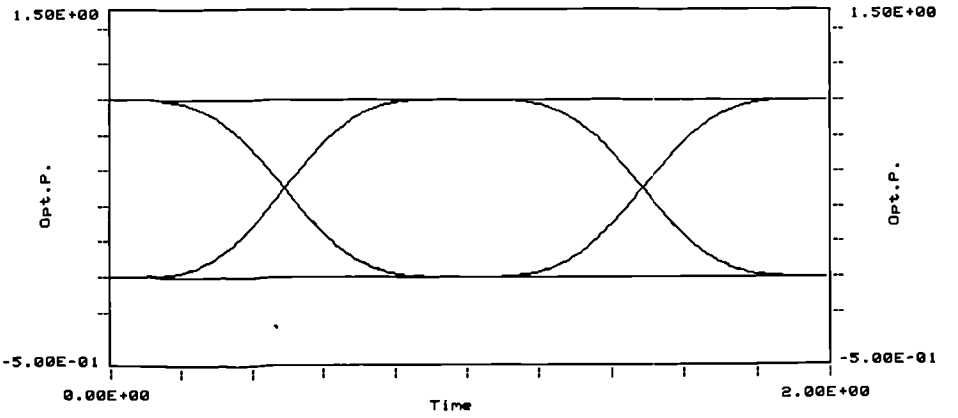

Fig. 2.5 Optical O/P Power 'Eye' for Bandwidth Limited Electrical Data I/P, with mean bias = $V_\pi/2$ and $V_{pp} = V_\pi$.

Considerable opening-up or bandwidth increase of the optical data 'eye' diagram is obtained. With a reduced electrical drive level ($V_{pp} = V_\pi/2$) either a less non-linear operation is obtained (mean bias $V_\pi/2$) at the expense of an extinction ratio penalty, or asymmetric pulse shaping is obtained as for example with a mean bias of $\frac{3}{4} \cdot V_\pi$ resulting in a high extinction ratio at the expense of an additional device insertion loss since the modulator is never fully 'on', as shown in Fig.2.6. These characteristics will be exploited in Chapter IV for the implementation of ultra-high speed optical data generation.

In addition to the traditional role of facilitating data modulation at high bit-rates, MZ modulators may also be employed for the implementation of signal shaping and multiplexing functions. In particular, modulators optimised for narrowband electrical drive at increased frequencies of several tens of GHz offer the potential for ultra-high speed signal processing which will be investigated in Chapter IV.

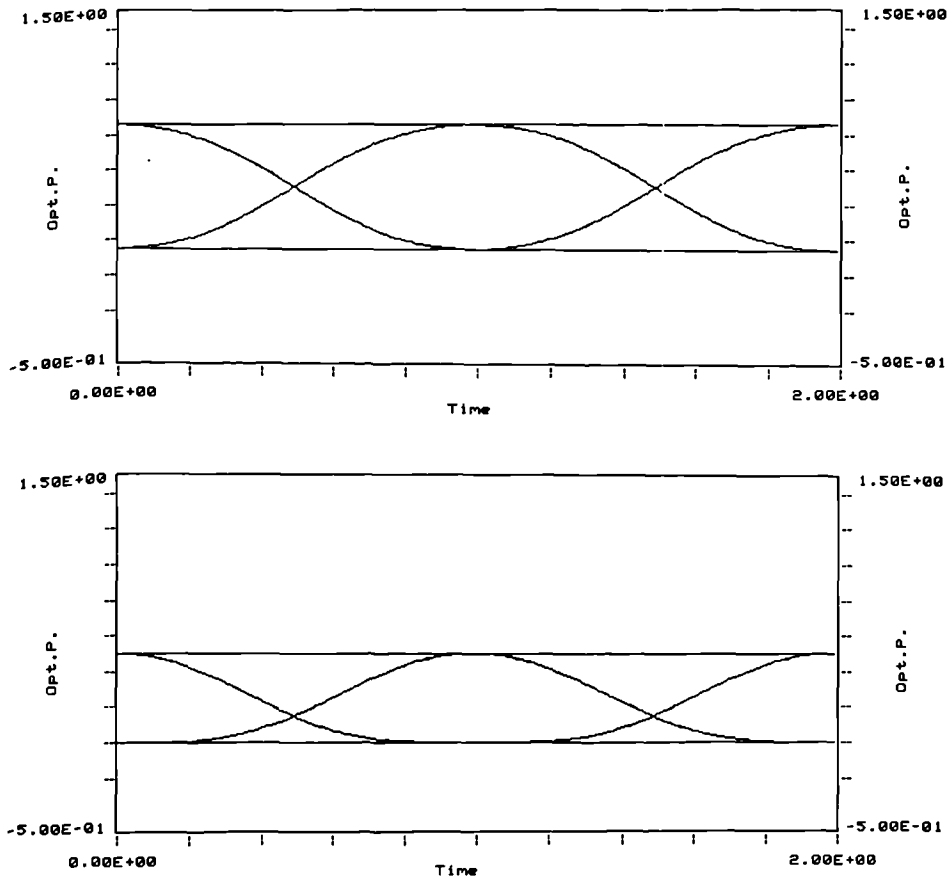

Fig.2.6 MZ Modulator with Bandwidth Limited Drive of Amplitude $V_\pi/2$, with Bias $V_\pi/2$ (upper), and with Bias $\frac{3}{4}\cdot V_\pi$ (lower).

II.4 OPTO-ELECTRONIC SIGNAL RESTORATION

For long distance transmission signal regeneration is required in regular intervals in order to compensate for signal attenuation and distortion. Whilst currently all installed systems employ full 3-R regeneration, advances in material and device technologies now allow large simplifications in the overall system design. Since in the latter part of this thesis the problem of signal attenuation is assumed to be solved as far as the systems under consideration are concerned, a brief summary of the available solutions is now provided to justify this assumption.

3-R Regeneration

Full 3-R regeneration (Reshaping, Retiming, Regenerating) has so far been the traditional approach to signal restoration. However, since this involves optical-to-electrical conversion, extensive analogue and digital electrical processing followed by electrical-to-optical signal conversion at each point of signal amplification, simpler and more flexible alternatives are required if the full potential of optical fibre transmission is to be realised. The main drawbacks of electro-optic regenerators are from an operational point of view that multi-wavelength signals need one regenerator for each wavelength, the regenerators themselves are bit-rate and signal format specific, and optically generated ultra-high speed transmission data rates would require optical as well as electronic time domain processing in each regenerator.

Linear Opto-Electronic Amplification

As a first step towards simplification of the intermediate line-equipment, the functions of timing extraction and digital signal regeneration may be eliminated. The result is a 'stripped-down' regenerator, in the form of a linear opto-electronic signal amplification stage suitable for applications in which not signal distortion but path attenuation is the main limiting factor. The linear opto-electronic repeater contains an optical receiver, linear electronic gain and an optical transmitter with sufficient bandwidth, such as a high speed directly modulated laser or an external modulator with CW optical signal source. This approach may be of interest for transmission routes of medium bit-rates upto maybe 2.5 Gbit/s, and systems requiring not more than ten amplification stages. The main limitations in such a system configuration are the overall system bandwidth after a linear cascade of bandwidth limited devices and the electronic system noise accumulation. In an experimental 420 Mbit/s system operating with two intermediate amplification stages, the feasibility of this approach has been demonstrated [Garnham and Blank]. Fig.2.7 shows the successive data 'eye' diagrams obtained at various points along the system, for the case of nominally

equal transmission bandwidth of all the optical receivers employed (565 Mbit/s circuits).

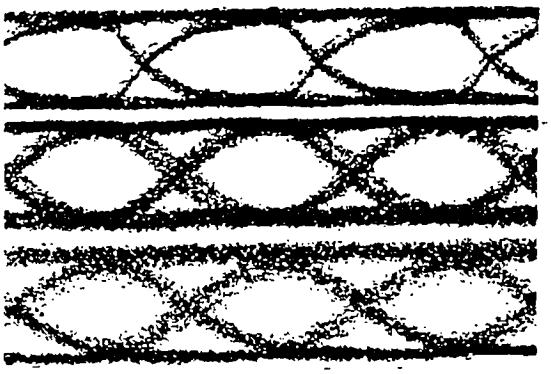

Fig.2.7 Linear Opto-Electronic Amplification at 420 Mbit/s:
'Eye' Diagrams after 1st, 2nd and 3rd Optical Receiver

A brief discussion of the required minimum receiver input signal levels at each intermediate repeater is included in [Garnham and Blank], with the experimentally observed system behaviour confirming that error-free transmission can be achieved if the signal-to-noise ratio is maintained at a sufficient level at the input of each subsequent linear repeater.

Based on current device technology, such linear opto-electronic repeaters are able to compete in terms of span capability with optical amplifier technology for single wavelength systems up to line-rates of 2.5 Gbit/s. At higher line-rates the deterioration in the optical receiver noise performance provides severe limitations, and optical amplifiers provide a more practical solution.

II.5 OPTICAL AMPLIFICATION

As long as signal attenuation is the main limitation to the achievable transmission distance, direct amplification in the optical domain is likely to be the preferred approach to signal restoration, especially in high performance, high capacity systems. For applications in the 1.3 and 1.55 μm wavelength windows semiconductor laser amplifiers have been

developed [O'Mahony (1)] which have allowed experimental system demonstrations with several cascaded amplifiers [Malyon and Stallard] and at Gbit/s line-rates [Malyon, Blank, Hobbs, Elton, Cockburn and Stallard]. More recently, fibre amplification has emerged as a high performance alternative for almost all transmission system applications, in the form of stimulated Raman amplification in standard or specially optimised silica fibres [Spirit, Blank, Davey and Williams] and optical gain in Rare Earth doped silica [Kaiser, Nagel, Shimada, Olsson and Payne] and fluoride fibres [Spirit, Walker, France, Carter and Szebesta]. In the context of high bit-rate optical systems the main amplifier issues are the available signal gain, the polarisation dependence of the gain, the optical bandwidth, linearity with signal power, and optical noise performance.

Prior to the availability of high performance doped fibre amplifiers travelling-wave semiconductor laser amplifiers were the main candidate for the provision of optical gain. Whilst single pass gains of upto 30 dB (optical) may be achieved, the main device limitations are due to their residual Fabry-Perot modes, the variation of the amplifier gain with input signal state of polarisation, the amplifier gain dynamics, and the effective amplifier optical noise figure in a system context. Semiconductor laser amplifiers based on only slightly modified laser structures have usually substantially different transverse electric (TE) and transverse magnetic (TM) optical gains due to their asymmetric device structure, giving a polarisation sensitivity of several dB (optical) unless especially designed device structures are employed. The amplifier gain dynamics are governed by the electronic carrier lifetimes as with semiconductor lasers below threshold. With gain recovery times of approximately 300 to 600 psec in bulk material semiconductor amplifiers, data patterning occurs at optical data-rates beyond approximately 1 to 2 Gbit/s, especially when the amplifier is operated in gain compression. Additionally, the intrinsic amplifier device noise figure of typically 4 to 6 dB is in practice deteriorated by the input fibre coupling losses, resulting in effective system noise figures no better than 6 to 8 dB at best. Whilst advances in materials and device designs promise improvements in gain recovery time and output power capability, the gain dynamics and the performance deterioration due to fibre coupling losses remain the main problems. Consequently, it is likely that semiconductor

amplifiers will find applications in non-linear optical and opto-electronic processing rather than in the context of basic linear optical amplification.

Compared with the above mentioned semiconductor laser amplifiers, fibre based optical amplification techniques offer a number of advantages. Although the basic processes involved have been known for a long time, advances in materials and device manufacturing were required to enable amplifier performances suitable for applications in fibre optic transmission systems. The main processes of interest for direct optical amplification in communication fibres are stimulated Raman gain and optical amplification in rare earth doped fibres.

Raman amplification in standard monomode optical fibre offers the prospect of long distance distributed optical amplification, in principle at any signal wavelength of interest. The disadvantages are the long interaction length of many km, thus ruling it out for standard discrete amplification applications, and the high power requirements of several hundred mW of pump power, even with specially optimised Raman fibres [Spirit, Blank, Davey and Williams]. Furthermore, when operating in gain saturation the sub-picosecond gain recovery times result in severe channel cross-talk in the case of WDM multi-channel operation, thus in any case not permitting system operation with high pump power utilisation. Consequently Raman amplification is now of limited interest for data transmission applications.

Rare earth doped fibre amplifiers have been developed only recently to the high level of performance required for transmission systems. Erbium doped silica fibres provide highly efficient signal amplification for operating wavelengths in the 1.55 μm low-loss fibre transmission window. The required optical pump wavelengths of either 980 nm or 1480 nm are compatible with near infra-red device technologies, providing an almost ideal amplification mechanism for high speed system applications. The main advantages are polarisation independence, high optical gain and low optical noise figure, allowing large numbers of amplifiers to be cascaded. Slow gain dynamics result in the amplifier effectively only responding to the mean optical signal power thus providing distortion-free linear optical amplification, and without channel cross-talk in multi-channel system

configurations. Furthermore, operation may be carried out well into amplifier saturation, allowing simple amplifier gain and power control schemes to be implemented. As a variation on the "discrete" amplifying fibres of a few metres length, ultra-low doping levels of Erbium over distances of many kilometres may provide distributed gain leading to effectively loss-less signal propagation [Spirit, Blank, Williams, Davey and Ainslie]. Potential applications for linear fibre propagation are as a distributed line amplifier or receiver pre-amplifier [Spirit, Wickens, Walker, Williams and Blank], allowing increased repeater spacings and extended repeaterless transmission spans, thus helping to overcome power budget limitations.

In the context of the system studies of this thesis, therefore, optical amplification by means of rare earth doped fibres is assumed to effectively remove the power budget limitations, at least for the number of amplification stages which may be required in the system configurations under study here. Thus system design and overall performance optimisation will be carried out with respect to limitations due to fibre chromatic dispersion only.

II.6 THE TRANSMISSION PATH

For high speed, long distance optical pulse transmission, the two main impairments are loss of signal due to fibre attenuation and pulse shape distortion due to fibre dispersion. Consequently all current and future planned high performance systems operate either in the 1.3 μm or the 1.55 μm low-loss windows of silica fibre, allowing spacings between linear electro-optic, regenerative, or optical amplifier based repeaters of typically 30 to 100 km. With the advent of doped optical fibre amplifiers with their excellent noise performance, however, digital systems can be envisaged with several hundred km fibre spans between fully regenerative repeaters, in which the optical amplifiers effectively remove the attenuation limit. The main consequence of the availability of optical amplifiers is therefore that high speed systems are limited by fibre dispersion. Two dispersive fibre

effects need to be considered with single mode optical fibres, namely the fibre chromatic dispersion and polarisation mode dispersion.

Standard step–index silica monomode fibre is characterised by an overall chromatic dispersion which originates from material dispersion and waveguide dispersion such that the waveguide dispersion cancels the material dispersion at a wavelength in the centre of the 1.3 μm low–loss fibre window.

The fibre transfer function may be expressed as:

$$H(f)= e^{(-j\cdot\beta\cdot L)} \tag{2.3}$$

with L being the fibre length in km, and β the propagation constant:

$$\beta = \tau\cdot(\omega-\omega_0) + \frac{d\tau}{d(\omega)}\cdot(\omega-\omega_0)^2 + \ldots \quad , \qquad \omega = 2\pi\cdot f, \qquad f_0 = \frac{c}{2\pi\cdot\lambda_0}$$

with $\dfrac{d\tau}{d(\omega)} = -\dfrac{D\cdot\lambda_0^2}{2\pi\cdot c}$, D being the first order dispersion parameter

For dispersion shifted fibre, the waveguide design has been altered through refractive index profiling such that the fibre waveguide and material dispersions cancel each other at $\approx$ 1.55 μm. The second and third order dispersion characteristics are similar to the standard step–index fibre case thus resulting – for the purpose of transmission system dispersion modelling – in a direct equivalence between system operation at 1.3 μm over standard step–index fibre and 1.55 μm operation over dispersion–shifted fibre.

In context of system modelling it is important to identify whether the value of the fibre chromatic dispersion varies significantly over the bandwidth of the optical signal. If this is the case, higher order dispersion terms need to be included for a full analysis of the system performance. Similarly, if dispersion compensation techniques are employed, such as through the addition of a fibre or a bulk optic device with a dispersion of opposite sign to the dispersion of the transmission fibre at the operating wavelength under

consideration, higher order dispersion terms may have to be taken into account which usually are not compensated for. In this work system operation is considered mainly over high dispersion fibre, such as 1.55 μm operation over step-index fibre. In this case the dispersion parameter D is sufficient to describe the fibre chromatic dispersion characteristics.

Although monomode fibre is designed to allow propagation of only one spatial mode to avoid the multi-path fibre dispersion of multimode fibres, it effectively provides for two propagating modes of orthogonal polarisation states. Small fibre asymmetries result in optical signal propagation with randomly varying coupling between the polarisation states leading to polarisation mode dispersion for the propagating optical signal of the order of 0.1 to 0.5 psec/km$^{\frac{1}{2}}$ [Poole, Bergano, Wagner and Schulte], [Poole], [Namihira, Kawazawa and Wakabayashi] which in turn results in a bandwidth limitation on the optical signal. Fortunately the dispersion value is small enough to allow polarisation mode dispersion to be ignored unless transmission distances reach many thousands of kilometers at multi-Gbit/s transmission speeds, or system speeds exceed 100 Gbit/s over more than hundred km.

II.7 OPTICAL RECEIVERS AND SYSTEM PERFORMANCE

In the context of high performance optical transmission systems the optical receiver has to fulfill several functions. Firstly, optical detection of the receiver input signal is to create an electrical copy of the signal power waveform without undue signal shape distortion. Secondly, the amount of electronic receiver noise added to the signal is to be minimised in order to maximise the receiver sensitivity. This requires low noise microwave components in optimised circuit designs, combined with suitable pulse shaping characteristics of the overall receiver. For binary digital transmission a near-optimum design target for the receiver output signal shape is given by the 100 % raised cosine signal frequency spectrum, resulting in a time domain pulse shape as shown in Fig.2.8 in 'eye' diagram form and providing maximum bandwidth limitation for minimum receiver noise whilst simultaneously ensuring low inter-symbol interference at the decision point.

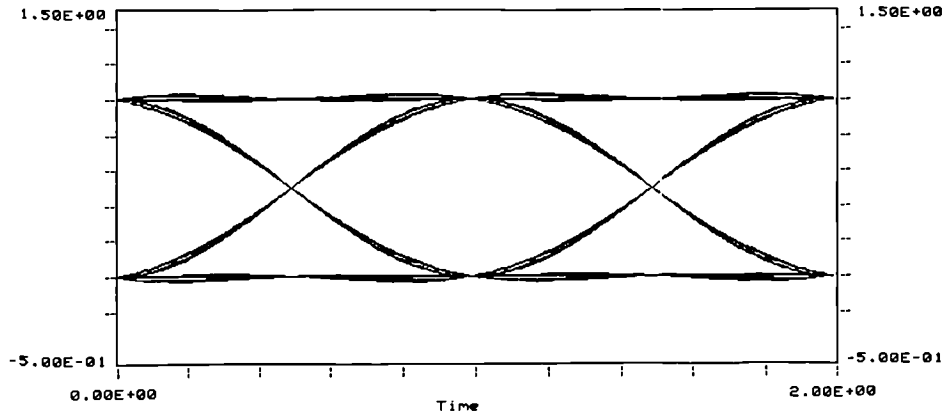

Fig.2.8 Raised Cosine Spectrum Time Domain Signal Shape ('Eye' Diagram)

Additional system performance improvements may be obtained through further optimisation, resulting in some variation in the exact receiver output pulse shape. In most cases, however, such additional optimisation yields receiver sensitivity improvements of the order of 1 to 2 dB optical [O'Mahony (2)], [O'Mahony (4)] which in terms of the system power budget is today of reduced significance due to the availability of highly efficient optical amplification techniques. Receiver optimisation may then be aimed at increasing the overall system tolerance to component variations and other system impairments. In the context of ultra-high speed systems the main system performance limitations originate from transmitter imperfections and the pulse propagation characteristics of the transmission path itself. Consequently, the system performance analyses and optimisations carried out in this work are concerned with identifying the system limitations due to dispersive fibre propagation and to identify system configurations with the potential for increasing these limits. In this context optical detection is assumed based on nominal raised cosine receiver filtering.

Overall system modeling is carried out by means of a series of computer programs covering a variety of system configurations and based on the individual device or subsystem characteristics as detailed above. Just as in an experimental system investigation, the starting point is an ideal electrical data waveform to be transmitted. The test signal consists of a 2^N–1 Pseudorandom Binary Sequence (PRBS) NRZ format waveform, which is

applied to a low-pass filter to simulate electrical bandwidth limitations within the transmitter drive circuitry. Appendices A2-3 and A2-4 show the block diagrams of the program structures for basic direct laser modulation and external modulation respectively. The filtered transmitter drive signal is applied to the transmitter opto-electronic device (laser or modulator), and after the generation of the complex electrical field description of the optical transmitter output signal, the effects of dispersive fibre propagation are evaluated, followed by optical power detection and electrical receiver filtering. The resulting electrical output waveform may then be displayed directly or alternatively can be processed further in order to generate the system output 'eye' diagram and a measurement of the effective 'eye' opening which would be available at the input to a following decision circuit.

In order to evaluate the dispersive fibre propagation performance of a particular system configuration and allow comparisons between alternative system designs, an analysis is required of system deterioration as a function of fibre distance. In the following investigations, this system performance analysis is carried out by means of an assessment of the deterioration of the system output 'eye' opening as a function of fibre distance. A full system analysis for back-to-back operation (no fibre) provides the reference 'eye' opening against which the results of all subsequent propagation calculations are normalised. Appendix A2-5 shows in schematic form the structure of the computer programs for carrying out the full system performance evaluation as a function of dispersive fibre propagation distance, based on a series of propagation calculations for increasing fibre distances. The results are then presented in the form of a graph of system penalty as a function of propagation distance, thus allowing straightforward performance comparisons between alternative system configurations.

Since the analysis is based on the relative 'eye' closure only, it neglects receiver noise and signal dependent noise terms. As far as receiver thermal noise is concerned, the assumption is that the receiver remains the same independent of propagation distance, as would be the case in a real system. Consequently receiver signal to noise ratio variations are due to variations in the signal level only, as evaluated with the analysis of 'eye'

opening. The situation is different for signal dependent noise terms, such as signal shot noise and signal spontaneous beat noise terms originating from the use of optical amplification. Therefore, a reduction in the 'eye' opening at the "on" level will also result in a reduction of the optical noise associated with that level, thus improving the real system signal–to–noise ratio beyond what the 'eye' diagram analysis indicates. However, any 'eye' closure due to an increase in the optical "off" signal level has the inverse effect since additional signal dependent noise is introduced. The basic approach adopted in this work does not cover those effects, i.e. assumes a thermal noise dominated detection process, and more detailed system analyses could take this signal dependent noise into account and also include additional receiver optimisation, especially in the context of multi–level optical signalling as studied in Chapter V. However, the investigations were aimed at identifying the basic system behaviour of a range of configurations, and the additional performance enhancements achievable through the detailed optimisation mentioned above will not alter the overall findings of this work.

II.8 SUMMARY

In this chapter a brief description has been provided of the main system components of high capacity digital optical transmission systems in preparation for their use in overall system modeling and performance analyses in subsequent chapters. In particular, the characteristics of semiconductor lasers and external modulators will play a major role in determining the overall system performance in the context of long distance dispersive fibre propagation. No attempt is made at optimising the optical receiver transfer function, instead standard raised cosine frequency spectrum signal shaping is assumed. Overall system performance analyses will be based on evaluations of system 'eye' diagram closure as a measurement of the system deterioration with dispersive propagation distance.

CHAPTER III

THE PERFORMANCE OF STANDARD SYSTEM DESIGNS

III.1 INTRODUCTION

The purpose of this chapter is to summarise the transmission performance limitations of standard system designs based on the components and subsystems described in the previous chapter. The results then represent a point of reference for the analysis of advanced high capacity system configurations in Chapters IV and V. The two main system limitations of concern are the maximum achievable data rate and the fibre dispersion-limited transmission distances, and consequently the discussion of system performance is presented in these terms.

In the context of high capacity optical fibre transmission systems the overall system performance is mainly determined by two components: the transmitter optical source and the transmission fibre. The characteristics of the optical source such as device speed limitations due to laser dynamics or the bandwidth of external modulators determine the maximum system operating speed. The transmitter spectral emission characteristics determine the rate at which dispersive fibre propagation leads to pulse distortion and overall system deterioration. The most widely employed laser sources are directly modulated Fabry-Perot lasers (Section III.2) and directly modulated Distributed Feedback Lasers (Section III.3). Further improvement in the transmitter spectral characteristics may be obtained with optical angle modulation achieved through direct DFB laser modulation followed by an optical demodulator (Section III.4). Finally, external modulation of a CW optical carrier signal leads to a transmitter output signal with minimum optical bandwidth, providing benchmark results for standard system configurations, with the system speed limited by the available modulator bandwidth and electronic processing capability and with the maximum transmission distance determined by the effects of chromatic dispersion on a minimum optical bandwidth signal (Section III.5).

III.2 FABRY-PEROT LASER SYSTEMS

Semiconductor Fabry-Perot lasers have been widely employed as the basic transmitter source for near-infrared optical transmission systems. At data-rates of 8 Mbit/s, 34 Mbit/s and 140 Mbit/s over propagation distances of no more than a few tens of km, early system designs were based on 1.3 μm lasers and standard step-index monomode fibre and were purely attenuation limited. The emergence of 1.55 μm wavelength operation and bit-rate increases to several hundred Mbit/s and beyond as well as large improvements in the system power budgets all resulted in fibre chromatic dispersion becoming the system performance limiting factor as a result of the broad optical spectrum of the Fabry-Perot laser. The main system effect of operating a Fabry-Perot laser over a dispersive transmission path is due to the differences in optical propagation delay between the optical powers in the individual laser modes. This results in a channel bandwidth which is propagation distance dependent. In addition, dynamic variations in the power distribution between the lasing modes (mode partitioning) lead to random variations in the channel transfer function, resulting in system mode partition noise.

III.2.1 Transmission Bandwidth

Based on the measured (time-averaged) optical emission spectrum of the transmitter laser, an effective channel bandwidth may be calculated as a result of the interaction of the laser spectrum and the fibre chromatic dispersion, leading to an equivalent electrical system transfer function of :

$$H(f) = \sum a_i \cdot \exp(-j2\pi f \tau_i) \qquad (3.1)$$

with a_i being the relative amplitude of the spectral line f_i,
and τ_i representing the relative delay after fibre propagation.

Fig.3.1 displays the measured laser spectrum of a 1.55 μm Fabry-Perot laser and the calculated absolute value of the channel transfer function H(f) for signal propagation

through 176 km of step-index fibre at 17 ps/nm/km chromatic fibre dispersion [Blank, Bickers and Walker]. The resulting bandwidth of ≈ 11.8 MHz is approximately half of that

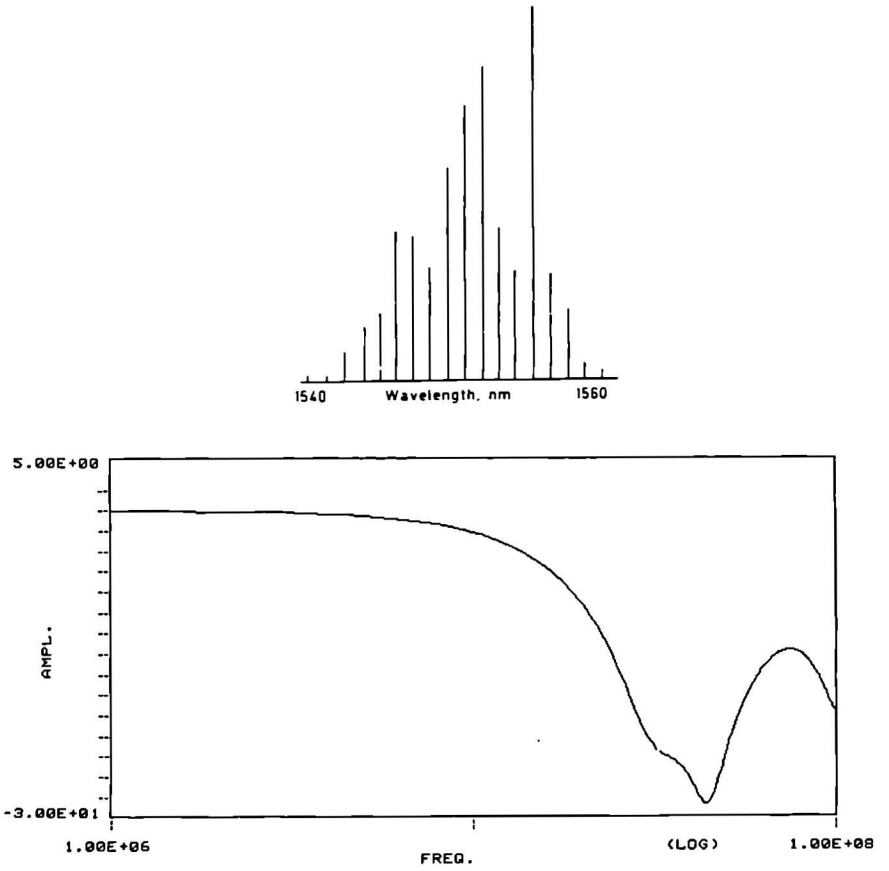

Fig.3.1 Measured Fabry-Perot Laser Spectrum (upper), and Calculated Channel Transfer Function (lower).

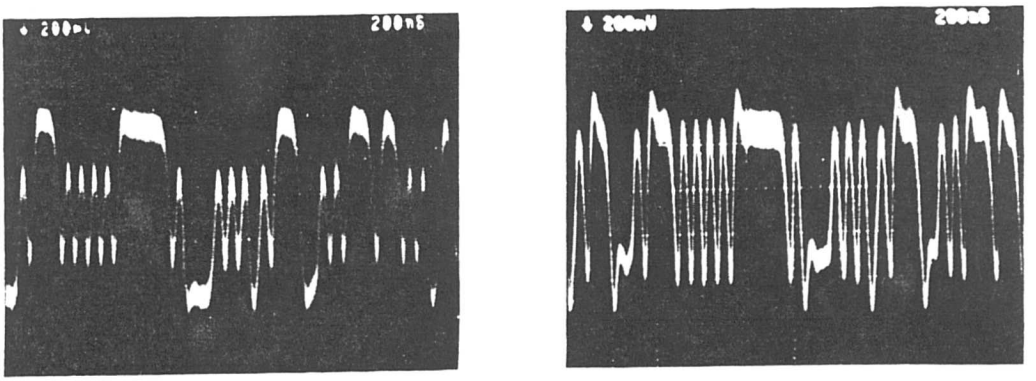

Fig.3.2 Bandwidth Limited 34 Mbit/s Optical Propagation: Data after 176 km (left), Electrically Equalised Data (right). (200 nsec/Div horizontal axis, 200 mV/Div vertical axis)

required for 34 Mbit/s transmission. However, by means of electrical equalisation after photodetection the channel bandwidth may be partially restored to allow system operation at this data rate (Fig.3.2).

For Gbit/s line-rates the laser operating wavelength therefore has to be close to the fibre wavelength of zero dispersion. Again the effective channel bandwidth may be computed. However, higher order fibre dispersion needs now to be taken into account due to the large relative variations in the first order fibre dispersion across the laser spectrum.

Fig.3.3 shows the measured spectrum of a high speed ridge waveguide 1.53 μm laser used for transmission over 100 km of dispersion shifted fibre. With a fibre dispersion of +1.5 ps/(nm·km) or −1.5 ps/(nm·km) at the laser centre wavelength (laser λ_c approximately 20 nm above or below the fibre λ_0) and with a second order fibre dispersion of 0.075 ps/(nm^2·km), the computed channel bandwidth (−3 dB electrical) is limited to approximately 400 MHz as shown in Fig.3.4. The second set of channel transfer functions shown in Fig.3.4 is for the laser spectrum of Fig.3.3 and a chromatic dispersion of +0.15 ps/(nm·km) and −0.15 ps/(nm·km) at the laser centre wavelength (a difference of 2 nm between the laser λ_c and fibre λ_0), again for 100 km propagation distance. The resulting bandwidths of ≈ 4.22 GHz for −0.15 ps/(nm·km) and 4.38 GHz for +0.15 ps/(nm·km) show that Gbit/s data propagation over distances approaching 100 km should be achievable with a Fabry-Perot laser diode as the transmitter optical pulse source.

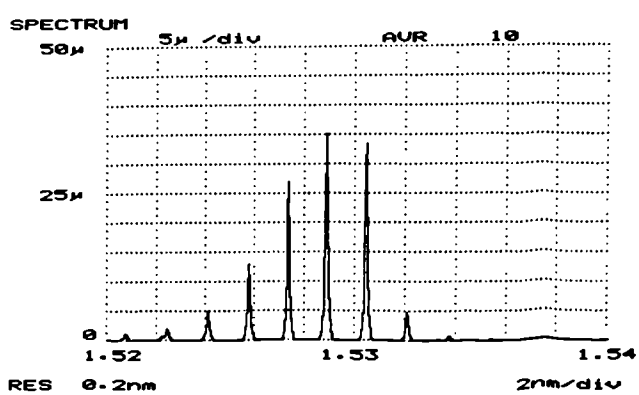

Fig.3.3 Optical Spectrum of Ridge Waveguide 1.53 μm Fabry-Perot Laser

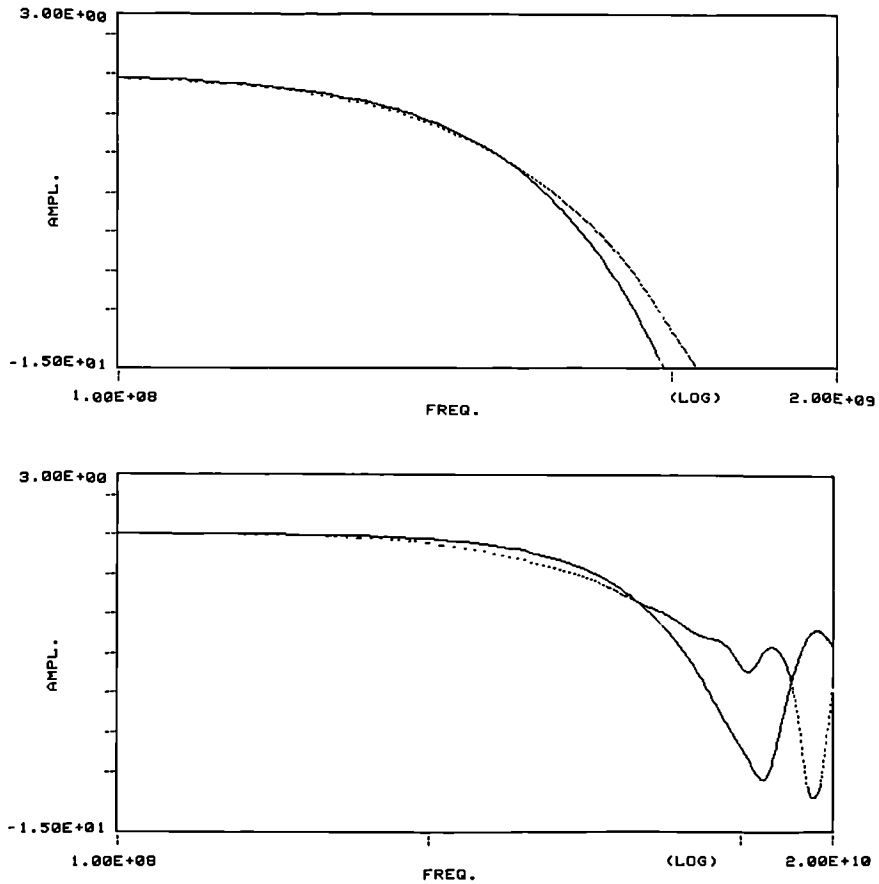

Fig.3.4 Channel Frequency Response for First Order Dispersion of ±1.5 ps/(nm·km) (upper) and ±0.15 ps/(nm·km) (lower), with 0.075 ps/(nm^2·km) Second Order Dispersion.

At high values of first order fibre dispersion the channel bandwidth reduces in proportion to the increase in fibre length, thus leading to a fixed bandwidth–distance product for a given laser spectrum and first order fibre chromatic dispersion value. At small fibre dispersions, however, the variation in fibre dispersion across the laser spectrum becomes significant, leading to finite system bandwidths even for laser operation perfectly aligned with the fibre zero dispersion wavelength. General discussions of pulse broadening as a function of distance and of the maximum achievable system capacity are normally based on theoretical calculations which rely on only the laser spectral width value rather than the actual spectral shape [Marcuse and Lin] [Ogawa] [Yamada, Kawana, Miya, Nagai and Kimura]. The results are general system bandwidth design curves which allow laser and fibre requirements to be approximated for a given application. However, due to the asymmetry in the laser spectra more detailed analyses are required to establish actual

limits, especially for high capacity system operation at low values of first order fibre dispersion. This is clearly demonstrated in Fig.3.4, with distinct differences in the system transfer functions for the two cases of +0.15 ps/(nm·km) and −0.15 ps/(nm·km) first order dispersion at the laser centre wavelength.

III.2.2 Transmission System Performance

The channel bandwidth limitation may to some extent be compensated for with electrical equalisation after photodetection, as shown in the example of Fig.3.2. In terms of the overall system performance, however, such equalisation leads to an increase in the receiver noise due to the enhancement of high frequency thermal and shot noise terms in the receiver output signal spectrum, thus resulting in a reduction in effective receiver sensitivity. Whilst this accounts for the deterministic changes in the overall channel bandwidth and noise performance, a further system deterioration results from laser mode partitioning during high speed direct laser modulation [Ogawa]. Although the total laser output power varies according to the rate equation description of the laser dynamics, the power in each individual mode and therefore the power distribution across the main lasing modes may vary considerably from one optical pulse to the next as well as throughout any individual pulse during high data rate direct laser modulation. A model for describing the effects of mode partitioning on the performance of high capacity optical fibre transmission systems operating over high dispersion fibre was proposed in [Okano, Nakagawa and Ito], followed by a modified analysis in [Ogawa] which allows system evaluations to be carried out based on only the measurement of the time avaraged laser emission spectrum. The latter model provides a reasonable approximation, especially if incomplete mode partitioning is also included by means of the mode partitioning factor k. Measurements of k have indicated that its value may range from almost 1 (full partitioning) to as little as 0.1 (largely stable laser spectrum) [Ogawa and Vodhanel]. Consequently, the overall system penalty is made up of two components, firstly a deterministic deterioration as a result of the channel bandwidth limitation (transformed into a receiver sensitivity penalty if

bandwidth equalisation is employed), and secondly an additional system noise term as a result of the combination of laser mode partitioning with dispersive fibre propagation (laser mode partition noise). Here, experimental system results are compared with the output of a computer model originally developed for the analysis of Fabry–Perot laser systems operating over high dispersion fibre [O'Mahony (3)] and amended to take second order fibre dispersion into account as well as incomplete laser mode–partitioning. Since the model only allows for variations in the laser spectrum at the onset of each new transition from low optical power to high optical power but not for variations within a given optical pulse, it can be expected that the k–values needed in the model to obtain agreement with the experimental results may be somewhat larger than the reported measured values, especially at Gbit/s system operating speeds.

Applied to the 34 Mbit/s, 176 km system of Fig.3.1, a calculated system penalty versus propagation distance is obtained as shown in Fig.3.5 for fibre dispersion of 17ps/(nm·km), second order dispersion of 0.075 ps/(nm^2·km), and with a laser mode partition k–factor of 0.4 as reported for low bit–rate modulation of buried heterostructure lasers [Ogawa and Vodhanel]. At 176 km the calculated penalty was 4.5 dB, dominated by a 4.2 dB equalisation noise penalty contribution. The measured system penalty was 4.0 dB,

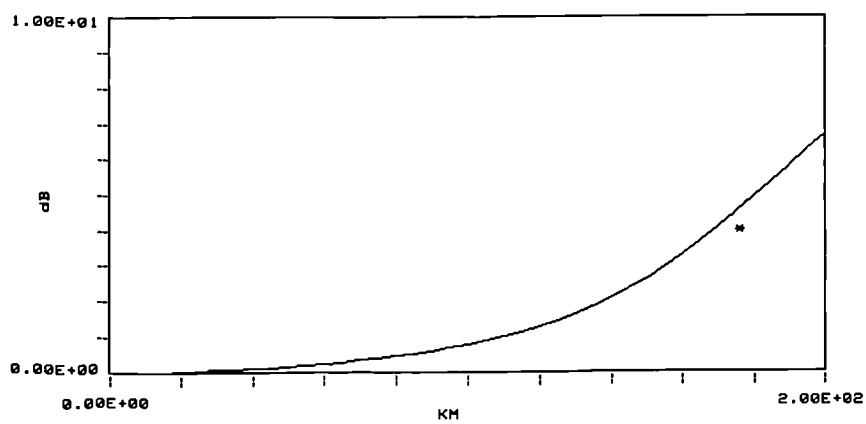

Fig.3.5 System Penalty vs Distance at 34 Mbit/s and 17 ps/(nm·km) (Experimental Result: *).

with the slight over–estimation in the model thought to be due to the fact that perfect channel bandwidth compensation is assumed upto the system clock frequency, whilst in the

experimental work a low order passive network filter was employed which provided the basic compensation required but not over the full frequency range assumed in the model. As a consequence of the small k-value, mode partitioning is not dominating the system behaviour, with the overall increase in receiver noise mainly due to channel bandwidth equalisation. This is reflected in Fig.3.2 which shows the bandwidth limitation without a visible increase in the noise level on the bandwidth limited pulses.

At Gbit/s line-rates the laser centre wavelength needs to be carefully aligned with the fibre wavelength of zero dispersion if propagation distances of more than a few kilometres are required. The potential for Gbit/s operation over long fibre distances was demonstrated early-on with an experimental system result at 2 Gbit/s over 51 km of dispersion-shifted fibre at 1.55 μm operating wavelength [Yamada, Kawana, Miya, Nagai and Kimura]. Two sets of experimental results are now presented, supported by system modeling to demonstrate how far such systems may be extended at operating speeds of 2 and 5 Gbit/s.

The calculated channel bandwidth results of Fig.3.4 indicated that the absolute value of the first order fibre dispersion at the laser centre wavelength needs to be well below 1.5 ps/(nm·km) if a 100 km span is to be achieved at a system line-rate of 2 Gbit/s. Fig.3.6 displays part of a pseudorandom data test sequence after fibre propagation over 92 km at approximately −1.5 ps/(nm·km) and 102 km at −0.15 ps/(nm·km). The system consisted of the 1.53 μm Ridge Waveguide laser with the emission spectrum as shown in

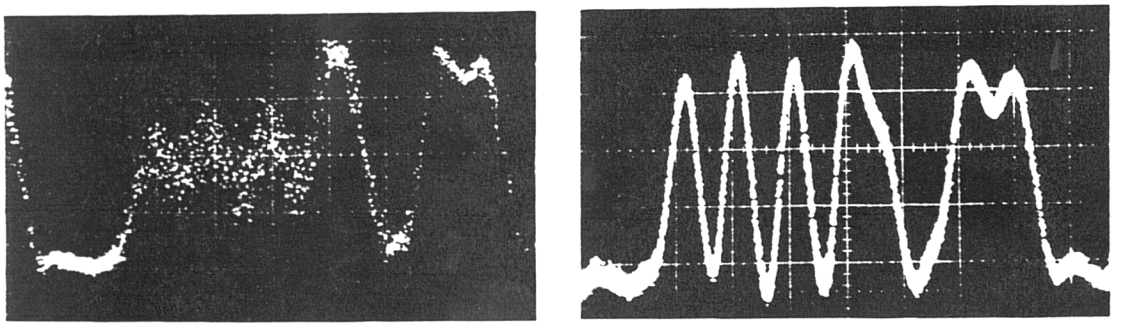

Fig.3.6 Pulse Train after 92 km propagation at −1.5 ps/(nm·km) (left), and after 102 km propagation at ≈ −0.15 ps/(nm·km) (right). (1 nsec/Div horizontal axis, 200 mV/Div vertical axis)

Fig.3.3 and dispersion shifted fibre with an average value of λ_0 of 1.55 μm [Blank, Garnham and Walker (2)]. After 92 km the pulse train shows clearly not only the severe bandwidth limitation but also mode partition noise. After propagation through the 92 km of dispersion-shifted fibre, followed by a further 10 km of standard step-index fibre which reduces the overall fibre dispersion at λ_c to approximately -0.15 ps/nm/km, both the bandwidth limitation and the mode partition noise have been reduced considerably. Full system bit error-ratio measurements revealed a system penalty of approximately 0.6 dB compared with back-to-back system operation.

The calculated system penalty as a function of propagation distance is shown in Fig.3.7 for both the 92 km and the 102 km experimental configurations, together with the

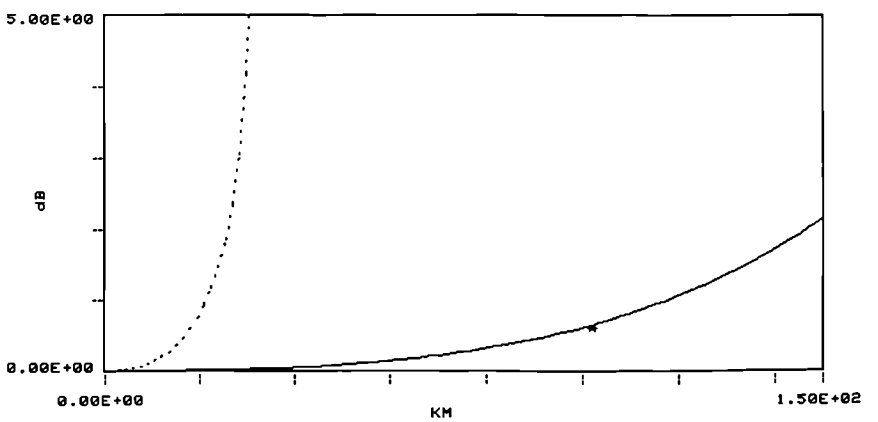

Fig.3.7 System Penalty as a Function of Distance for First Order Fibre Dispersion of -1.5 ps/(nm·km) (dashed) and -0.15 ps/(nm·km) (solid). 102 km Experimental Result: *

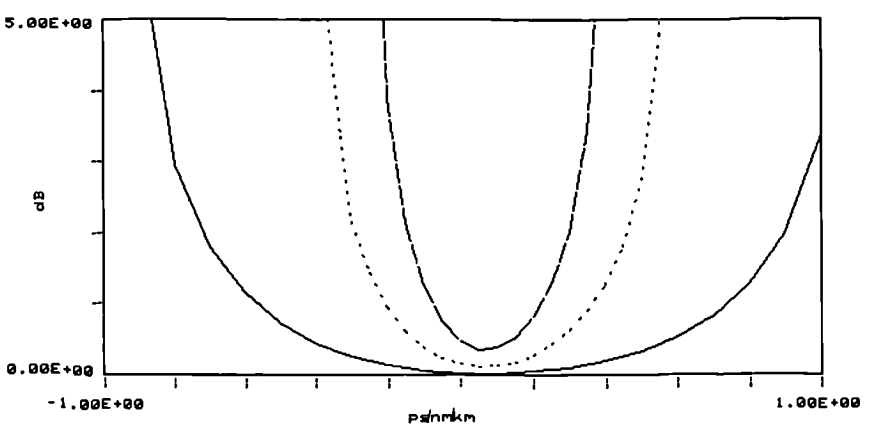

Fig.3.8 System Penalty as a Function of First Order Fibre Dispersion for 50 km (——), 100 km (· · ·) and 150 km (– –) Propagation.

experimental result. Fig.3.8 displays the calculated system penalty as a function of the first order fibre dispersion value at the laser centre wavelength for 50 km, 100 km and 150 km transmission, showing how the required wavelength matching accuracy increases with increasing distance, and also demonstrating clearly how the asymmetry in the laser emission spectrum leads to an offset of the optimum laser centre wavelength away from the fibre wavelength of zero dispersion. This is of particular importance in the context of maximising the tolerances on the laser and fibre specifications for a given application.

As an alternative to high bit-rate data transmission in the 1.55 μm wavelength window which necessitates the use of dispersion-shifted transmission fibre, operation in the 1.3 μm wavelength range allows operation over the widely installed standard step-index fibre. To demonstrate the potential at multi-Gbit/s line-rates if the laser centre wavelength λ_c is matched sufficiently well to the fibre λ_0, experiments have been carried out at 5Gbit/s with a wavelength selected laser diode. The design of the optical receiver and the electronic processing employed in the system experiment are described in [Walker, Blank, Garnham and Boggis]. A laser launch power of approximately -3 dBm was available together with a receiver sensitivity of -25.5 dBm, thus providing a system power budget sufficient for propagation over at least 50 km at 1.3 μm, including allowance for some system dispersion penalty and a system margin. The centre wavelength of a commercial, wavelength-selected high speed semiconductor laser diode (λ_c = 1.313 μm) was sufficiently close to the λ_0 of fibre available for the system studies (λ_0 = 1.317 μm). System measurements over 53 km of fibre revealed that error-free transmission could not be achieved as long as the laser was biassed at threshold (optical extinction ratio of approximately 30 to 1), but that satisfactory system operation was possible with a slightly increased laser bias resulting in a reduced optical extinction ratio of approximately 8 to 1. Since the average optical laser spectrum (Fig.3.9) was found not to change significantly over this range of laser bias adjustment, the differences in system performance can be attributed mainly to a reduction in the laser mode partitioning characteristics.

The reduction in laser extinction ratio resulted in an effective receiver sensitivity deterioration to -24.1 dBm before any dispersive fibre propagation. After propagation over

53 km of standard step-index fibre the additional penalty due to fibre chromatic dispersion was 0.5 dB, as shown in Fig.3.9. Fig.3.10 shows the computed system penalty as a function of dispersive propagation distance, based on the measured laser spectrum and for

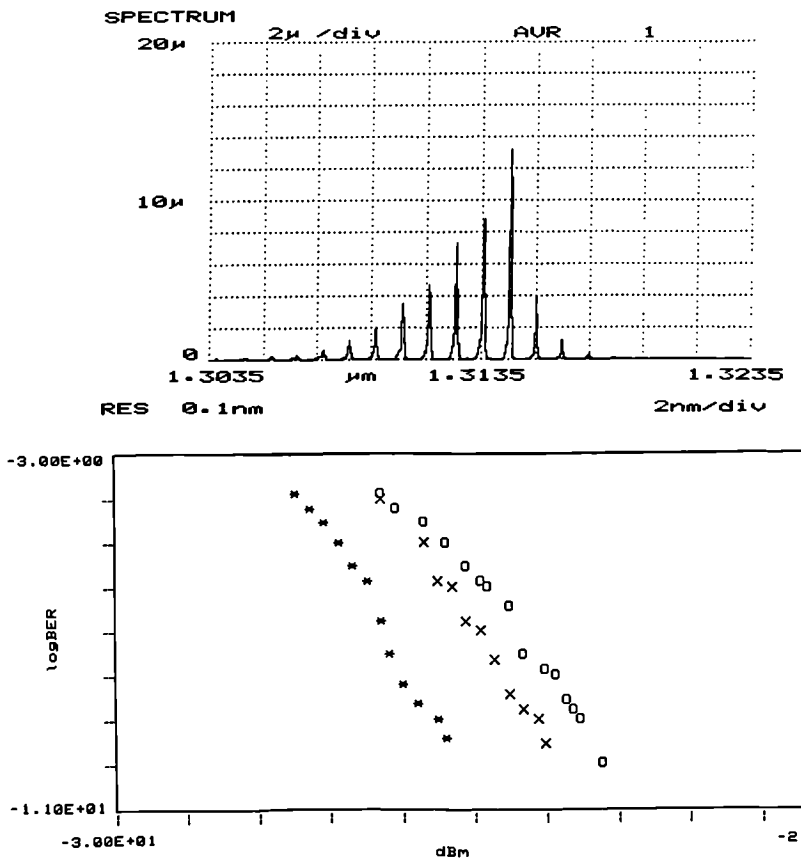

Fig.3.9 5 Gbit/s Fabry-Perot Laser System: Optical Spectrum under PRBS Data Modulation (top), and BER Measurements after 0 km with 30:1 Extinction (*), 0 km with 8:1 Extinction (x), and 53 km with 8:1 Extinction (o).

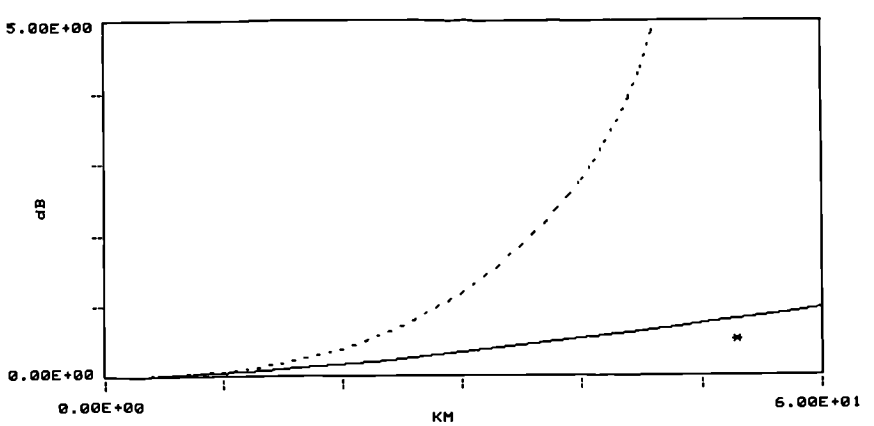

Fig.3.10 System Penalty as a Function of Dispersive Propagation Distance: -0.35ps/(nm·km), k=1.0 (dashed), and k=0.4 (solid). 53 km Experimental Result: *.

laser operation from threshold (laser mode partitioning factor k = 1.0) and for operation with reduced extinction ratio (k = 0.4), demonstrating the importance of the level of laser mode partitioning for the overall system behaviour.

These experimental results, which at both operating speeds represent the longest transmission distances reported for Fabry–Perot laser based transmitters, demonstrate that high bit–rate and long distance optical fibre transmission systems may be operated successfully provided that the laser wavelength is matched sufficiently well to the zero dispersion wavelength of the fibre. Basic system modeling has been employed to analyse the experimental results and to provide some insight into the tolerancing required on the laser centre wavelength with regard to the fibre zero dispersion wavelength. The results also demonstrate that the asymmetric emission spectra of long–wavelength semiconductor lasers lead to asymmetric system penalty behaviour for operation below and above the fibre zero dispersion wavelength. Consequently the more detailed analysis is required based on a representative optical laser spectrum rather than theoretical calculations relying only on the laser optical spectral width, if the limits are to be explored for Gbit/s optical pulse propagation. The same applies for establishing maximum tolerances for the laser and fibre characteristics for a given system data rate and propagation distance.

In conclusion, the combination of high speed Fabry–Perot lasers and low dispersion monomode fibre allows multi–Gbit/s system speeds to be achieved over propagation distances of interest. In principle, operating speeds are limited by the maximum speed of the electronic circuitry as well as the laser response times, and the propagation distances are limitated by the effects of residual fibre dispersion. In practice, the tolerances achievable on the laser and fibre characteristics determine the maximum capacity.

III.3 INTENSITY MODULATED DFB LASERS

In the Distributed Feedback Laser the internal grating along the laser length ensures that only one optical wavelength may be emitted, thus reducing the width of the optical spectrum from a few nm, as in the case of the Fabry-Perot laser, to a few MHz for CW laser operation. As a result, Gbit/s data propagation is possible over high dispersion optical fibre such as 1.55 μm operation over standard step-index fibre. However, as outlined in Chapter II, dynamic wavelength shifts (chirp) during direct laser modulation broaden the spectrum to several Angstroms, which represents many times the information bandwidth of the modulating signal even at multi-Gbit/s data rates. As a result, laser wavelength chirp provides the limiting factor for high speed direct laser modulation with propagation over dispersive fibre.

The particular characteristics of a range of laser structures have been analysed and demonstrated experimentally [Tucker], with the aim of identifying from a device point of view how to maximise the laser direct modulation speed capability. Overall system performance analyses have been presented [Linke], [Koyama and Suematsu], [da Silva and O'Reilly], [Koch and Corvini], [Heidemann], [Vodhanel, Elrefaie, Iqbal, Wagner, Gimlett and Tsuji], which provide general system design guidelines and include comparisons between laser structures. In practice, often only a limited choice is available for the implementation of a particular system, and it is then important to optimise the device operating conditions in order to achieve maximum system performance. In the following, the system behaviour is analysed for one particular laser design, demonstrating the principle considerations to be applied in the design of such Gbit/s systems based on directly modulated DFB lasers.

The laser relaxation oscillation on switch-on, both in the time domain and in the wavelength domain (Chapter II.2.3), results in strongly non-linear laser behaviour during direct data modulation. The duration of these non-linear distortions is determined by the laser parameters and the drive conditions, through the laser relaxation oscillation frequency and the laser damping factor. Since the non-linear laser response is independent of the

modulating data rate, the consequences on the overall system performance vary considerably with the data rate applied. At low bit-rates (upto a few hundred Mbit/s) the non-linear signal distortions affect only a small fraction of the total data pulse energy, and thus in the limit of very low bit-rate operation are neglegible. At higher bit-rates a large part of the pulse is affected, thus leading to considerable dispersive pulse distortion during fibre propagation. However, for a given laser the operating conditions may be optimised to maximise the achievable propagation distances. At bit-rates approaching the maximum laser speed capability the whole pulse is affected, leading to a more substantial effect on the overall system performance whilst at the same time providing less options for system optimisation. The fact that following pulses in a long sequence of "1"s are not subject to the laser non-linear signal distortions is of minor importance for the overall system performance in a digital transmission system operating at low bit-error-ratios. Since the average number of consecutive "1" data pulses is small in a random data stream, the performance of the distorted data pulses dominates the system behaviour at low bit-error-ratios. On the other hand, remedial action such as increased laser bias for reduced laser non-linearity affects all data pulses, leading to a rapidly increasing system penalty due to the reduction in optical extinction ratio [Koch and Corvini]. To what extent optimisation of the laser operating conditions may result in major improvements is therefore dependent on the data line-rate employed. Equation 2.1 detailed how the laser wavelength chirp depends on the laser linewidth enhancement factor α and the laser output power waveform. Although a small value is desirable for α, obtainable through optimised device design [Westbrook (1)], [Ogita, Yano and Imai], the laser operating conditions affect greatly the value of d/dt[ln(P(t))], thus device optimisation with regard to the laser transient behaviour is at least as important. Whilst purely from a laser point of view this suggests the use of a slow laser operated at small driving levels for achieving minimum wavelength chirp, this needs to be balanced against the requirement to have as little of the overall pulse energy distorted in the time and optical frequency domains, which in turn requires a fast laser operated at the highest possible drive levels.

Consequently, the performance of a particular laser at a given data rate is dependent on

the interworking between the fundamental laser behaviour and the system requirements in digital pulse modulation systems. Techniques developed for reducing the inherent laser wavelength chirp through laser current waveform shaping are an attempt to improve on the natural laser output pulse shape. However, in practice they are often difficult to implement at higher bit-rates where they might offer the greatest benefit [Bickers and Westbrook], [Olshansky and Fye].

The results of some system modeling will now be used to discuss these issues in more detail. The basis for the computer analysis of the overall system behaviour is the ridge waveguide DFB laser introduced in II.2.1 which has been used at BT Laboratories for system investigations and which is also available from commercial suppliers. The analysis is carried out at data-rates of 2 Gbit/s and 5 Gbit/s, the latter being the maximum operating speed for direct intensity modulation of the particular device employed. At lower data-rates of upto several hundred Mbit/s, only a small fraction of the optical pulse energy at the rising edge suffers from wavelength chirp, which disperses quickly during initial fibre propagation to leave a remaining transform-limited optical signal. Consequently, after an initial small system penalty the performance then stabilises to provide overall system characteristics almost as for ideal intensity modulation. Under certain circumstances similar behavior may be obtained even at Gbit/s system speeds, as will be shown below.

2 Gbit/s Data Rate:

At Gbit/s data rates the laser relaxation oscillation is present for a large part of an individual optical pulse thus resulting in considerable excess pulse distortion during dispersive fibre propagation. If the laser relaxation frequency at the "on" level is substantially larger than the bit-rate, the system performance is only weakly dependent on the laser drive level employed, whilst it is strongly dependent on the laser bias which determines the laser dynamics during switch-on. Fig.3.11 displays the electrical drive signal and the resulting laser output power waveform for a laser bias near threshold. Fig.3.12 shows the system penalty as a function of distance for two drive levels, firstly for laser operation from threshold to 2.2 times threshold, secondly from threshold to 3 times

threshold. In both cases the laser drive current is bandwidth limited to twice the bit-rate, i.e. 4 GHz, thus providing fast rise and fall times relative to the bit-interval.

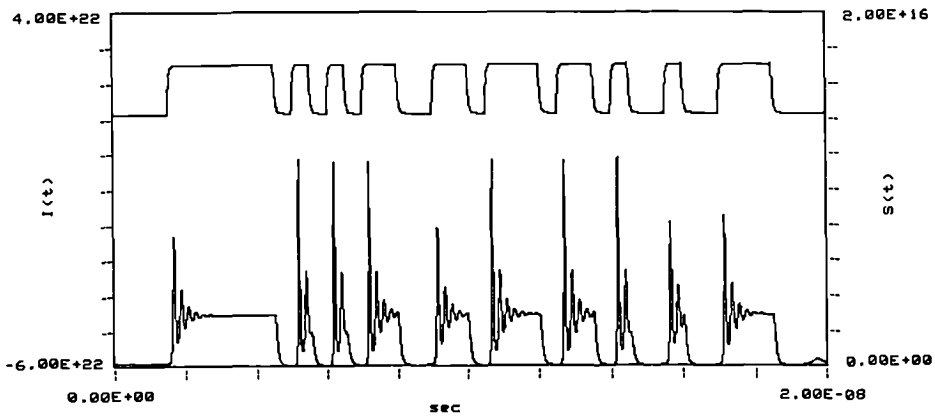

Fig.3.11 Laser Drive Waveform and Resulting Output Power Signal

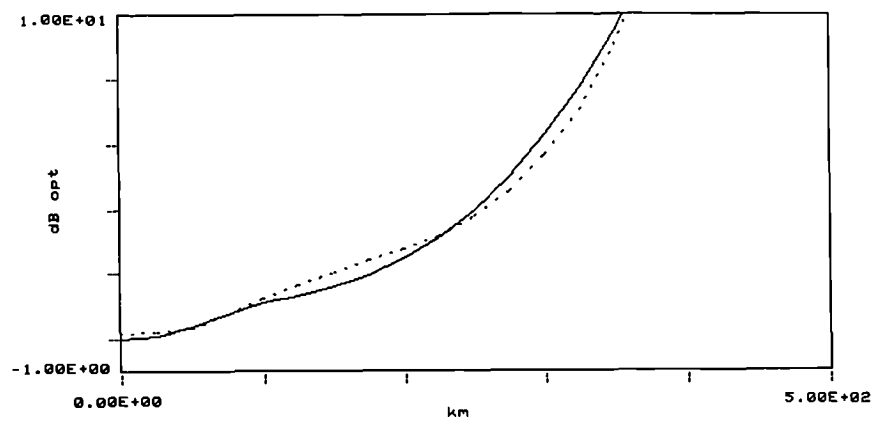

Fig.3.12 System Penalty for two Laser Drive Levels: Threshold to 2.2 times Threshold (dashed), and Threshold to 3 times Threshold (solid).

With the laser intrinsic speed substantially faster than the data rate, a reduction in the drive signal bandwidth may be employed to dampen the laser relaxation oscillations during switch-on (Fig.3.13) without risking overall speed limitations in the system. Fig.3.14 displays the resulting penalty curves for a transmitter electrical signal bandwidth limited to approximately 80 % of the system clock frequency, resulting in major improvements at higher system penalties and again showing only minor differences between the two laser drive amplitudes.

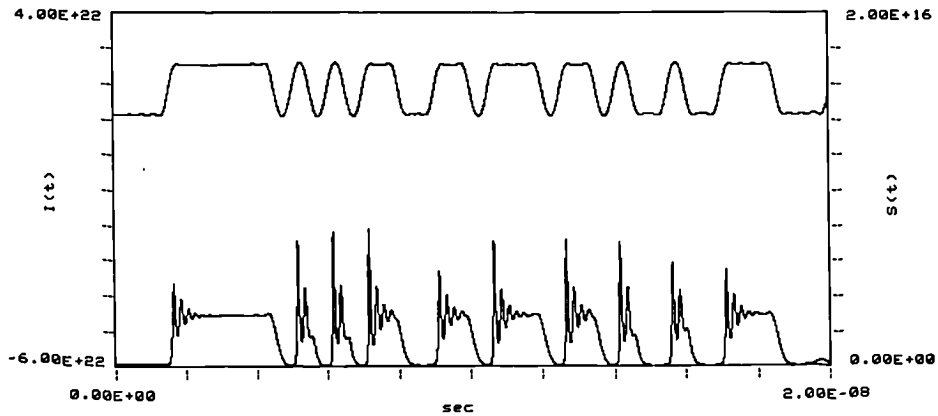

Fig.3.13 Bandwidth Limited Laser Drive Waveform (upper), and Resulting Optical Power Signal (lower).

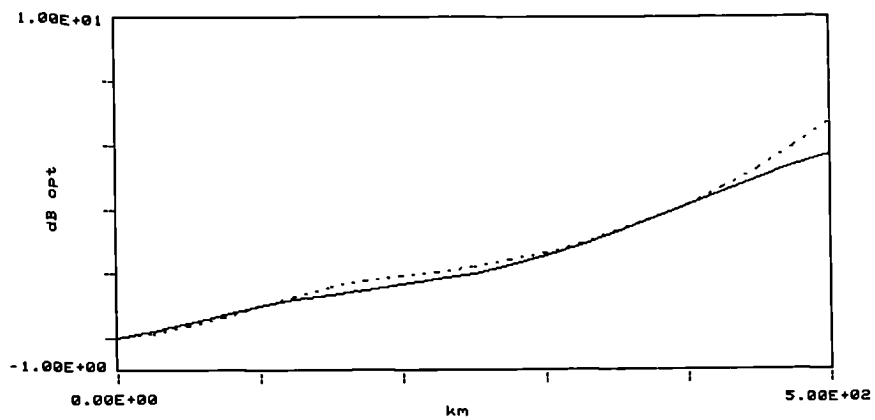

Fig.3.14 System Penalty for two Laser Drive Levels (Bandwidth Limited): Threshold to 2.2 times Threshold (dashed), and Threshold to 3 times Threshold (solid).

Further improvements in system performance are achievable through increasing the laser bias and thus allowing a reduction in the transmitter optical extinction ratio. The combination of the resulting increased laser speed leading to a smaller portion of the pulses being distorted together with a larger damping in the laser relaxations at high power operation leads to substantial improvements in dispersive signal propagation. Fig.3.15 displays the results for laser operation with the same electrical data amplitudes as before but with a reduced optical extinction ratio of approximately 4 to 1. System sensitivity deterioration due to the additional shot noise with low extinction ratio optical transmitter operation has not been included here, but would not alter substantially the overall system behaviour in the context of dispersion limited data propagation.

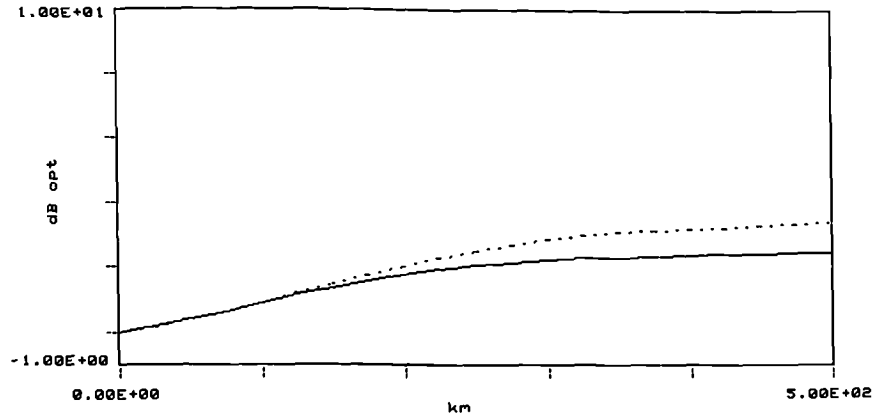

Fig.3.15 System Penalty with Laser Optical Extinction of 4:1, and Laser peak-to-peak Modulation Amplitudes of 1.2 times Threshold (dashed) and 2 times Threshold (solid).

The leveling-off of the penalty curves at around 2.5 and 3.3 dB is due to complete dispersal of the chirped part of the pulse out of the bit-interval, leading to a "background" penalty whilst their remaining unchirped pulse energy then deteriorates according to the transform-limited optical spectrum, resulting in a second rise in the penalty curve after approximately 1500 to 2000 km (Fig.3.16), as appropriate for 2 Gbit/s transform-limited pulses (see III.5).

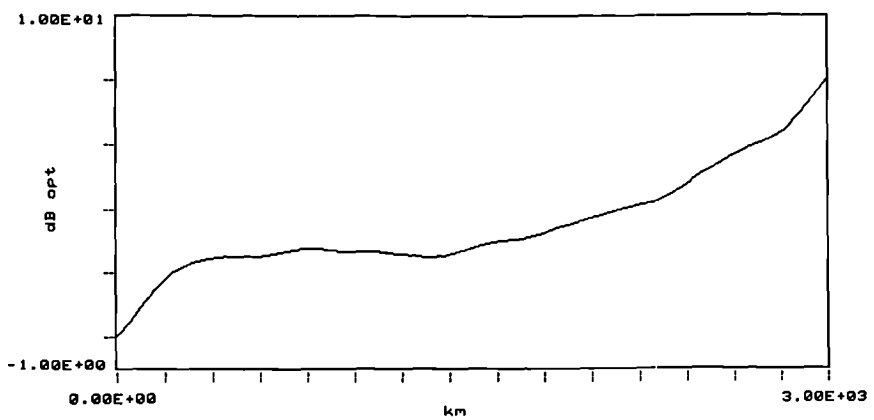

Fig.3.16 System Penalty Curve for 2 Gbit/s at 4:1 Laser Optical Extinction Ratio.

This demonstrates that if the distorted portion of the optical pulse is kept sufficiently small, propagation distances may be achieved similar to those for ideal chirp-free intensity modulation, just as in the case of low bit-rate system operation.

5 Gbit/s Data Rate:

For the particular laser structure employed here, a data rate of 5 Gbit/s is the maximum system speed achievable. A single data pulse now consists of simply the first cycle of the switch-on relaxation oscillation, resulting in strong data patterning and large wavelength chirp as shown in Fig.3.17. Consequently, unlike in the case of lower bit-rate operation, the drive level employed when the laser is biassed at threshold does make a substantial difference to the overall system performance since it affects both the optical pulse shape and the wavelength chirp, with the laser speed of response increasing as the

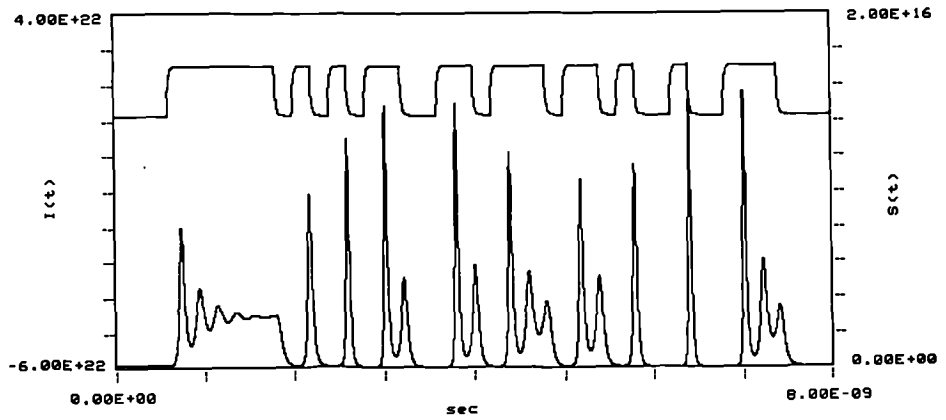

Fig.3.17 Laser Drive Current (upper) and Optical Power Waveform (lower) at 5 Gbit/s.

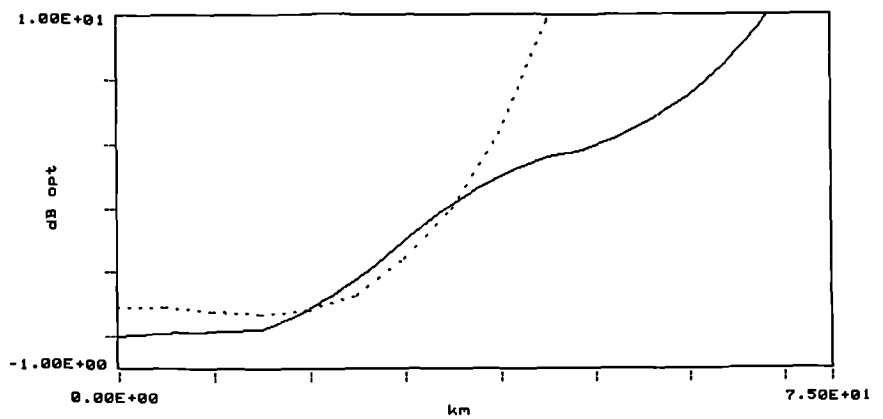

Fig.3.18 System Penalty for Laser Drive from Threshold to 2.2 times Threshold (dashed) and to 3 times Threshold (solid).

drive level increases. In particular, the laser relaxation oscillation may lead to considerable 'eye' closure for back-to-back system operation depending on the laser drive level. Fig.3.18 displays the system penalty curves, showing the smaller drive level incurring a

relative penalty without fibre propagation, due to stronger data patterning which reduces and moves to higher frequencies as the drive level is increased. This also accounts for the better system performance of the high drive level result after extended propagation.

With the system data-rate close to the intrinsic laser speed, bandwidth limiting of the electrical drive signal has only a minor effect, since the laser in any case can not respond to harmonic frequency terms in the drive current. This has been confirmed with full system calculations and is reflected both in an unchanged shape of the transmitter output signal and substantially unaltered dispersive fibre propagation performance.

On the other hand, raising the laser bias level results in a considerable improvement in system performance due to an increase in the laser speed (reduced data patterning) and stronger damping in the laser relaxation oscillations. The resulting system penalties are shown in Fig.3.19 for the same two electrical laser drive amplitudes employed previously, but with the laser bias adjusted in each case for an optical extinction ratio of approximately 4 to 1.

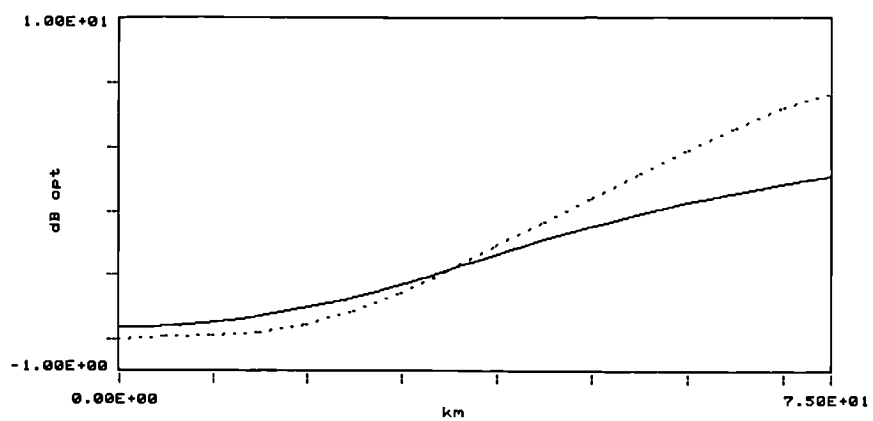

Fig.3.19 5 Gbit/s System Penalty for 4:1 Optical Extinction Ratio, with a Drive Signal Amplitude of 1.2 times Threshold (dashed) and 2 times Threshold (solid).

Further laser chirp reductions may be obtained through laser bias increases until the optical extinction ratio falls to 3:1 or 2:1. However, under those operating conditions the overall system performance suffers from a large amount of excess shot noise in the receiver, especially with Avalanche Photodiodes or optical pre-amplification, and is therefore not considered to be practically useful. The extreme case of relatively small

intensity modulation on a large optical "bias" will be discussed below in Section III.4 in the context of optical frequency modulation.

In conclusion, direct injection current modulation of DFB laser diodes allows substantial improvements in the achievable dispersion limited propagation distances compared with Fabry-Perot lasers, and in particular allows operation over high dispersion fibre up to data-rates of several Gbit/s. At these line-rates, however, the laser wavelength chirp limits the maximum propagation distances, with the system behaviour depending critically on the laser parameters and operating conditions. In the limit of low bit-rate modulation, system distances as with ideal external modulation may be achieved, whilst at operating speeds close to the intrinsic laser speed limit the system behaviour is totally dominated by the laser chirp characteristics. If, on the other hand, operation is considered over low dispersion fibre such as with a 1.55 μm laser wavelength over low-loss dispersion-shifted fibre, the system operating speed is mainly limited by the intrinsic response times of the laser and the electronic processing devices in the system. Long distance propagation is accomplished straighforwardly, especially with fibre based optical amplifiers, until non-linear fibre propagation effects begin to play a major role. The fact that at lower bit-rates only the initial part of the optical pulses contain any excess wavelength chirp may be exploited in the context of optical processing for chirp-free ultra-high speed optical data generation and will be discussed in Chapter IV.3.2.

III.4 OPTICAL ANGLE MODULATION

As outlined above, the two main limiting factors of the DFB laser based system design are the laser speed limitation at Gbit/s line-rates due to the slow laser response close to threshold and the laser wavelength chirp. Whilst laser operation well above threshold leads to higher device speed as well as a far more linear response to the electrical drive signal, the resulting poor optical extinction ratio prohibits this approach for high speed intensity modulated digital systems. In particular, a poor extinction ratio

reduces the available modulated signal launch power, results in additional shot noise in the optical receiver, and also leads to increased non-linear signal distortions along the transmission span, such as in semiconductor optical amplifiers and also in the transmission fibre itself.

In the limit, however, a small modulation signal applied to a laser biassed well above threshold results in a small optical amplitude modulation index whilst at the same time linear optical frequency modulation occurs, with a large laser bandwidth available as appropriate for the high laser bias employed [Elrefaie, Vodhanel, Wagner, Atlas and Daut]. For notionally rectangular binary digital data modulation, this results in the emission of two optical frequencies, one for the electrical "0" level and a second for the "1" level of the modulating bit stream. If the laser is followed by an optical filter centered on one of the two transmitter frequencies intensity modulated optical data are obtained [Saito, Yamamoto and Kimura]. Due to the extended laser bandwidth, optical intensity modulation may thus be achieved at data rates beyond the direct intensity modulation laser capability, and also with a narrower optical spectrum than with direct intensity modulation. In general, however, the optical emission spectrum of the demodulated signal still contains some residual chirp. Commonly employed optical filters are Fabry-Perot etalons and Mach-Zehnder delay demodulators. In both cases the filter passband and out-of-band rejection characteristics determine the FM modulation depth to be employed, and thus the level of residual wavelength chirp. Optical FM modulation with Mach-Zehnder delay demodulation is of particular interest in the context of high speed systems and the basic system operation and performance considerations are summarised now. A practical implementation of a Mach-Zehnder delay demodulator consists of two fibre 3 dB couplers, spliced together with an appropriate differential propagation delay (fibre length) between the two arms and including polarisation control to ensure maximum interference at the output coupler. The transfer function of the demodulator is given by Eq.3.2, with η representing the output intensity at the output port.

$$\eta = \cos^2(\Delta\varphi/2) = \tfrac{1}{2}\cdot(1+\cos(\Delta\varphi)), \qquad (3.2)$$

($\Delta\varphi$: differential optical phase at the output 3 dB coupler).

This is of the same form as the electro-optic transfer function of a Mach-Zehnder intensity modulator (Chapter II.3) since it is based on the same principle. However, the Mach-Zehnder modulator has a notionally zero differential propagation delay between the two arms and is being modulated to achieve a differential phase shift of π, resulting usually in a transfer function which is only weakly dependent on the input signal optical wavelength. Here, however, the differential path delay is considerable in order to achieve the required wavelength selectivity. Consequently the question is to what extent direct laser angle modulation with optical demodulation may in system terms be equivalent to external intensity modulation by means of a Mach-Zehnder modulator.

The maximum value for the differential time delay τ is equal to the bit interval T of the data stream and the minimum peak-to-peak optical frequency modulation Δf which can be employed is $\frac{1}{2}\cdot f_c$, where f_c is the system clock rate. Simultaneous use of τ=T and $\Delta f=\frac{1}{2}\cdot f_c$ however leads to an optical demodulated signal with slow optical rise and fall times. In most cases, therefore, a somewhat larger frequency deviation is employed, combined with a reduced time delay in the Mach-Zehnder demodulator. However, chirp-free modulation, i.e. as with ideal external modulation, is only obtained if the maximum and minimum values of τ and Δf respectively are employed simultaneously [Shirasaki, Nishimoto, Okiyama and Touge].

Further constraints to be satisfied for successful FM signal generation and conversion to IM are given by the need for optical signal polarisation matching at the output coupler of the Mach-Zehnder interferometer, matching of the laser optical frequencies and the demodulator characteristics, and sufficiently low laser phase noise to prevent system penalties resulting from FM noise to AM conversion in the demodulator. Either laser bias control or Mach-Zehnder differential path length control is required to ensure that stable system operation is achieved. All these requirements, however, can be fulfilled relatively straightforwardly [Bryant, Carter, Lewis, Spirit, Widdowson and Wright].

Consequently, direct laser frequency modulation with optical Mach–Zehnder delay demodulation offers the advantages of low electrical drive levels, system speeds to beyond the direct intensity modulation capability of laser diodes as demonstrated with successfull system operation at 20 Gbit/s [Shirasaki, Yokota and Touge] and with substantially reduced transmitter chirp, at the expense of an optical filter and tight control over the operating point of the laser and the filter centre wavelength. Since this system configuration provides in the limit the same performance as ideal external intensity modulation, an analysis of maximum system performance (maximum path dispersion for a given bit–rate) is left to Section III.5 (external modulation). In most practical cases, the system performance will be worse by typically a factor 2 to 3 in terms of transmitter optical bandwidth due to some residual wavelength chirp, thus providing a practical solution for applications where the full advantages of external modulation are not needed, but where some improvement over the speed and dispersion limits of directly intensity modulated DFB lasers is required.

III.5 EXTERNAL MODULATION

External modulation techniques allow the separation of the optical signal generation and data modulation processes such that non–linear interactions may be avoided during signal generation between the electronic signal, the optical intensity and the optical phase, as occur in directly modulated semiconductor lasers. Typical examples are Mach Zehnder external modulators implemented in a variety of material technologies, electro–absorption modulators, and semiconductor optical amplifiers used as optical gates. Of these three types of device only the Mach–Zehnder modulator has the potential for providing truly chirp–free data modulation, since with both other devices large variations in electron carrier density occur leading to a certain amount of signal wavelength chirp [Suzuki, Noda, Kushiro and Akiba]. With a Mach–Zehnder modulator the optical signal may have an optical spectrum of minimum bandwidth for the signal pulse shape generated thus allowing substantially longer propagation distances over dispersive optical fibre. Since the optical

bandwidth is then determined solely by the data rate and is not dependent on fundamental laser characteristics such as the Fabry-Perot spectral width or the DFB laser chirp characteristics, a straightforward relationship is obtained for the maximum achievable transmission distance as a function of the data rate employed, for a given fibre chromatic dispersion parameter and optical pulse shape. If, starting from some reference data rate and propagation distance, the line-rate is increased by a factor N, the optical bandwidth increases also N-fold leading to N times the pulse broadening. Since, however, at N times the data rate only 1/Nth of the absolute value of pulse broadening is permissible in order to obtain the same level of relative pulse broadening or intersymbol interference, the maximum propagation distance is reduced by a factor N^2. Consequently a constant value C_{max} may be derived which describes the maximum channel capacity based on the system line-rate B and the total fibre dispersion D_{tot}, the product of the first order fibre dispersion parameter D and the propagation length L_{max} :

$$B^2 \cdot D_{tot} = B^2 \cdot D \cdot L_{max} = C_{max} \qquad (3.3)$$

The value of C_{max} depends on the definition of maximum allowable propagation length (e.g. whether for 1 dB or 2 dB system penalty) and on the exact optical pulse shape at the transmitter output.

Due to the relatively large electrical drive powers required for current Mach-Zehnder modulators at Gbit/s operating speeds, the device and drive amplifier bandwidths tend to be kept to a minimum, resulting in a bandwidth limited electrical drive signal to the modulator arms, with a resulting optical pulse shape as shown in Fig.2.5 after the non-linear modulator transfer function. Optical propagation through dispersive fibre then leads to signal shape distortions and intersymbol interference as depicted in Fig.3.20 with the system 'eye' diagrams for 10 Gbit/s operation back-to-back and after 100 km of fibre at 15 ps/(nm·km). Identical signal shapes (change of time axis only) are obtained at for example 5 Gbit/s over 400 km, in accordance with Equation 3.3 above.

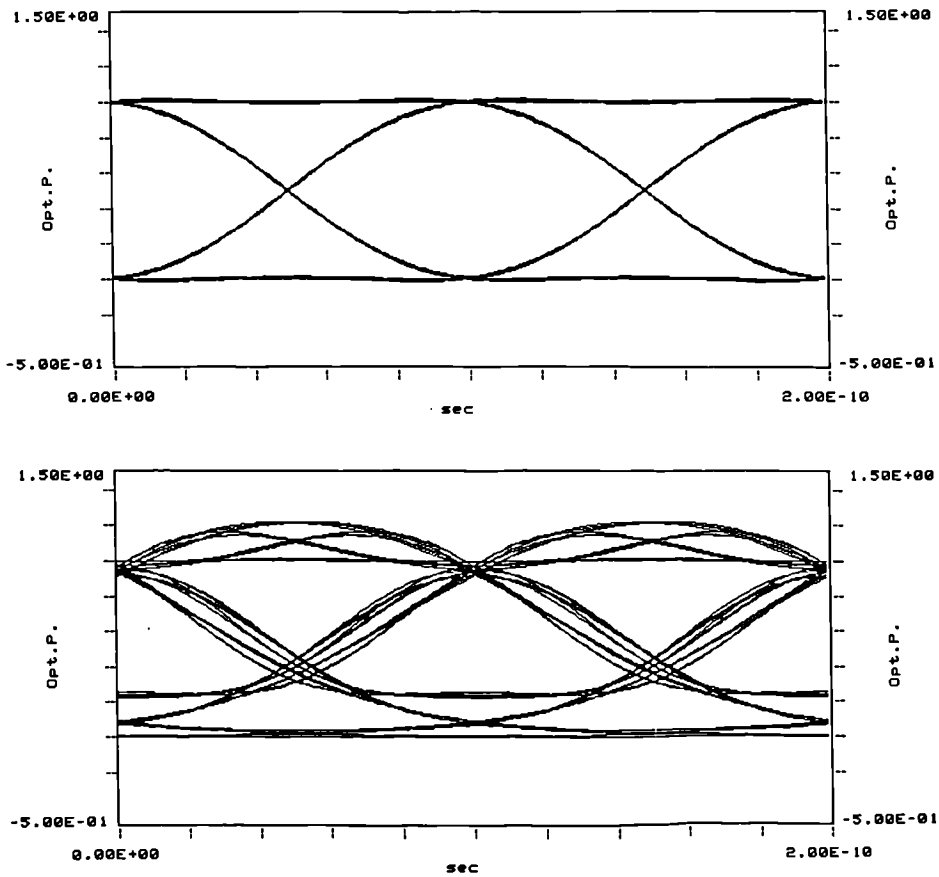

Fig.3.20 10 Gbit/s System 'Eye' Diagrams after 0 km (upper) and 100 km (lower) Fibre Propagation with 15 ps/(nm·km) Chromatic Dispersion.

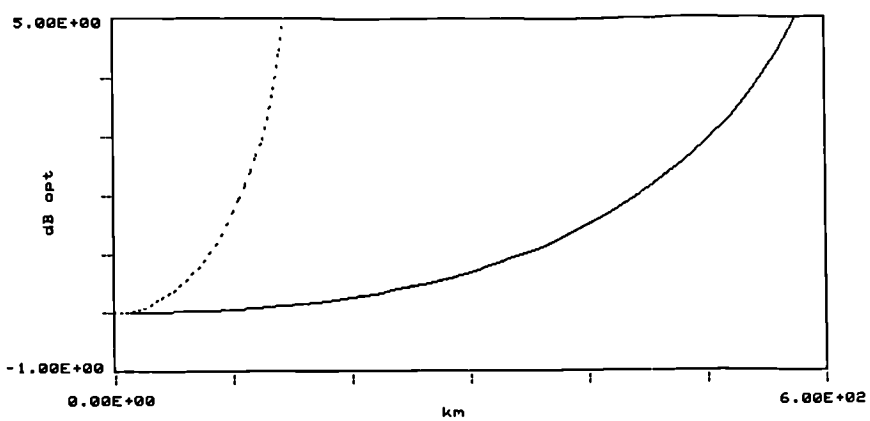

Fig.3.21 System Penalty as a Function of Distance for 5 Gbit/s (solid) and 10 Gbit/s (dashed).

Clearly visible is a reduction in 'eye' opening (1.7 dB optical) with both the "on" and the "off" levels deteriorating. System penalty calculations carried out according to the flow charts given in Annex A2–5 provide graphs of system penalty versus propagation distance

for 5 Gbit/s and 10 Gbit/s operation as shown in Fig.3.21. The propagation distances for 1 dB and 2 dB optical system penalties are 80 and 106 km for 10 Gbit/s and 320 and 426 km for 5 Gbit/s respectively, leading to a value of C_{max} of 120 $Gbit^2 \cdot psec/(s^2 \cdot nm)$ for 1 dB system penalty, and 160 $Gbit^2 \cdot psec/(s^2 \cdot nm)$ at a 2 dB penalty level. These results demonstrate the large improvement over system operation based on directly modulated DFB lasers, at the price of a separate modulation stage unless the two functions can be integrated into a single device.

Whilst the inherent wavelength chirp of directly modulated standard DFB lasers leads to severe system limitations compared with external modulation as discussed above, the external modulation system configuration also allows the introduction of controlled optical chirp onto the carrier signal independent from the data modulation process. For system operation at 1.55 μm wavelength over standard step-index fibre, controlled chirping to shorter wavelengths during each emitted data pulse leads to initial pulse compression during propagation, followed by pulse broadening once a minimum optical pulse width is reached. This may be achieved through direct FM modulation of the CW laser source in the external modulation transmitter configuration [Koch and Alferness]. For practical reasons guard bands are required between data pulses to allow a wavelength "reset" of the optical source between pulses if ideal chirping characteristics are to be implemented, making this approach particularly applicable to Optical Time Division Multiplexed system configurations. An experimental demonstration of the pre-chirping technique in an OTDM context [Olsson, Agrawal and Wecht] employed optical self-phase modulation in an optical semiconductor amplifier in gain saturation and providing the required wavelength chirp to shorter wavelength during each data pulse. Alternatively, sinusoidal frequency modulation of a DFB laser source may be used resulting in some limitations due to non-linear chirp throughout each optical pulse but still permitting increases in the dispersion limited transmission distance as demonstrated with 5 Gbit/s RZ data transmission over 200 km of high dispersion fibre [Henmi, Saitoh, Fujita, Yamaguchi, Asano, Mito and Shikada] and 5 Gbit/s NRZ system operation over 450 km [Ellis, Pycock, Cleland and Sturrock].

III.6 SUMMARY

This chapter has provided a summary of the performance of the main standard system configurations of interest for high capacity digital optical data transmission. In particular, the system dispersion limitations have been presented for transmitter optical sources based on (in increasing order of performance) Fabry–Perot lasers, Distributed Feedback lasers and External Modulation. With Fabry–Perot lasers Gbit/s operation is only possible over low–dispersion fibre, and if optimised sufficiently both the laser speed limitations and the system dispersion penalties limit the achievable system capacity. DFB lasers allow the use of high dispersion fibre to some extent, with further performance improvements possible through phase or frequency modulation of laser diodes. Over low–dispersion fibre, the intrinsic laser speed limits the maximum data–rate, whilst long distance propagation is possible until non–linear fibre effects begin to dominate the system performance. Finally, external modulation provides the minimum optical transmitter bandwidth, limited in the maximum data–rate only by the rising drive power requirements for ultra–wide–bandwidth external modulators, and thus by the signal processing speeds in the electronic domain. Some further improvement in the dispersion limited transmission distances may be obtained by means of controlled optical chirping of the externally modulated data stream, but relying on chirp optimisation for a particular propagation distance of interest. Over high dispersion fibre external modulation therefore provides the longest propagation distances, whilst over low–dispersion fibre chromatic dispersion is less of a problem with non–linear fibre propagation effects beginning to dominate over the long distances available from a chromatic dispersion point of view.

In the next two chapters techniques will be investigated for increasing substantially the optical line–rates as well as improving the dispersion–limited propagation distances. The aim is to achieve these improvements based on the same bandwidth limited components as employed in the standard system configurations described above.

CHAPTER IV

TECHNIQUES FOR ULTRA-HIGH SPEED SYSTEMS

IV.1 INTRODUCTION

Optical transmission system designs currently employed in the network may be developed further to transmission speeds of several Gbit/s whilst still capable of operation over distances of a few tens of km, as analysed in Chapter III. An example is the worldwide adopted standard of 2.488 Gbit/s for the STM-16 level of the new Synchroneous Digital Hirarchy (SDH). However, even the introduction of such multi-gigabit/s capacity links in the core transmission network of the major telecommunication network providers is unlikely to be sufficient to cope with capacity demands in the longer term future. Whilst current high speed system designs are likely to be engineered to cover capacity requirements from $\approx$ 2 Gbit/s to $\approx$ 10 Gbit/s, new design approaches may be required to allow further substantial increases in transmission speed. Attempts at employing current designs for this purpose will encounter restrictions mainly in the two areas of device speed limitations and signal distortion during fibre propagation. Whilst the inherent transmission capacity of optical fibres may be substantially larger than is currently utilised, the opto-electronic interface will provide a speed bottle neck. The direct modulation capability of semiconductor lasers is limited by the device dynamics as described in Chapter III, similarly optical modulators and opto-electronic receivers with tens of GHz bandwidth are difficult to implement. At the electronic level, signal processing required for the multiplexing of ultra-high speed TDM signals will also face limitations in terms of fundamental device speed. Since both electronic and opto-electronic device limitations are to be overcome, alternative system configurations are required which allow the electrical domain signals to remain within the bandwidths and processing speeds available, as well as ensuring that the signal translation between the electrical and optical domains also requires only components with practically obtainable bandwidth.

In this chapter techniques will be analysed for the generation and processing of ultra-high speed TDM signals by means of optical processing, thus employing Optical Time Division Multiplexing (OTDM) to circumvent the traditional speed limitations imposed by practical device characteristics. In an OTDM approach (Fig.4.1) [Alping, Anderson, Tell and Eng], several channels of lower speed optical data are either optically processed in order to obtain an optical Return-to-Zero (RZ) signal format from the standard NRZ signal, or are generated directly in an RZ format, allowing subsequent interleaving of the tributary channels for the formation of the high speed optical data stream. After fibre propagation, an optical demultiplexing process is carried out, resulting in individual optical RZ output data streams at the original tributary data-rates, which can be detected by standard bandwidth optical receivers. Several advantages are obtained, in particular the ultra-high speed multiplexing and demultiplexing processing functions are carried out in the optical domain, thus reducing the requirement for broadband electronic signal processing.

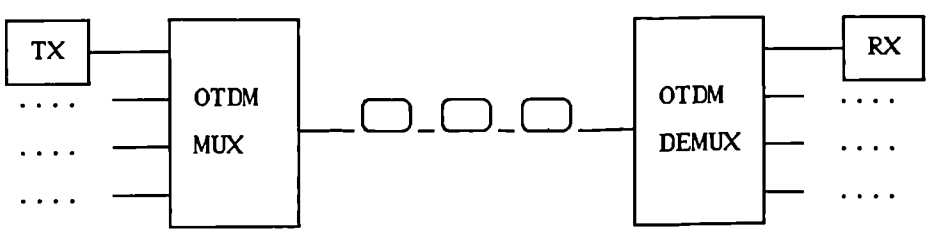

Fig.4.1 Basic OTDM Systems

This chapter is concerned with optical pulse generation and subsequent data modulation issues, with the aim of maximising the OTDM system line-rate whilst minimising the performance requirements of individual system components.

For use in OTDM fibre transmission systems, one requirement is for an optical pulse source which operates at a pulse repetition rate equal to the line-rate of each electronic tributary, producing pulses of sufficiently short duration to allow subsequent interleaving of several channels. Whilst in an ideal situation this pulse source may be modulated directly at the tributary line-rate to create in one step modulated RZ optical pulse streams, additional system design flexibility may be obtained if pulse generation and data modulation

are carried out separately, thus permitting optimisation of both the optical pulse generation and the data modulation processes. In the following, Section IV.2 will be concerned with techniques for the generation of suitable optical pulse streams whilst in IV.3 several options will be studied for the implementation of data modulation, followed by a discussion of overall system issues in a full OTDM configuration in IV.4. Fibre propagation limits will be addressed in Chapter V.

IV.2 OPTICAL PULSE SOURCES

The aim of the optical pulse generation process is to create pulses of sufficiently short duration at repetition rates equal to the line-rate of the tributary (electrical) data streams, without a requirement for ultra-broadband electrical or opto-electronic devices. To achieve this objective, non-linear device behaviour may be utilised such that only low frequency (preferably narrowband) electrical drive signals are required to the active devices. Approaches are of interest which are either based on direct modulation of a laser diode or may employ external modulation of a CW optical signal.

IV.2.1 Pulsed Laser Sources

The optical output power from a semiconductor laser diode was shown in Section II.2 for laser drive signals with a fast rising edge (step-function or square wave). The resulting laser relaxation oscillation results in signal waveform distortions with direct data modulation. The underlying laser device dynamics, however, can be made use of in repetitive optical pulse generation by means of suitable repetitive electrical drive to the laser, resulting in what is known as laser gain switching [Van der Ziel and Logan]. By providing an electrical drive signal of suitable shape, level and bias, only the first peak of the laser relaxation oscillation will be emitted, resulting in a single optical pulse for each electrical pulse and thus providing a continuous optical pulse train. With typical high speed

semiconductor laser diodes of today this process results in the generation of optical pulses of typically a few tens of psec duration, obtainable at pulse repetition frequencies to several GHz. Fig.4.2 shows the laser output power waveform and emission wavelength as a function of time for sinusoidal electrical drive at a frequency below the laser relaxation oscillation frequency.

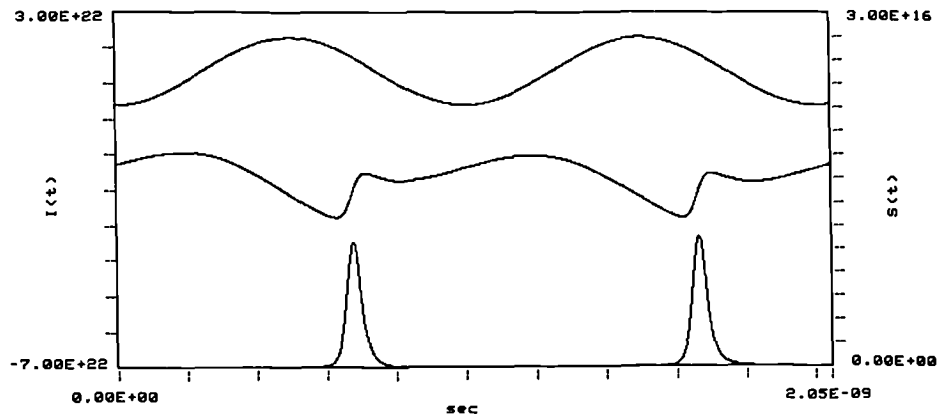

Fig.4.2 Electrical Drive (top), Laser Wavelength (centre), and Optical Power (bottom)
(Laser Bias: 0.5 times Threshold, Drive Amplitude : 2 times Threshold)

With a laser bias increased to beyond the value required for minimum output pulse width secondary peaks of the laser relaxation oscillation appear. Since this situation is to be avoided under all circumstances in an OTDM application, laser operation needs to be controlled to remain within a bias level range in which deviations from the optimum operating point only lead to increased pulse width without any secondary optical pulse emission. The gain switching process results in rapid carrier density variations during the optical pulse, which in turn lead to a strong frequency (wavelength) variation accross the pulse. However, during the time period of significant optical intensity emission the optical frequency varies almost linearly with time, resulting in an optical spectrum as shown in Fig.4.3 for the operating conditions as in Fig.4.2 above. The main disadvantage of gain switching at high repetition frequencies is its dependance on an electrical drive waveform with a small value time derivative at the point of optical pulse emission, which results in a relatively large amount of timing jitter in the pulse generation process.

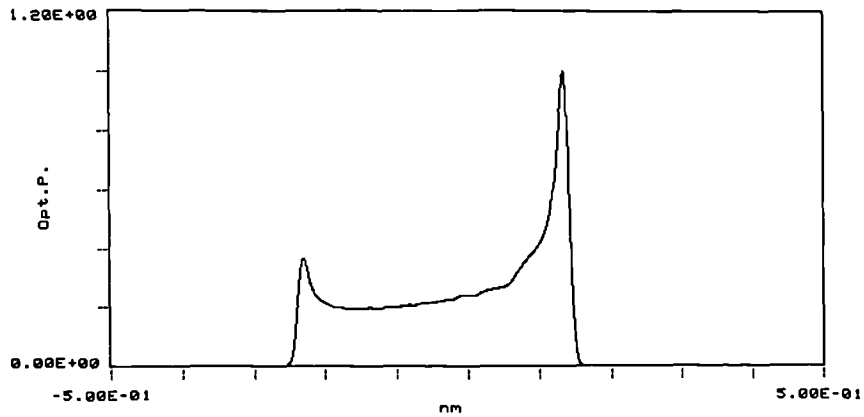

Fig.4.3 Optical Spectrum for Gain Switched DFB Laser

Since the wavelength chirp of the gain switched DFB laser shows a dominant linear component, dispersive pulse compression may be employed to reduce the optical pulse width, until the optical spectrum represents approximately the transform limit of the created time domain optical pulse [Takada, Sugie and Saruwatary]. Alternatively, optical filtering techniques may be employed to reduce the optical spectral width, again until the spectrum is approximately the transform limit of the optical pulse [Nakazawa, Suzuki and Kimura]. Whilst the dispersive pulse compression technique leads to short pulses of a few psec, the optical filtering approach results in near transform limited optical pulses of several tens of psec, and the choice of technique is therefore determined by the target pulse width required in any particular application.

An alternative optical source with built-in optical spectral control is the semiconductor mode locked laser (MLL). The addition to a standard laser chip of an external cavity with some optical frequency selectivity allows the generation of transform limited optical pulse trains, at pulse repetition rates in the region of one to twenty GHz. Descriptions of device operation and stability issues may be found in for example [Lowery and Marshall] and [Lowery, Onodera and Tucker]. Whilst a high degree of optimisation of the external cavity optical characteristics together with the semiconductor chip operating conditions is required for best performance, the laser does provide the facility to adjust the pulse temporal characteristics as well as signal operating wavelength. Similarly, the advent of highly efficient erbium doped fibre amplification permits the construction of a variety of

configurations of fibre model locked lasers, capable of high power, transform limited optical pulse generation. At high pulse repetition rates, however, the current lengths of the erbium fibre in the MLL necessitates laser operation at a high harmonic of the basic fibre laser mode locking frequency. Consequently a large number of independent, i.e. "time-interleaved" optical pulse trains are being generated, with the potential for insufficient pulse-to-pulse stability for data transmission system applications. Laser tuning techniques will have to be developed to allow laser operation synchronised to the required system line-rate, complemented by stabilisation techniques for achieving the required temporal and spectral pulse stability [Shan, Cleland and Ellis].

With all the above methods, the exact pulse shape and spectral characteristics are critically dependent on laser bias and modulation parameters, and on the correct alignment with additional external components. This makes the techniques useful for laboratory trials of high speed system configurations, whilst further development work is needed, such as full integration of all the components to reduce the need for precision external alignment and control, before they may be considered for real system applications.

IV.2.2 External Modulation

In Chapter II, the basic transfer function of a Mach-Zehnder intensity modulator and its use for standard external data modulation were summarised. However, it will be shown that external modulation may find applications far beyond the basic usage so far considered, and that it may form the basis for ultra-high speed optical pulse generation, optical signal conditioning and optical multiplexing beyond the capabilities of directly modulated semiconductor lasers. In particular, optical data generation and multiplexing are possible to optical line-rates 4 to 6 times higher than the highest electrical signal frequency employed anywhere in the system. This section provides an introduction to prepare for the subsequent multiplexing and system concepts under study here.

By applying a sinusoidal electrical drive signal to the modulator ($V_{pp} = V_{\pi}$, from fully "off" to fully "on"), at the system clock frequency for CW optical input, an optical

pulse train with a repetition frequency equal to the clock rate and a duty cycle of 50% is obtained. As in the case of bandwidth limited electrical data drive signals (Fig.2.5) the non-linear transfer function of the modulator results in optical output pulses with reduced rise and fall times, suitable for optical interleaving with a second channel (Fig.4.4).

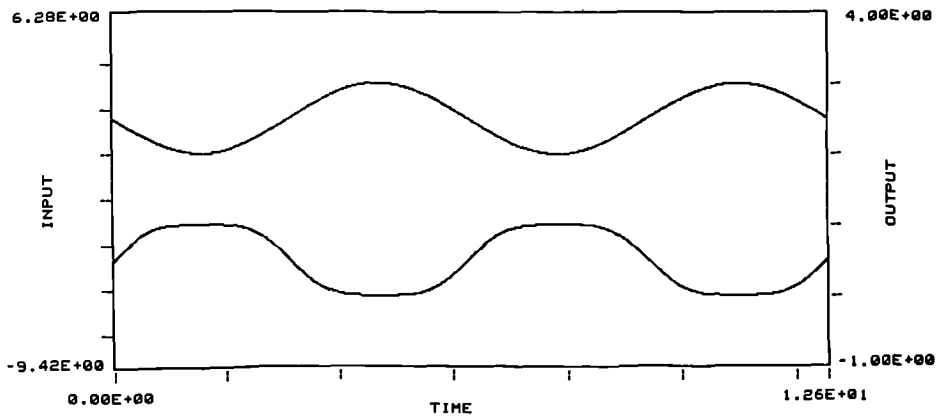

Fig. 4.4 Optical Modulator O/P for CW Optical I/P and Electrical Drive at $f=f_{clock}$, amplitude V_π, bias $V_\pi/2$ (time axis in radians).

By increasing the electrical drive level from $V_{pp} = V_\pi$ to $V_{pp} = 2 \cdot V_\pi$, and selecting a bias point of $V_{bias} = 0$ (fully "on"), during each cycle of the sinusoidal drive waveform the modulator is driven twice through the "on" position, resulting in a repetition frequency of the optical output pulse train of twice the frequency of the electrical drive signal (Fig.4.5) [Haus, Kirsch, Mathyssek and Leonberger]. Additionally, the non-linear transfer function provides for a duty cycle of the generated pulse stream of 0.33 (based on FWHM pulse width), thus enabling further time domain interleaving of such pulse trains to be carried out [Blank]. This mode of operation of a Mach Zehnder intensity modulator will form the basis for optical data generation at line-rates of upto six times the highest electrical signal frequency employed anywhere in the system, and it offers the potential for ultra-high speed signal generation employing trade-offs between maximum required electrical frequencies and maximum electrical drive levels.

Further reductions in the pulse width of the generated optical pulse streams can be realised by not restricting the electrical modulator drive signal to the fundamental frequency component. The addition of a small number of harmonics results in an electrical

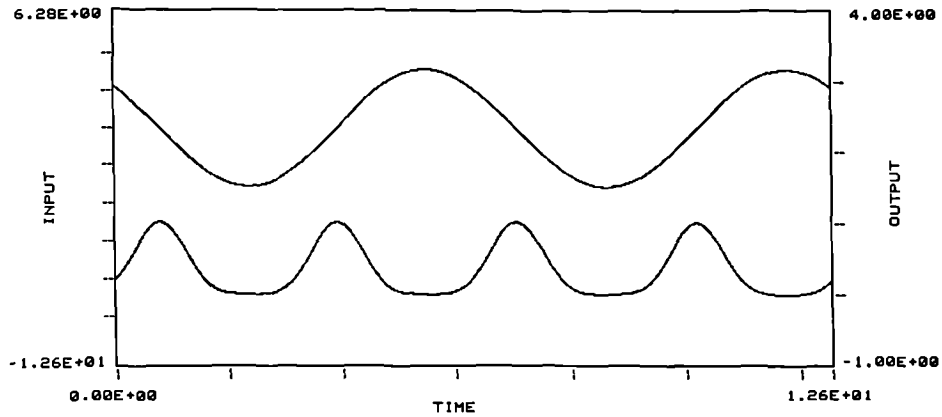

Fig. 4.5 Optical Pulse Train for CW Optical Modulator I/P, Single Frequency Electrical Drive at $V_{pp} = 2 \cdot V_{\pi}$, $V_{bias} = V_0$.

waveform with reduced rise and fall times, and if the modulator design is specifically optimised for fundamental plus harmonic operation (whilst maintaining the lowest possible switching voltage), operation at $2 \cdot V_{\pi}$ peak-to-peak drive level leads to a frequency doubled pulse repetition rate in conjunction with shortened optical pulse width.

If the fundamental frequency component plus a limited number of harmonic terms equal to the lower frequency components of a square wave signal are employed, the desired effect is obtained in principle. Fig.4.6 shows the case for inclusion of the $3 \cdot f_0$ and $5 \cdot f_0$ harmonics. However, the oscillations in the electrical drive waveform due to the missing higher order frequency terms lead to a deterioration of the optical extinction ratio, thus providing a source of strong channel crosstalk if several pulse trains were to be interleaved.

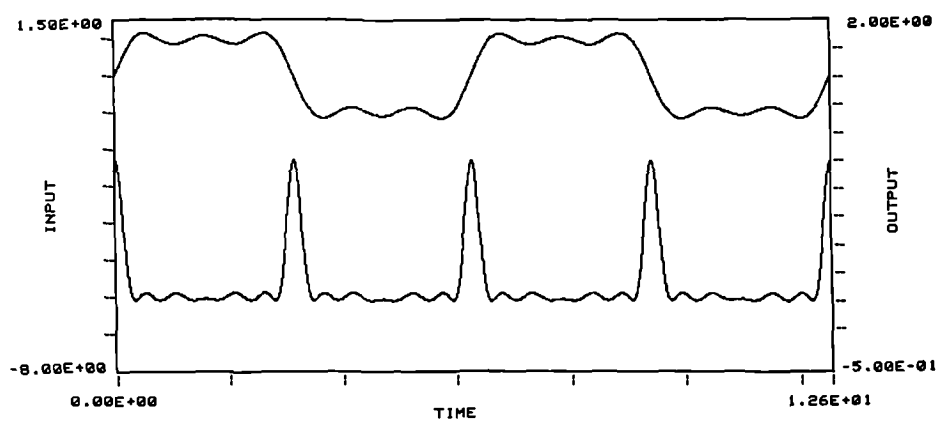

Fig.4.6 Electrical Waveform and Optical Output with $3 \cdot f_0$ and $5 \cdot f_0$ Harmonic Terms

Table 4.1 summarises the optical pulse width (relative to the pulse repetition interval) and the optical crosstalk levels for electrical drive signals as described above.

Frequencies ($/f_0$)	Rel.Amplitudes	Rel.Pulse Width	Crosstalk (dB optical)
1	1	0.333	---
1 + 3	1+0.33	0.131	-11.5
1 + 3 + 5	1+0.33+0.2	0.087	-14.5 (Fig.4.6)
1 + 3 + 5 + 7	1+0.33+0.2+0.14	0.068	-13

Table 4.1 Optical Pulse Width and Crosstalk Levels

In order to reduce the level of crosstalk, optimisation of the drive waveform is required by means of adjusting the relative amplitudes of the harmonic terms. Fig.4.7 shows the optical power waveform obtained for a modulator drive signal containing modified f_0, $3 \cdot f_0$ and $5 \cdot f_0$ harmonic terms. Optical extinction between the pulses is now −22 dB, whilst the relative optical pulse width is increased to 11% compared with the original 8.7%. Table 4.2 summarises the new operating conditions and the characteristics of the generated optical pulse trains, for up to 3 harmonic frequency terms in the electrical drive signal to the modulator.

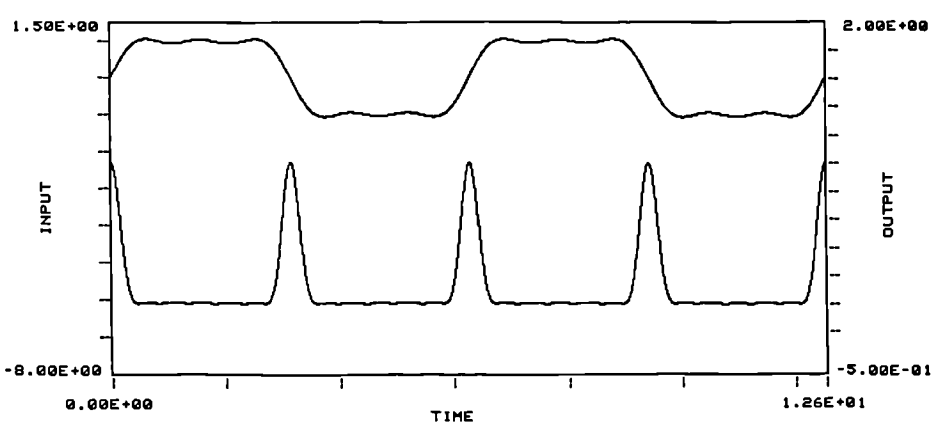

Fig.4.7 Optical Pulse Train for $2 \cdot V_\pi$ Electrical Drive with 3rd and 5th Harmonics with Optimised Amplitudes

Frequencies ($/f_0$)	Rel.Amplitudes	Rel.Pulse Width	Crosstalk (dB optical)
1	1	0.333	---
1+ 3	1+0.20	0.173	-24
1 + 3 + 5	1+0.28+0.12	0.111	-22 (Fig.4.7)
1 + 3 + 5 + 7	1+0.30+0.15+0.07	0.083	-23

Table 4.2 Optical Pulse Widths and Crosstalk Levels with Optimised Electrical Drive

The optical pulse widths of Table 4.2 suggest that the pulse trains will be suitable for optical interleaving of 3, 6, 8 and 12 channels, respectively. However, due to the particular pulse shapes under consideration, this would lead to a "bandwidth-limited" quasi-NRZ type line signal, whilst a more conservative approach of 2, 4, 6 and 8 channels, respectively, leads to a final line signal of RZ format, thus providing a degree of tolerance with regard to minor variations in the actual pulse width generated. If a full $2 \cdot V_\pi$ drive level is not realised, a reduction in duty cycle results, but most seriously, a considerable reduction is obtained in the optical on-off modulation ratio. Fig.4.8 shows the optical pulse train under electrical drive conditions as in Fig.4.7, but with a drive amplitude reduced to V_π . The resulting optical signal is unsuitable for optical multiplexing applications, due to the poor optical extinction ratio of only 2 to 1.

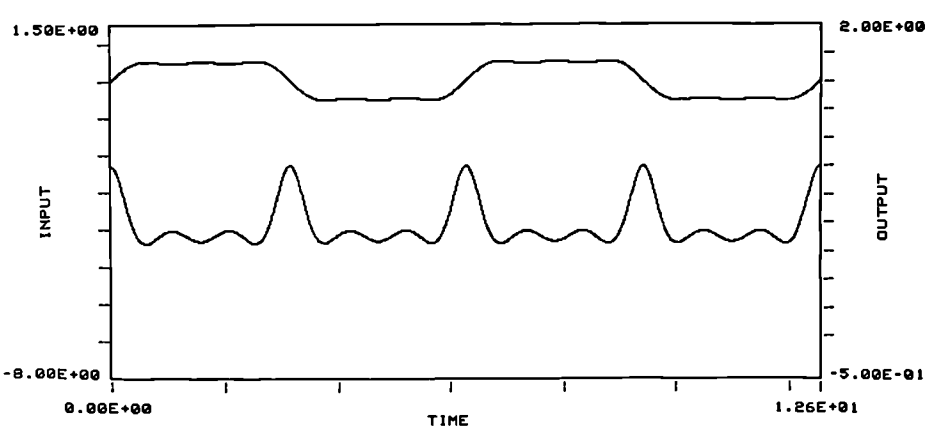

Fig.4.8 Operation with Reduced Electrical Drive Level

However, the situation may be improved considerably with the modulator bias adjusted from "on" to "off", thus guaranteeing maximum extinction at the expense of an additional effective device insertion loss (Fig.4.9). The resulting output signal shape may not be of interest for optical pulse generation, but is suitable for the implementation of optical gating and sequential optical signal processing, which will be considered in Section IV.4.

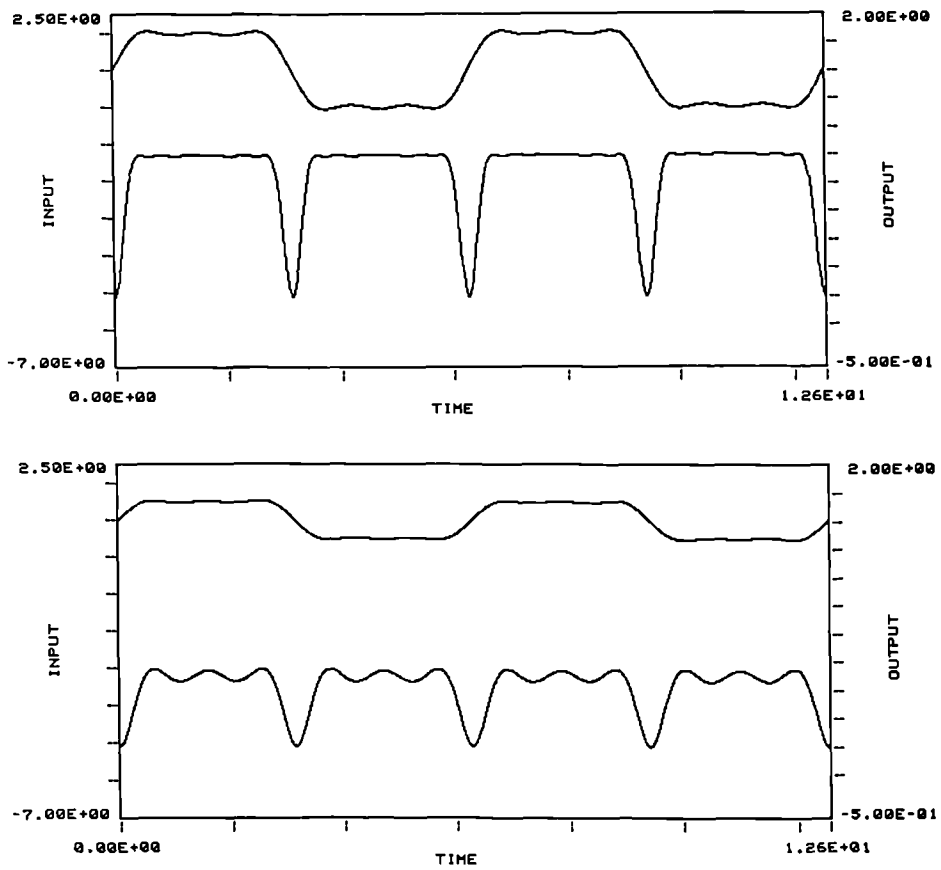

Fig.4.9 Optical O/P for Bias "off" : $2 \cdot V_\pi$ drive (upper), V_π drive (lower)

For single frequency electrical drive at $2 \cdot V_\pi$ amplitude, the result of frequency doubling combined with 33% relative width optical pulse generation is important in a systems context. In the case of $2 \cdot V_\pi$ modulator drive with additional harmonic terms as analysed above, the comparison has to be made with the electrical signal requirements for standard modulator operation in order to achieve equivalent optical pulse generation. Fig.4.10 depicts the electrical drive waveforms for V_π modulator drive (upper trace) and $2 \cdot V_\pi$ modulator drive (lower trace, Table 4.2, 4th option), in both cases for obtaining optical pulse trains suitable for subsequent 8-channel multiplexing (low duty cycle optical pulse

generation). Fig.4.10 then also displays the electrical drive signal spectra, clearly demonstrating that for $2 \cdot V_\pi$ operation (lower trace) not only the fundamental component is at half the frequency but that also only half the number of harmonic terms are required, thus placing far less stringent requirements on the frequency responses of the modulator and the drive electronics. Consequently, $2 \cdot V_\pi$ modulator operation offers considerable advantages not only for operation with single frequency electrical drive but also in the case of low duty cycle optical pulse generation. In the example given here, the reduction in the required modulator bandwidth of a factor of two also leads to to a reduced value of modulator V_π such that the resulting electrical drive amplitude becomes the same for both the V_π and $2 \cdot V_\pi$ system configurations, whilst the $2 \cdot V_\pi$ approach necessitates only half the drive electronic and modulator bandwidth.

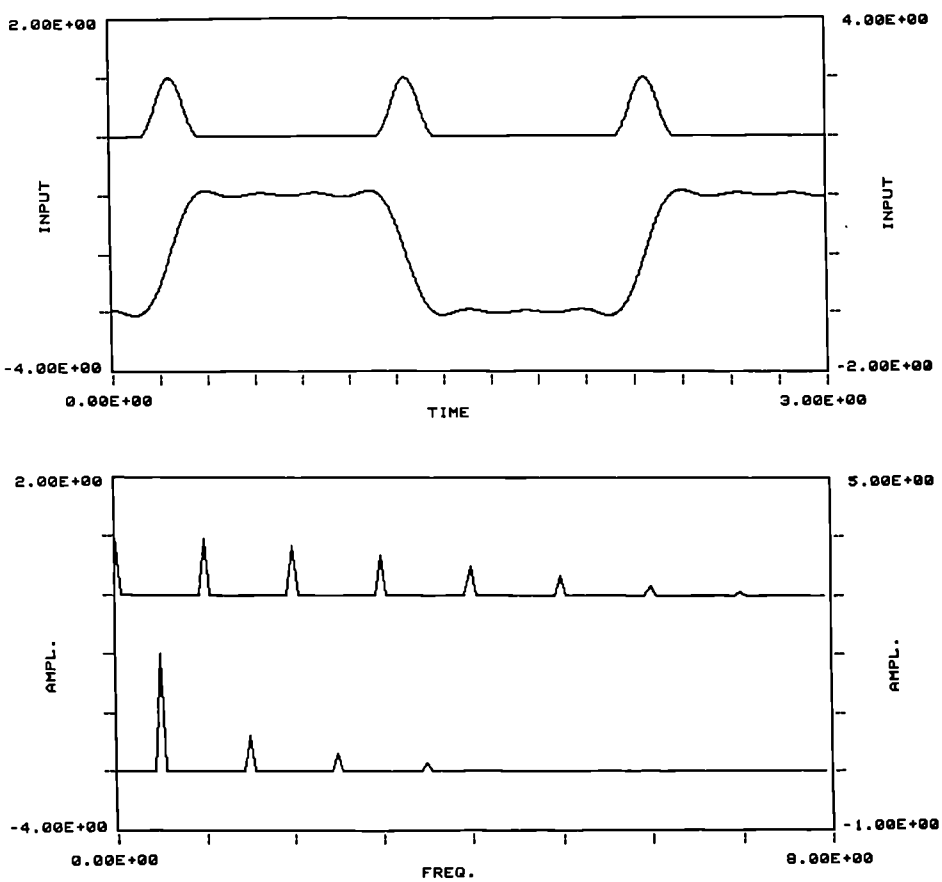

Fig. 4.10 Electrical Drive Waveforms (first graph) and Spectra (second graph) for Low Duty Cycle Pulse Generation, with V_π drive (upper traces) and $2 \cdot V_\pi$ drive (lower traces)

IV.2.3 Optical Angle Modulation

Section III.4 described the use of direct laser frequency modulation with subsequent optical demodulation for low chirp optical data modulation at system speeds approaching the maximum small signal modulation bandwidth of the laser diode. Only under special circumstances, however, is this technique equivalent to ideal intensity modulation as obtainable from a Mach-Zehnder opto-electronic modulator, whilst in the general case the optical data thus created contains some wavelength chirp. In the context of repetitive optical pulse generation, however, this approach may be employed for the generation of optical pulse trains with characteristics similar to ideal external modulation as analysed in IV.2.2 above. The aim is to provide a sinusoidal variation of the differential optical phase at the output signal combiner of the interferometer. This can be obtained by sinusoidal phase modulation of a CW optical carrier, followed by a Mach-Zehnder (MZ) interferometer with differential path delay τ equal to one half of the period of the optical input signal phase modulation ($\tau = 1/(2 \cdot f_c)$) [Shirasaki, Nishimoto, Okiyama and Touge]. In a similar way low duty cycle optical pulse generation may be obtained through optical phase modulation with fundamental plus harmonic electrical drive signal components. The advantage of such a configuration is that an optical phase modulation of a peak-to-peak amplitude of $\pi/2$ is required in order to obtain a differential phase shift of π at the interferometer output, representing a factor of two improvement compared with the operation of a MZ intensity modulator. Consequently, if an electro-optic phase modulator is employed for the generation of the phase modulated CW signal a fourfold reduction in electrical drive power is achieved compared with the intensity modulator of IV.2.2. This is a considerable advantage, especially in the case of frequency doubled pulse generation, requiring $2 \cdot V\pi$ drive to the intensity modulator but only $V\pi$ drive to a phase modulator followed by an interferometric delay demodulator.

Alternatively, direct laser phase (frequency) modulation may be employed, followed by the same delay demodulator with $\tau = 1/(2 \cdot f_c)$. Given a laser frequency modulation

sensitivity of η_{fm} (in MHz/mA), an electrical modulating signal s_e leads to sinusoidal optical phase modulation $\Phi(t)$:

$$S(t) = S_0 \cdot \cos(\omega_0 \cdot t + \Phi(t))$$

with

$$\Phi(t) = 2\pi \cdot \eta_{fm} \cdot \int_0^t s_e(t')\, dt'$$

and

$$s_e(t) = s_{e0} \cdot \cos(\omega_s \cdot t)$$

or

$$\Phi(t) = 2\pi \cdot \eta_{fm} \cdot 1/\omega_s \cdot s_{e0} \cdot \sin(\omega_s \cdot t) \qquad (4.1)$$

Equation 4.1 allows the necessary electrical drive level ($\pm s_{e0}$) to be determined for achieving a required peak optical phase modulation. For example, a typical DFB laser FM modulation sensitivity of 500 MHz/mA at 10 GHz modulation frequency requires a value for s_{e0} of 15.7 mA to achieve a peak-to-peak phase modulation of $\pi/2$. After the delay demodulator this provides for an optical pulse train as with V_π modulation of the Mach-Zehnder modulator, or $V_\pi/2$ drive to the phase modulator and delay demodulator combination. With currently available electro-optic device technologies the electrical drive signal requirements are considerably reduced in the case of the direct laser PM modulation approach. In a 50 Ω microwave environment, at 10 GHz drive frequency, the required ± 15.7 mA laser drive corresponds to 1.57 V_{p-p} drive voltage, compared with approximately 5 V_{p-p} for $V_\pi/2$ drive of a current $LiNbO_3$ phase modulator of suitable characteristics, or 10 V_{p-p} for V_π drive of an equivalent Mach-Zehnder intensity modulator, all of which result in the same optical output signal. The limitations to practically achievable speed of operation are given in the case of electro-optic modulators by the large electrical drive power requirements at multi-GHz signal frequencies and in the case of direct laser modulation by the detrimental effects of increasing residual amplitude modulation for high frequency phase modulation. The main difficulty of operating a "long" interferometer with optical phase or frequency modulation of the optical source is the tight control required over the differential path delay. As with a standard MZ interferometer it relies on the optical coherence between the two paths at the output signal combiner, but it employs an

optical path length difference between the interferometer arms which is orders of magnitude larger than in a MZ modulator. As a result, accurate dynamic interferometer path length or optical signal frequency control is required to overcome environmental effects on the laser source and interferometer.

In conclusion, a range of devices and modulation techniques has been described for the generation of short optical pulses, in preparation for an investigation into optically multiplexed ultra-high capacity transmission systems. In particular, the use of direct laser gain switching and $2 \cdot V_{\pi}$ drive of Mach-Zehnder modulators both result in the generation of short optical pulses with selectable duty cycles, depending on the exact drive and bias conditions. The requirements for sources of well defined short optical pulse trains as a basic building block for ultra-high capacity systems may thereby be satisfied.

IV.3 DATA MODULATION

The limitations of employing directly modulated single frequency laser diodes and the potential advantages of external modulation have been described in Chapter III. Whilst the use of external modulation may lead to chirp-free (transform-limited) optical pulses and thus allows a considerable extension of the system dispersion limit, the advantage is obtained at the expense of stringent practical device operating requirements. At line-rates above a few Gbit/s the modulator drive power required with present technologies is increasingly large. Alternatively, for a given limited electrical modulation power the achievable device extinction ratio may be compromised as a result of not turning the modulator fully off, or alternatively the effective device insertion loss increases considerably if the modulator bias is adjusted to ensure a high extinction ratio and consequently is never switched fully on. At system speeds beyond 10 Gbit/s the electronic multiplexing of the tributary data channels itself becomes a major problem.

Consequently, for single channel externally modulated system applications of conventional design (CW laser, electrical TDM data applied to the modulator), a system

approach will be of importance which minimises the modulator drive power requirements and maybe also leads to optical output data with reduced optical bandwidth for increased system path dispersion capability. Such system configurations will be investigated in IV.3.1.

For ultra-high speed system operation beyond the speed capability of electrical multiplexing equipment and broadband optical modulators, optical time division multiplexing of individual RZ data streams requires the generation of optical RZ modulated data streams. In this case optical modulation is required only upto the highest electrical interface line-rate. Again, techniques are sought which minimise the electrical bandwidth and power requirements. For the analysis of two fundamentally different approaches to the problem of combining the processes of short optical pulse generation and data modulation, in preparation for subsequent optical interleaving of all the tributary data streams, the common starting point shall be the same as in electrical TDM: N electrical data channels of line-rate $B_0 = 1/T_0$ (T_0 being the bit-interval) are assumed to be available in NRZ format and are to be multiplexed to form a new bit stream of line-rate $B_N = N \cdot B_0$ with a new bit-interval $T_N = T_0/N$. Three alternative approaches will be investigated for conversion of the electrical NRZ input data into optical RZ pulse streams of suitable characteristics :

a) Standard electrical-to-optical conversion is carried out at the tributary line-rate B_0 (standard transmitters, Sections II.2 and II.3), and is then followed by processing in the optical domain to convert the optical NRZ data to RZ format, in preparation for subsequent interleaving of all N tributary optical RZ channels.

b) Direct conversion from electrical NRZ to Optical RZ is effected by means of a single Mach-Zehnder electro-optic modulator.

c) An optical pulse train is generated at a pulse repetition frequency equal to B_0 (see above), followed by external modulation to impress the electrical data information onto the pulse train ("gating" of the optical pulses).

These three approaches will be analysed in detail in IV.3.2, IV.3.3 and IV.3.4, respectively, with the main aim being the identification of transmitter configurations which maximise the achievable line-rate whilst simultaneously minimising the electrical signal bandwidths and drive powers.

IV.3.1 External Modulation with Reduced Bandwidth Drive

At high bit-rates the electrical drive power requirement for external modulation becomes a major issue. As an example, currently available travelling-wave electro-optic modulators (Lithium Niobate, KTP, Polymers, etc.) typically have a V_π switching voltage of 3 to 4 V for 4 GHz bandwidth, rising to approximately 10 V peak-to-peak modulation signal for 10 GHz bandwidth devices. The increase at higher speeds is a result of the shorter (travelling wave) electrodes required for higher bandwidth modulator operation in order to keep the walk-off between the electrical signal and the optical signal to an acceptable level. Even optimised novel modulator structures still require drive levels well beyond the signal level capability of digital high speed circuitry. As the device switching voltage increases approximately linearly with the modulator bandwidth, the drive power requirement for full on-off digital modulation increases as the square of the device bandwidth, posing a major problem for the provision of broadband electronic drive circuitry for the modulator. Consequently, any system design approaches which minimise the device bandwidth requirements are of considerable interest.

For single channel systems, the modulator bandwidth may be halved by employing three-level duobinary signalling in the electrical path to the modulator. Through an appropriate choice of the bandwidth of the electrical drive amplifier plus the modulator electrode transfer function, the standard NRZ electrical input data can be converted into duobinary electrical data. The optical output signal may then also be of duobinary form, with the optical waveform a reshaped replica of the effective electrical modulator drive signal due to the non-linear transfer function of the MZ modulator. Alternatively, the same electrical duobinary data signal may be converted back into a two-level optical signal

by means of a suitably modified modulator bias point. Both approaches are potentially of interest in a systems context and are analysed below in detail.

Optical Duobinary Data Generation:

The use of multi-level signals is well known in the context of high capacity transmission systems, as for example summarised in [Bruce Carlson]. With optical transmission, however, the availability of what used to be viewed as "unlimited" transmission bandwidth has resulted in the main research and development efforts being directed towards increasing binary system speeds and improving path loss capability. To this extent, the advantages to be gained in terms of receiver noise performance have been analysed for duobinary optical signal detection [O'Mahony (2)] and for combined duobinary signalling and Decision Directed Feedback equalisation [O'Reilly, Duarte and Blank], [De Oliveira Duarte]. The results demonstrate that some improvements in receiver sensitivity may be obtained when the receiver noise is dominated by high frequency noise terms. With transmission limits now being approached in terms of high capacity binary optical signalling over dispersive propagation paths, coding and modulation techniques which offer bandwidth efficient channel utilisation may find applications in the field of optical transmission.

In the context of this work, three level signalling will be investigated as a means of relaxing the transmitter modulator specifications as well as improving long distance high capacity transmission system performance. With the same assumptions as in Section II.3 (modulator frequency response included in the electrical drive bandwidth for convenience of modeling), a limited electrical signal bandwidth of approximately one quarter of the signal clock frequency (-3dB bandwidth), or as a specific example a raised cosine frequency spectrum appropriate to one half the actual data rate, will result in a standard duobinary and bandwidth limited effective signal pulse shape (Fig.4.11, first graph). The non-linear MZ modulator transfer function leads to a reshaping of the three-level pulse train as shown in Fig.4.11. Some variation in the exact pulse shape may be obtained through the precise choice of the electrical filter function. However, the optical pulse shape remains

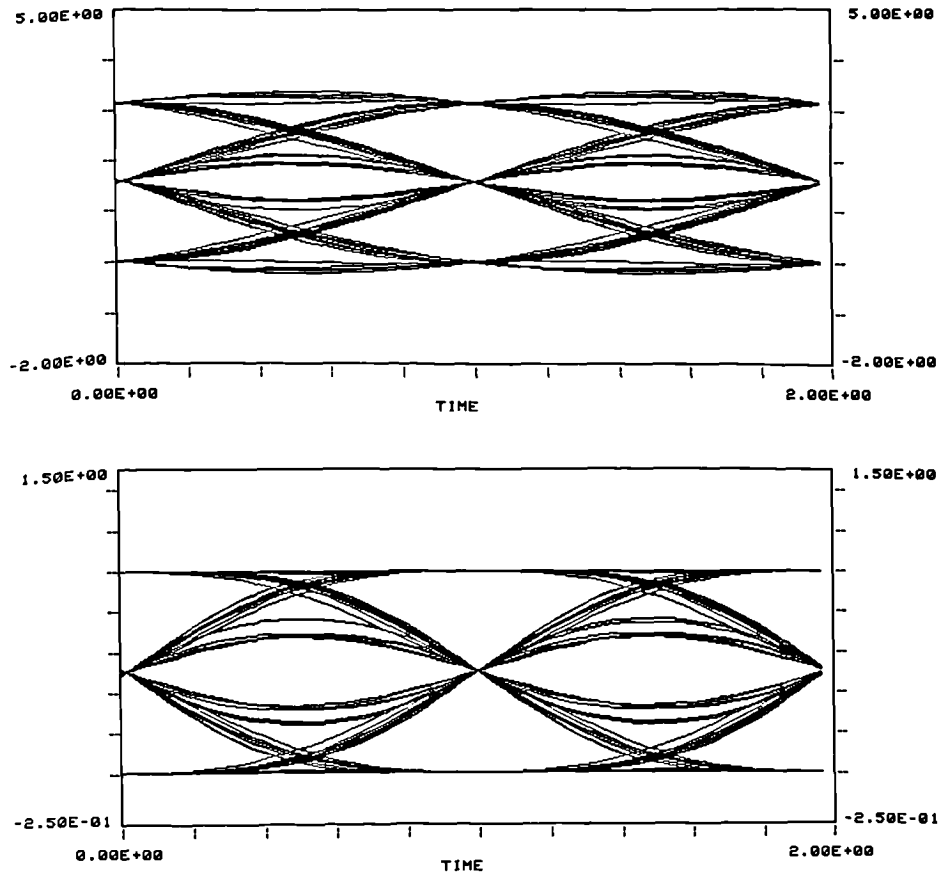

Fig.4.11 Generation of Optical Duobinary Signal :
Electrical Input 'Eye' Diagram (upper), Optical Output 'Eye' Diagram (lower)

dominated by the modulator non-linear electro-optic transfer function as long as no harmonic frequency terms are contained in the electrical drive spectrum.

The three-level optical signal benefits from a substantially narrower optical spectral width compared with its two-level counterpart for the same data-rate, and therefore a distinct increase in the fibre chromatic dispersion limited maximum transmission distance may be achievable. This will be investigated further in Chapter V.

Electrical Duobinary Data Converted Into Optical Binary Format:

The approach described above combines the advantages of low electrical bandwidth requirement (leading to low modulator drive power) with a narrow optical bandwidth of the generated three-level line-signal. For applications where the three-level line-signal is not acceptable, a change to the modulator bias from the usual mean level (around which

the ac-coupled electrical modulating signal operates) of "half-on" to either fully "off" or fully "on" leads to the demodulation of the three-level signal back to a standard binary optical line-signal. In this operating mode advantage is taken of the repetitive electro-optic transfer function of a Mach-Zehnder modulator as well as its non-linear transfer function. At the expense of suitable precoding of the data the original data pattern is recreated in the optical domain, although a modulator and electrical drive circuit with only half the usually required bandwidth are employed, resulting in substantially reduced electrical drive power requirements.

Fig.4.12 depicts the varying signal waveforms from the original electrical data signal through the coder, the bandwidth limiting modulator drive circuit, and finally the optical data signal, as a correct reproduction of the original electrical input data sequence. Issues of concern are the effective device insertion loss, the optical extinction ratio achievable, and the detailed optical pulse shape, all as a function of the modulator bias and the peak-to-peak electrical modulation amplitude.

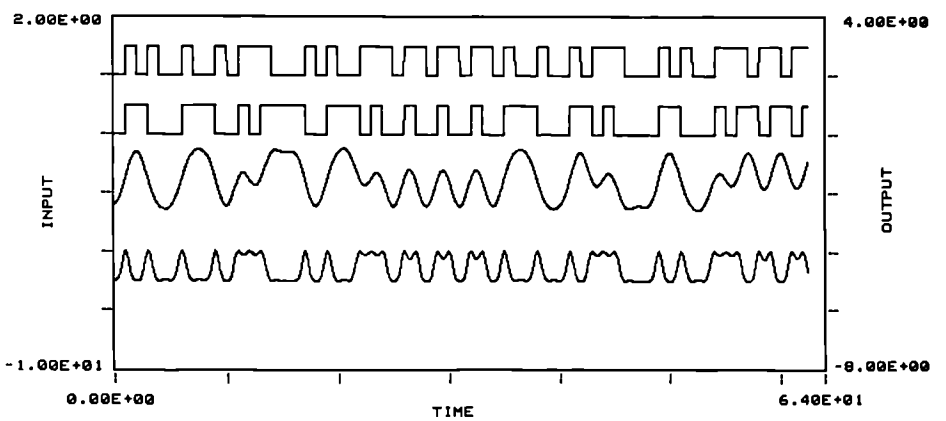

Fig.4.12 Pulse Shapes through the two/three/two-level transmitter configuration (Data; Coded Data; Three-Level Electrical Signal; Decoded Two-Level Optical Data)

In order to analyse which particular settings are of practical interest the overall performance is now considered as a function of the electrical data drive level applied to the modulator:

- *Full $2 \cdot V_\pi$ peak-to-peak signal amplitude:* the choice of mean modulator bias point is between "on" and "off" (V_{bias}= V_0 or V_π), resulting in either the original data or the inverted data in the optical domain. No extinction ratio penalty and no additional "functional" device insertion loss is introduced beyond the basic fibre-to-fibre loss of the modulator. The electrical precoded and filtered three-level data 'eye' diagram (raised cosine frequency spectrum filter at half the data line-rate) is of the same shape as in Fig.4.11, the difference being a doubling of the peak-to-peak amplitude and a shift in the mean bias level from $V_\pi/2$ to V_0 or V_π (fully "on" or fully "off") . The resulting decoded optical data 'eye' diagrams are shown in Fig.4.13.

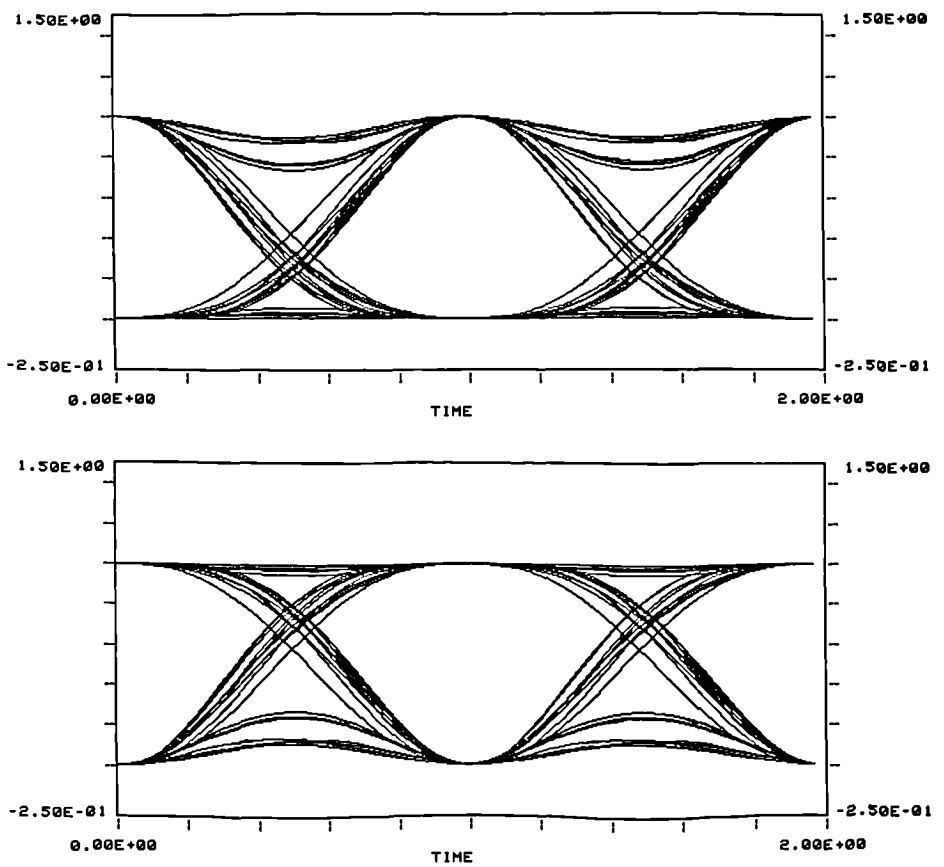

Fig. 4.13 Demodulated Optical 'Eye' Diagrams: Bias V_0 (upper), Bias V_π (lower)

- *Less than $2 \cdot V_\pi$ modulation amplitude:* only a mean modulator bias at the "off" position allows a good optical extinction ratio to be achieved. For V_π data amplitude, 'eye' diagrams are obtained as shown in Fig.4.14, with either a 3 dB reduction in the peak optical signal level ("off" bias), or the emergence of a poor extinction ratio in

addition to the same 3 dB reduction in modulated signal level ("on" bias). Whilst a 3 dB reduction in signal level might be acceptable in a system context, the poor extinction ratio with an "on" bias would in most cases be unacceptable. Further reductions in the electrical 3-level signal amplitude only lead to minor additional changes in the output optical pulse shape. However, due to the non-linear modulator transfer function, a rapid increase in the effective additional device insertion loss results or a further deterioration of the optical extinction ratio.

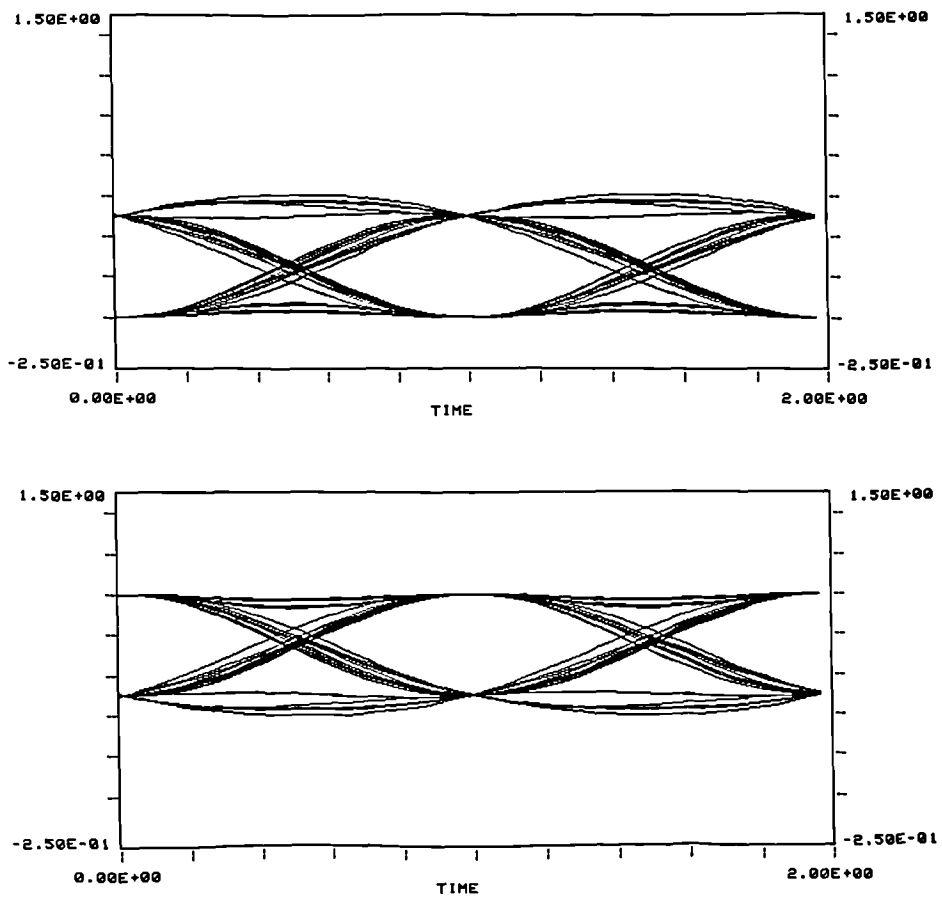

Fig.4.14 Electrical data amplitude V_π: Bias V_π (upper) and Bias V_0 (lower)

When analysing the overall performance achievable with a mean modulator bias in the "off" position, allowance needs to be made for a finite maximum extinction ratio of the basic MZ modulator itself, such as for example 20 or 30 dB (optical). Any reduction in the peak transmitted optical signal level then in turn also leads to a deterioration of the

achievable optical extinction ratio of the optical data. Fig.4.15 shows the effective additional device insertion loss and the maximum achievable optical extinction ratio as a function of the electrical signal peak-to-peak amplitude, for basic modulator device extinctions of 10, 20 and 30 dB (optical). From the graph it is clear that in order to make use of the advantages of low electrical bandwidth which generates the opportunity for low electrical modulator drive power, the effects on effective optical insertion loss and achievable optical extinction ratio need to be taken into account.

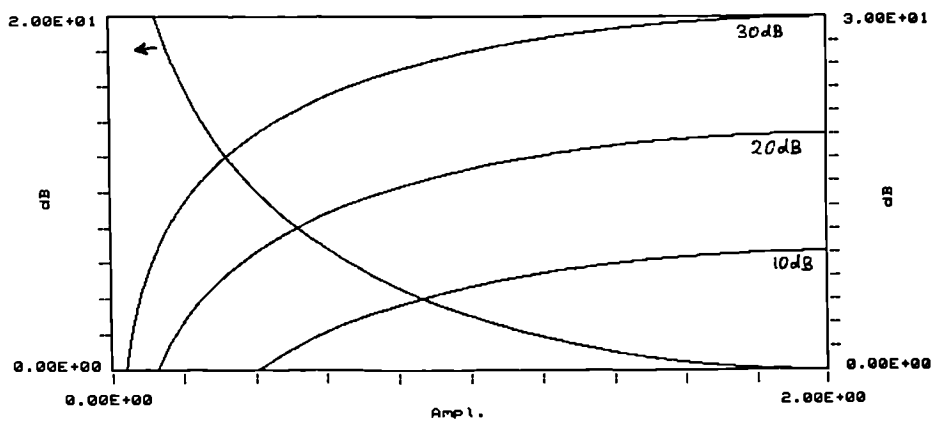

Fig. 4.15 Excess Insertion Loss (left hand y-axis) vs Drive Amplitude (0 to $2V_\pi$), Effective Optical Extinction Ratio (right hand y-axis) vs Drive Amplitude, for Device Extinction Ratios of 10, 20 and 30 dB optical.

It is imperative that the electrical drive peak-to-peak amplitude does not fall below the modulator V_π value in order to avoid a large excess optical insertion loss as well as significant deterioration in the optical extinction ratio, especially with limited basic device extinction. With an electrical peak-to-peak amplitude of $\frac{1}{2} \cdot V_\pi$, the additional optical insertion loss is $\approx$ 8.3 dB, and the optical extinction ratio falls to $\approx$ 1.7 dB for a device extinction ratio of 10 dB, to $\approx$ 11.7 dB for a 20 dB device, and to $\approx$ 21.7 dB for a 30 dB device. Effectively, the value of the additional optical loss due to the incomplete switching of the MZ modulator is equal to the reduction in achievable optical extinction ratio (in optical dB). Consequently, the use of a high extinction ratio modulator (better than 30 dB) together with optical amplification for overcoming the additional insertion loss

the incoming data, with the gating shape determined by the bias and drive level of the electrical control signal as discussed in IV.2.2. In particular, a sinusoidal electrical modulator drive signal of V_π amplitude at the clock rate of the input optical NRZ data leads to a Return-to-Zero (RZ) output data format, with a pulse width equal to 50% of the bit-interval and with an "almost" square pulse shape, as per Fig.4.4. An electrical modulator drive level of $2 \cdot V_\pi$ around an "on" mean bias modulator point, at half the data clock frequency, leads to an optical output RZ data stream with a pulse width of 33%, of shape as in Fig.4.5. Cascading of two such stages, the first operating at V_π and f_{clock}, the second at $2 \cdot V_\pi$ and also at f_{clock} results in optical pulse narrowing to 50%, followed by subsequent narrowing to 16.5%, suitable for interleaving of a total of 4 to 6 channels (see below for further details).

The alternative approach of non-sinusoidal electrical drive signals (i.e. fundamental plus harmonics) has been described in IV.2.2 for optical pulse generation and is of particular interest in this context. A fixed input channel line-rate of NRZ or 50 % RZ format may be the starting point, with the requirement for an optical output pulse width depending on the number of channels to be multiplexed. In contrast to the single frequency electrical modulator drive descibed above, where multi-stage processing is required if a substantial reduction of the pulse width is to be achieved, a suitably chosen fundamental electrical drive frequency, combined with the appropriate number of harmonic frequency terms as described in IV.2.2 allows single-stage optical processing from optical NRZ data input format to low duty-cycle optical RZ output format.

In addition to providing the required optical pulse narrowing, the use of the optical modulator "gate" may give the additional benefit of laser wavelength chirp reduction for high capacity data generation and propagation. At modulation speeds upto Gbit/s data rates the wavelength chirp of directly modulated DFB laser diodes may be mainly confined to the initial part of each optical pulse, where on switch-on considerable ringing of the optical waveform is accompanied by large wavelength variations. By adjusting the timing of the optical sampling process such that only the later part of the pulse is sampled, the excessive optical bandwidth associated with the front part of the optical pulses can be

removed. In Fig.4.16 the spectrum of a DFB laser modulated directly with 3 Gbit/s NRZ data shows the typical broadening due to wavelength chirp. Subsequent simultaneous processing of two such pulse streams in a 2x2 optical switch, which was driven electrically at 3 GHz with V_π peak-to-peak amplitude, resulted in the NRZ-to-RZ optical gating function on each optical input signal followed by pulse train interleaving. The spectrum of the output signal shows the removal of the excess optical bandwidth of the original 3 Gbit/s input data. Fig.4.16 demonstrates clearly the principle of combined optical pulse shortening and optical spectral narrowing, resulting in transform-limited optical signal generation at high speed optical line-rates based on standard, chirped optical input data streams.

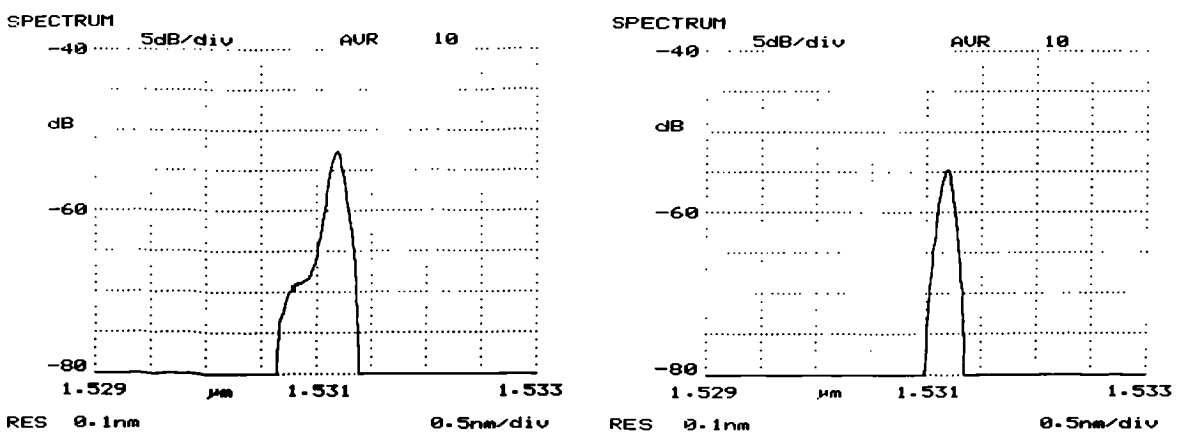

Fig. 4.16 Optical Spectra: Chirped 3 Gbit/s NRZ Data (left),
Chirp-free 3 Gbit/s RZ Constituent of 6 Gbit/s NRZ Data (right).

IV.3.3 Electrical NRZ to Optical RZ Conversion

One of the techniques described in IV.2.2 for the generation of short optical pulses can be extended to simultaneous optical pulse generation and data modulation. Fig.4.5 and Fig.4.6 showed the resulting optical pulses for single frequency and for fundamental plus harmonic electrical drive respectively, of amplitude $2 \cdot V_\pi$ around an "on" modulator bias point. The result was frequency doubling as well as RZ optical pulse generation, with the

pulse width depending on the slope of the electrical drive waveform around the mean signal level. If on the other hand the electrical data stream is precoded, such that the electrical waveform applied to the modulator changes level when a digital "1" is to be transmitted and remains at its current level for a digital "0", then direct optical RZ pulse modulation is achieved, with the pulse width determined by the slope of the electrical drive signal at the transition point as in the case of the frequency doubled optical pulse generation of IV.2.2. Specifically, sinusoidal electrical signal waveforms will result in 33%

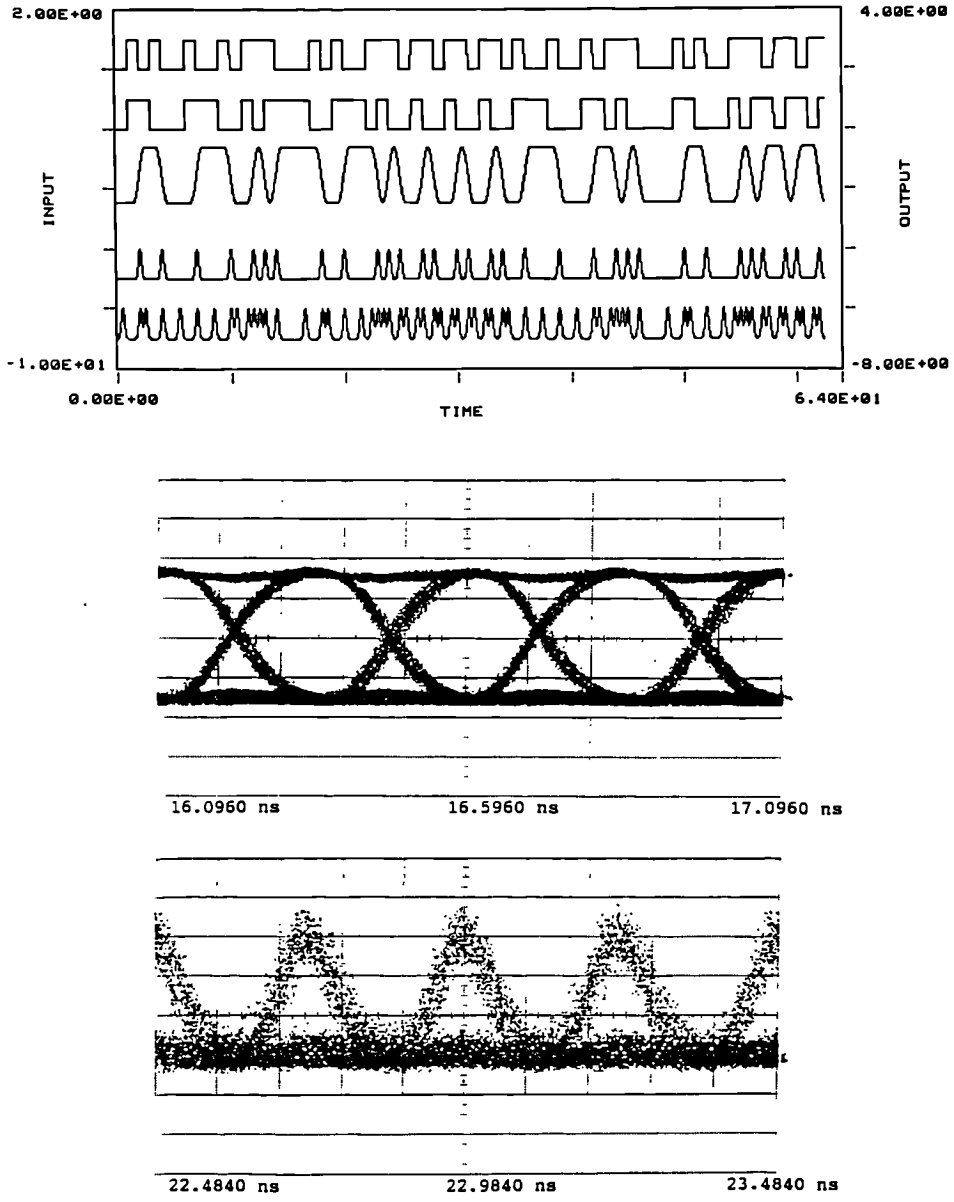

Fig.4.17 Optical RZ from Electrical Bandwidth Limited NRZ Data.
Top: Data/Coded Data/Modulator Drive/Optical Output Signal/2–Channel Multiplex.
Middle: Experimental 'Eye' Diagram, Electrical Drive at 4 Gbit/s NRZ.
Bottom: Experimental 'Eye' Diagram, Optical Output Signal at 4 Gbit/s RZ.

duty cycle optical pulses, just as in the case of high speed optical pulse generation based on single frequency $2 \cdot V_{\pi}$ electrical drive. The first graph of Fig.4.17 shows a full sequence of signal shapes, starting with the digital input data, followed by the coded data, the raised cosine frequency spectrum bandwidth limited electrical drive signal, and then the resulting optical output data pulse train. The fifth and final trace depicts the optical signal after a 2:1 time domain multiplexing operation of two such channels (time interleaving of two separate channels), demonstrating how the modulation process has resulted in RZ optical pulses derived from bandwidth limited NRZ input data, suitable for two-channel multiplexing / interleaving without further optical processing. If the bandwidth of the electrical coded and filtered data signal is twice the value of that in Fig.4.17, optical pulses with 16.5% duty cycle are generated, suitable for subsequent interleaving of at least 4 optical channels. Fig.4.18 summarises the resulting signal shapes, including the final optical signal after interleaving of two channels, showing continued RZ format suitable for further multiplexing. Such multiplexing issues will be discussed further in Section IV.4.

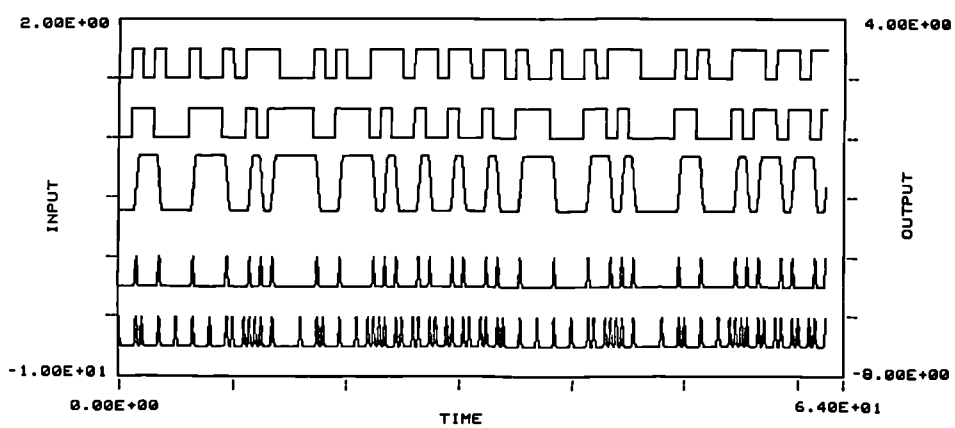

Fig. 4.18 Optical RZ from Electrical NRZ Data (traces as in Fig.4.17)

Also of interest is the case of opposite modulator bias. With the average bias value set to V_{π}, data inversion and at the same time inversion of the optical signal shape is obtained. The resulting optical output signal shows a Return-to-One (RO) format instead of the standard Return-to-Zero (RZ) (Fig.4.19). Whilst the data inversion may be dealt with in the electrical precoding stage, the optical pulse shape inversion will find applications in high bit-rate optical multiplexing in Section IV.4.

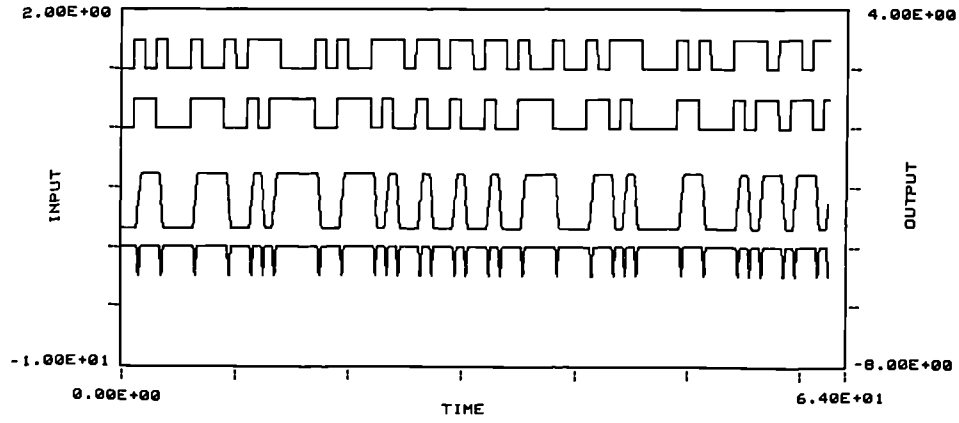

Fig.4.19 Optical "Return-to-One" from Electrical NRZ Data.

IV.3.4 External Modulation of Pulsed Sources

Having investigated options for efficient optical NRZ-to-RZ conversion of standard format optical data (ready for subsequent optical multiplexing) and the simultaneous generation and data modulation of low duty-cycle RZ optical data from NRZ electrical data, this section will now be concerned with efficient electrical data modulation of low duty-cycle optical pulse trains. Fundamentally this will be based on the same principles as established in IV.3.1 for data modulation of a CW optical carrier. Now the CW carrier is replaced with a synchronised optical pulse source of suitable characteristics, and the data modulation process takes the form of a "pulse gating" operation. In the limiting case of an optical pulse width substantially shorter than the data bit-interval, the exact optical gating window shape is of little importance, as long as the window is either fully open or fully closed for the duration of the short optical input pulse. If, however, the optical pulse width is non-neglegible compared with the bit-interval, some shaping of the optical pulse will take place in addition to the data modulation process itself, since the MZ modulator in effect multiplies the optical power waveform with the effective gating waveform. Consequently the analysis in IV.2.2 and IV.3.1 with regard to electrical to optical waveform conversion applies in this context directly. In particular, standard electrical NRZ modulation, electrical duobinary signal modulation with automatic demodulation in the modulator, and differentially encoded NRZ data drive for achieving short optical gating

windows (IV.3.3) may all be employed, depending on the system requirements.

Under such circumstances the aim is to minimise the electrical data modulation requirements, whilst the use of a separate optical pulse source permits the provision of optimised pulse characteristics suitable for subsequent multiplexing and dispersive fibre propagation. Consequently, it is important to identify the maximum optical pulse width which does not suffer unduly from optical pulse shape changes due to the chosen data modulation process.

With standard electrical data drive to the modulator, even when electrically filtered down to a minimum bandwidth such as the raised cosine frequency spectrum, a well opened data 'eye' diagram is obtained (flat top and bottom) due to the MZ nonlinear transfer function. Consequently, an optical pulse source with pulse widths less than one half the bit-interval (50 % duty cycle) will not be subjected to any significant pulse shaping during the data modulation process. However, the bandwidth and power efficient data modulation approaches analysed above lead to narrower optical "gating window" shapes. In the following a brief summary of the performance of the main combinations of optical pulse source and data modulation approaches of practical interest will be presented.

Electrical Duobinary / Optical Binary Data Modulation :

With a duobinary electrical data drive to the modulator of $2 \cdot V_{\pi}$ peak-to-peak amplitude a modulation 'eye' diagram results in the optical domain as shown in Fig.4.12. Replacing the CW optical input with a 50 % duty cycle optical pulse source (sinusoidal

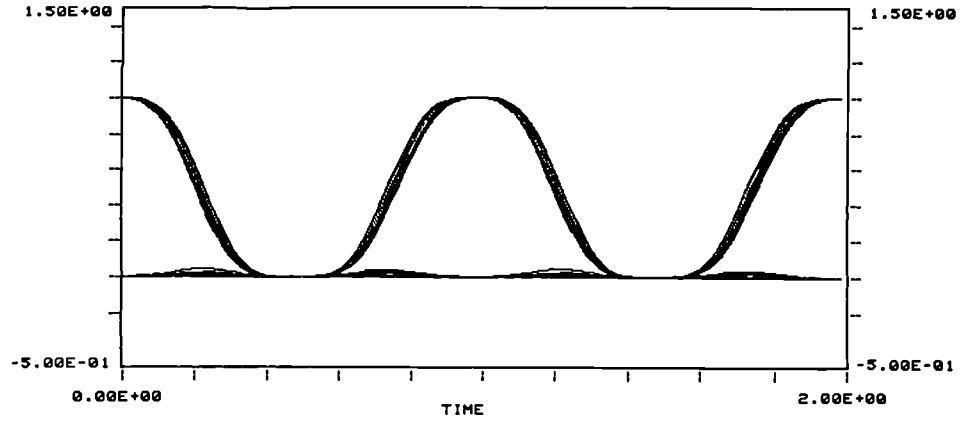

Fig.4.20 Optical Data 'Eye' Diagram for 50% Duty Cycle Input Pulses

electrical modulator drive at f_c, amplitude V_π), the resulting optical data 'eye' diagram takes the form shown in Fig.4.20. Clearly visible is some pulse width modulation as a consequence of the interaction between the data modulation and the shape of the incoming optical pulses. By changing the optical pulse source to 33 % duty cycle ($2 \cdot V_\pi$ modulator drive at $f_c/2$), only a minor amount of pulse shaping remains (Fig.4.21). Therefore, optical pulses with a duty cycle of no more than 0.3 will allow duobinary electrical data modulation to effectively result in a pure optical gating process, with the data modulated optical pulse characteristics solely determined by the optical pulse source employed.

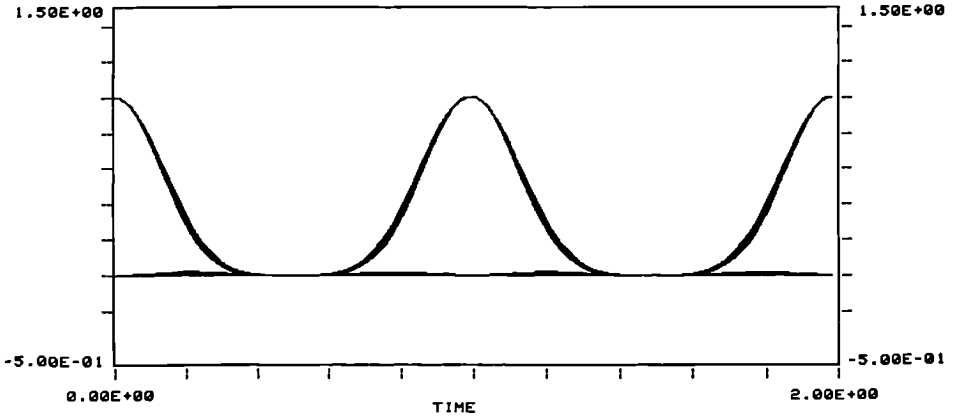

Fig.4.21 Optical Data 'Eye' Diagram for 33% Duty Cycle Input Pulses

If the electrical amplitude of the duobinary data modulation is reduced to V_π as in Fig.4.14 (upper), the level of data dependent pulse shaping increases for a given optical input pulse width due to the changed optical gating window width under these operating conditions. An analysis of the overall performance for various configurations reveals that the duty cycle of the input optical pulse train should now be no more than 20 % as obtained for example with pulse generation listed as the second option in Table 4.2.

Three-Level Optical Data Generation :

In Section IV.3.1 the generation of three-level optical data was investigated by means of duobinary filtering of the electrical data, followed by standard bias and drive level of the Mach-Zehnder modulator. As in the above examples for binary optical data modulation, the modulation process may be employed to "gate" a low duty cycle input

pulse train. The main difference in this case, however, is the generation of a three level RZ signal. Whilst the optical modulation waveform at the "1" and the "0" levels is well suited as a gating function (remaining either fully "on" or fully "off" for a large percentage of the bit-interval), the "½" level features either a rising or falling "gating waveform". Fig.4.22 shows the resulting output 'eye' diagram for a 50 % duty cycle input pulse train. Severe patterning occurs for the "½" level pulses.

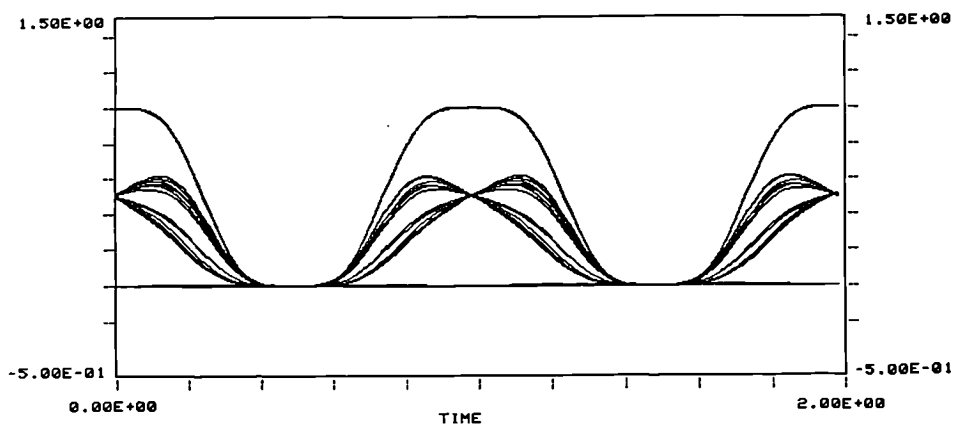

Fig.4.22 Optical Output for Three-Level Optical Modulation as in Fig.4.11, with 50% Duty Cycle Input Pulses.

The situation is considerably improved for optical input pulses of 17 % duty cycle (Table 4.2, 2nd option), with a reduced but still clearly visible level of data dependent pulse shaping at the "½" level (Fig.4.23).

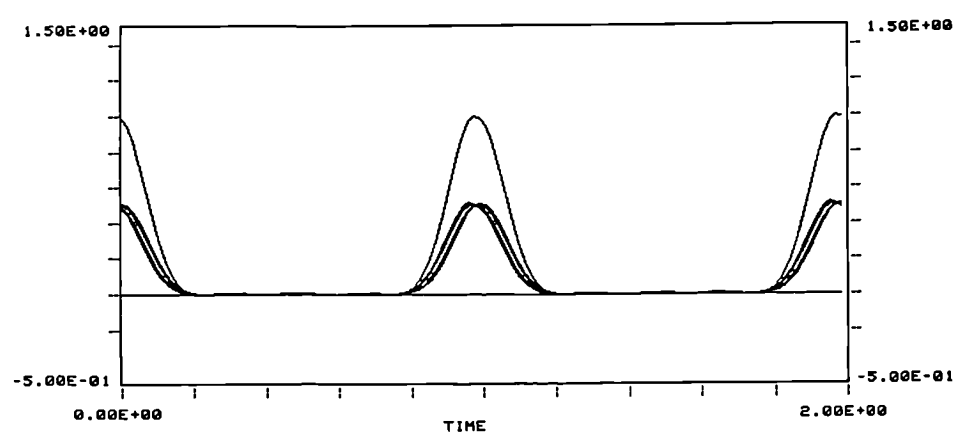

Fig.4.23 Optical Output for Three-Level Optical Modulation as in Fig.4.11, with Optical Input Pulses as per 2nd Option, Table 4.2 .

The pulse shaping effectively leads to a small amount of pulse position modulation (left / right from the centre position in the bit-interval by ± 1.6%). Further reductions in the relative pulse width down to ≈10 % (e.g. Table 4.2, third option, Fig.4.7) then limit this pulse position modulation to approximately ±0.6 % of the bit-interval, a level at which it is unlikely to cause problems.

However, due to the RZ nature of the resulting three-level pulse train, and the loss of the correlation between adjacent pulses once optical interleaving with other channels has taken place, little advantage would be gained as far as the optical spectral width of the generated data is concerned, and thus no benefit will be gained in the context of dispersive fibre transmission. This approach is therefore only of interest if advantages can be identified in the optical receiver/post-detection processing after optical demultiplexing back to the original "duobinary RZ" signal.

Optical "Return-to-One" Data Modulation :

At the end of Section IV.3.3, Fig.4.19 demonstrated the effect of adjusting the modulator bias level from "on" to "off" when the operating conditions are optimised for electrical NRZ to optical RZ conversion. The resulting optical Return-to-One modulation format leads in the context of low duty cycle pulse train data modulation to individual pulse re-shaping but this time for the "unwanted" pulses. The narrow width of a "0" data waveform is likely to lead to incomplete suppression of the incoming pulse unless the optical pulse is substantially shorter than the data modulation window. Fig.4.24 shows the resulting 'eye' diagram for data modulation and optical input pulses with both approximately 17% width relative to the bit-interval, i.e. $2 \cdot V_{\pi}$ drive with a 3rd harmonic term for the optical pulse generation, and data modulation according to Fig.4.19. The potential benefit of operating such a configuration is its ability to selectively modulate one time slot in N, with the other N-1 pulse positions unaffected by the processing in the selected channel. Potential applications for this approach will be described later in this chapter.

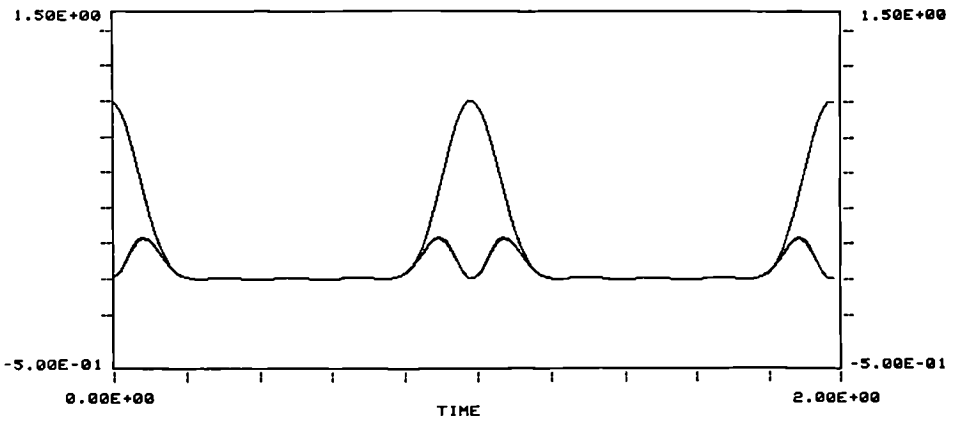

Fig.4.24 Return-to-One Data Modulation applied to a Low Duty Cycle Optical Input Pulse Train

In order to achieve better extinction of the remaining two small pulses for "zero" data, the input optical pulse width needs to be substantially reduced. As an example, if it is halved (Table 4.2, 4th option), the optical extinction improves from approximately −6.5 dB (relative peak level of the residual pulses in Fig.4.24) to −12.5 dB. Also visible in Fig.4.24 is a small amount of crosstalk signal in between the selected pulse positions, due to the finite extinction in the optical pulse generation process as discussed in IV.3.3. The relative importance of these two main sources of channel crosstalk (namely optical pulse source characteristics and the performance of the data modulation process) in an optical multiplexing context will differ depending on the exact system configuration.

IV.4 OPTICAL MULTIPLEXING AND DEMULTIPLEXING

In the previous sections a number of techniques have been developed for the generation of data modulated return-to-zero optical pulse streams. The remainder of this chapter will now be concerned with multiplexing of tributary optical data streams, and with the question of subsequent optical demultiplexing of the resulting ultra-high speed OTDM signals for the recovery of the original data channels.

IV.4.1 Optical Multiplexing

Optical Time Division Multiplexing (OTDM) of a number of tributary data channels may be implemented in a variety of ways, and it is therefore useful to first identify the main options for the format of the ultra-high speed optical data stream. The system requirement may be to provide optical data in the currently most widely employed Non-Return-To-Zero (NRZ) format. Alternatively, an individual pulse shape with a FWHM value less than the bit-interval may be acceptable, resulting in an "almost Return-to-Zero" line-format. Finally, for some system applications such as ultra-long distance non-linear data transmission, non-linear optical pulse propogation (soliton transmission) may require an RZ signal format with a low duty cycle of typically less than 20%. In the following, three basic configurations will be analysed, based on the optical pulse generation and data modulation approaches described earlier in this chapter.

Option 1 : Active Multiplexing based on Optical Switches and Modulators

So far in this chapter the Mach Zehnder electro-optic intensity modulator has been the basis for the high speed optical signal processing studies. However, the somewhat more complicated 2 by 2 directional coupler electro-optic switch shows the same electro-optic transfer function as the MZ modulator, but with the advantage of two optical inputs and two outputs. Consequently, if used with one optical input signal only, one of the optical outputs will provide the same signal as a single-input MZ modulator whilst the second output shows the inverted optical signal. With the second optical input available, either Input 1 is connected through to Output 1 and Input 2 to Output 2 (for 0 V electrical signal), or alternatively Input 1 is linked to Output 2 and Input 2 to Output 1 (V_π electrical signal). Thus one 2x2 switch may fulfill simultaneously the functions of NRZ-to-RZ conversion of two NRZ optical input channels, plus optical interleaving of the two data streams to form an NRZ output line signal at twice the data rate of the individual channels, for example at Output 1. Output 2 is then available as a monitor port, to ensure correct phasing of the optical input channels and the electrical drive signal

to the switch. The electrical signal need only be of sinusoidal form, at the clock frequency of the input data channels. Four channel OTDM multiplexing may then be carried out by repeating the same operation at the higher data rate, requiring a switch with electrical sinusoidal drive of twice the original tributary data clock frequency (or half the final multiplexed optical data clock frequency) for the second level 2:1 multiplex. A detailed discussed of the configuration is provided in [Blank]. The line signal 'eye' diagram after a complete four channel multiplexing operation is shown in Fig.4.25. The shape of the optical data at both the 2:1 and 4:1 level is determined by the combination of sinusoidal electrical switch drive and the non-linear electro-optic transfer function (Fig.4.4), thus providing for a final NRZ format optical line signal suffering from no intersymbol interference at the center of the bit-intervals, and only minor patterning near the bit-interval edges. Additional advantages in the context of input data pulse streams with optical wavelength chirp were identified in IV.3.2, Fig.4.16.

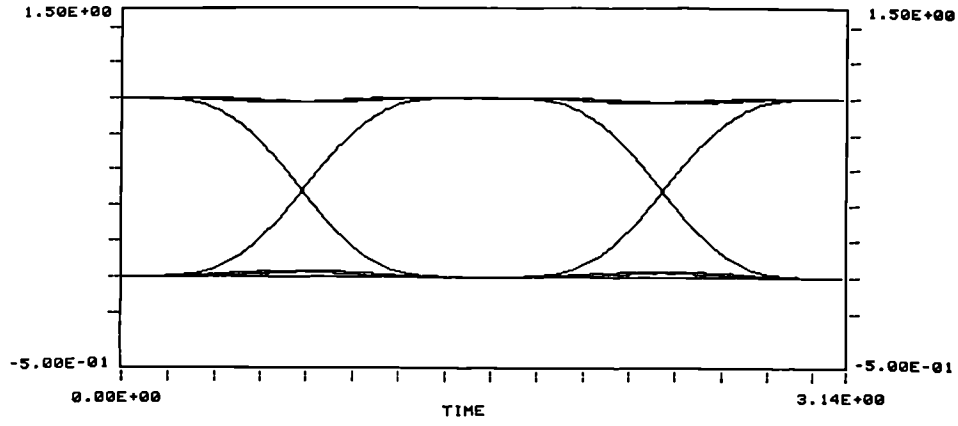

Fig. 4.25 Four-Channel Active Multiplexing With 2x2 Optical Switches

If however the requirement is for the electrical control signals in the multiplexer not to exceed the clock frequency of the optical input data, only the first level 2:1 multiplexing process is implemented with 2x2 switches, with the resulting output signals individually converted from NRZ to RZ format via $2 \cdot V_{\pi}$ drive operation of MZ modulators, as described in IV.2.2, Fig.4.5, followed by passive interleaving to form the 4:1 multiplexed optical line signal [Blank]. The resulting 'eye' diagram for the full multiplexer is shown in Fig.4.26, again demonstrating that the pulse shape is determined by the optical

multiplexing action, since it is identical to the signal shown in Fig.4.5 for straight optical pulse generation. Fig.4.26 also provides experimental verification of the second level signal shaping and subsequent interleaving process to a final data rate of 16.6 Gbit/s. The 'eye' diagram shows some slight bandwidth limitation compared with the computed result due to an optical detection and oscilloscope display bandwidth of 18 GHz.

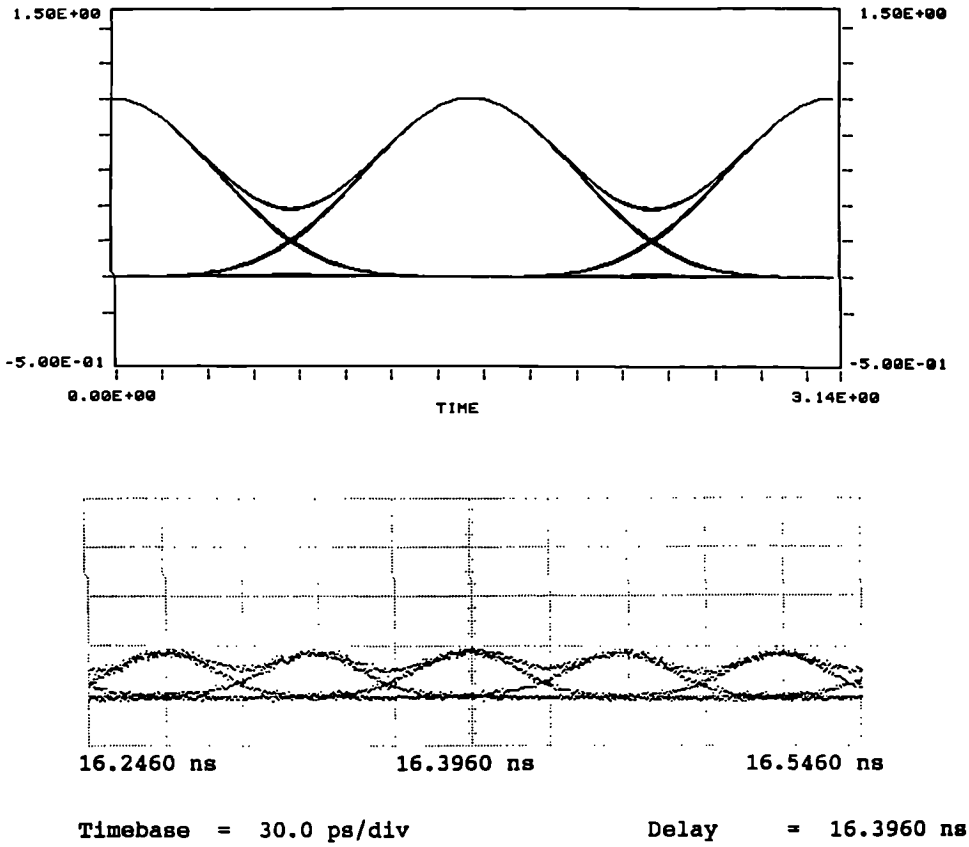

Fig.4.26 Four Channel Active Multiplex with Minimum Electrical Drive Frequencies and Experimental Verification at a Multiplexed Line Rate of 16.6 Gbit/s

Option 2 : Passive Multiplexing of Optical Input Channels

If the tributary optical data channels are available in low duty cycle RZ format, through either of the techniques discussed earlier in the chapter, then passive interleaving of suitably phased optical channels leads directly to the desired full line-rate multiplexed optical signal. Whilst in Option 1 above the active switching element ensured that the level of intersymbol interference between multiplexed channels is kept to a minimum

(determined only by the particular switch operating condition chosen and the switch extinction ratio), passive interleaving of a large number of channels (e.g. 4 or 16) relies on the quality of all the contributing optical input channels. Consequently, the maximum number of channels which may be combined depends not only on the Full Width Half Maximum (FWHM) value of the optical pulses but also on the particular pulse shape. While Fig.4.26 depicts the output line signal for a four channel multiplexing operation, six input channels containing identical pulses may be interleaved by appropriate phasing to provide a bandwidth limited NRZ format, at the expense of some intersymbol interference.

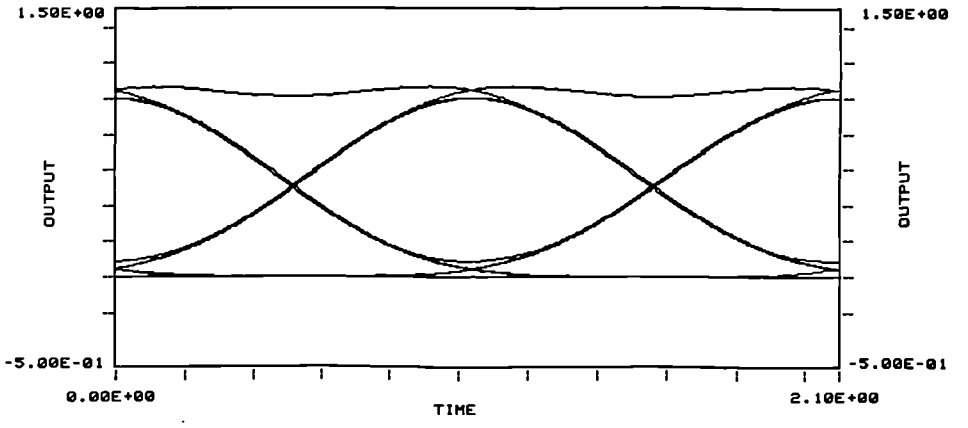

Fig. 4.27 Six–Channel Optical Multiplex based on Optical Pulses as in Fig.4.26

A detailed analysis of how closely channels can be aligned as a function of the detailed pulse shape will be carried out in Chaper V.

Option 3 : Sequential Multiplexing (Electrical Input – Optical Output)

In Options 1 and 2 above the multiplexing operation is based on N individual tributary optical input channels of either NRZ or RZ format. Alternatively, a single source of optical pulses at a repetition frequency of $N \cdot f_0$, i.e. the full system line–rate, may be followed by "modulation" stages which each carry out the data modulation of one of the N time slots. Fig.4.28 depicts the optical modulation waveform 'eye' diagram for electrical drive to the modulator as in Fig.4.19, and the output signal 'eye' after one modulation stage with an optical input pulse train at the full line–rate (N = 4).

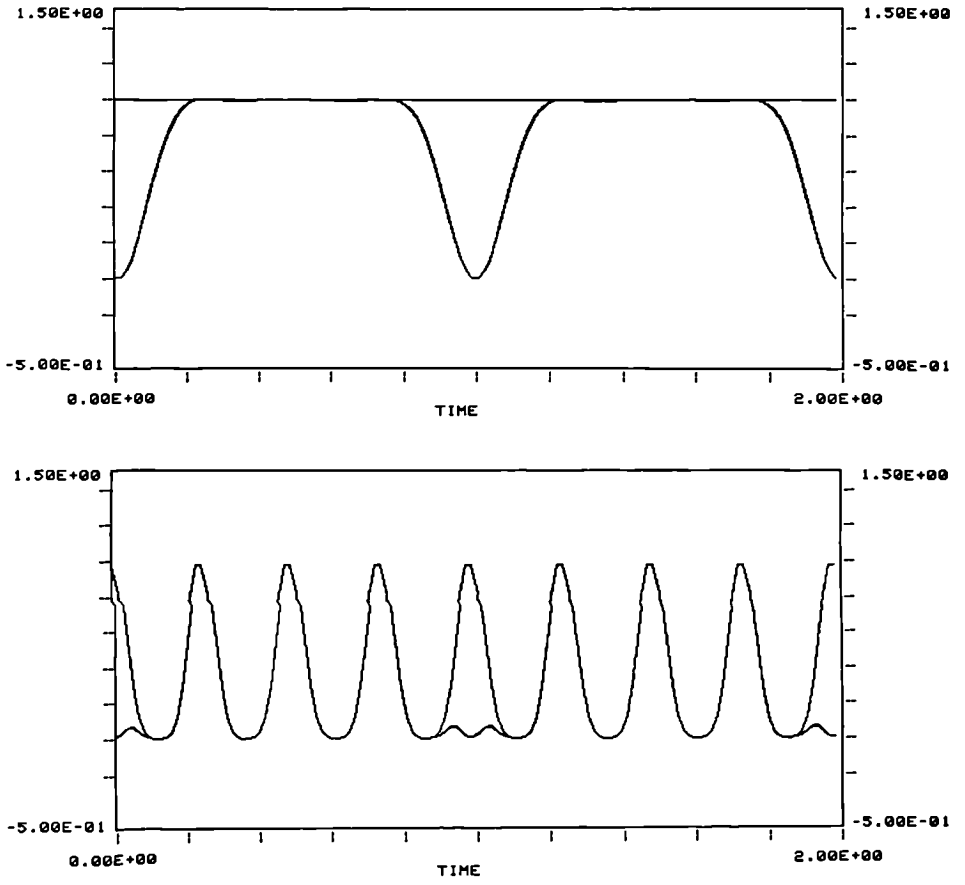

Fig.4.28 Optical Modulation 'Eye' Diagram (upper)
and Line Signal 'Eye' Diagram after One Multiplexing Stage (lower).

Subsequent multiplexing stages will modulate the remaining N–1 channels. The main advantages of this configuration are firstly that only one optical pulse source is required, and secondly that equal signal amplitudes are guaranteed for all channels. The use of one single optical source facilitates operation in for example a bus or ring configuration, where the modulating stages or tributaries are at separate locations. With operation according to Option 1 or Option 2 above, each tributary either needs to derive its optical carrier signal from a common source in order to guarantee close matching of optical frequencies for subsequent fibre propagation – practical only if at the same location – or has to provide a separate optical source with accurate local control over its characteristics. The second advantage of guaranteed equal pulse amplitude in all the channels (assuming equal modulator operating conditions) may be of particular advantage in applications where fibre non–linearities cannot be neglected, such as in high signal power transmission over

extended fibre distances, thus requiring identical pulse amplitudes in order to avoid differing optical pulse propagation behaviour between the different channels. In both basic configurations, namely the tree-structured multiplexer based on 2x2 switches or the sequential multiplexer, particularly suited for distributed processing, the number of electro-optic switches/modulators is identical, and the main differences are in the end-to-end signal attenuation through the full N channel multiplexer, and in the electrical data signal requirements. The difference in processing insertion loss may be considerable for larger numbers of channels, with the optical source signal having to pass through $\log_2 N$ switches in the first case, but N modulators in the second. Typical individual device insertion losses of 5 dB (optical) therefore will result in a difference of 25 dB between the two approaches, for an eight channel system. At this level, careful positioning of the optical amplification stages would be required in order to avoid system penalties due to a deteriorating optical signal-to-noise ratio throughout the processing structure.

IV.4.2 Optical Demultiplexing

Having achieved efficient optical multiplexing of a number of tributary data channels, the objective of the optical demultiplexing process -whether in one location or distributed- is to recover a representative version of the individual tributary input data with again a minimum requirement on electrical bandwidth. In contrast to the multiplexing process which may be carried out passively or actively, demultiplexing requires active processing to separate the channels, resulting in optical output signals of RZ format. The main performance measurements of an optical demultiplexing configuration are the maximum speed of operation, the level of data patterning after a channel has undergone a complete multiplex-demultiplex cycle, and the level of interference from adjacent or possibly even all other N-1 data channels. Due to the availability of optical amplification, the demultiplexing architecture is not strongly constrained by device insertion or signal splitting losses, and overall system optimisation may concentrate on the time domain performance of any particular configuration, in particular the resulting signal shapes and the levels of

intersymbol interference between the channels.

Two main demultiplexer configurations are of interest. Firstly, the multiplexing configuration of Option 1 above may be operated with the optical signal travelling in the opposite direction, resulting in the demultiplexing of the N channel OTDM signal back into its constituents. However, depending on the exact configuration, pulse width modulation will occur, leading to data patterning. Also, the sinusoidal electrical drive signal to the switches or modulators allows only a 1 into 2 demultiplexing process at each stage. Thus for N channels, $\log_2 N$ processing stages are required to access any particular channel. Secondly, as an alternative option sinusoidal electrical drive with harmonic frequency terms, of between V_π and $2 \cdot V_\pi$ amplitude, allows direct access to any particular level of the multiplexed hierarchy, and most importantly, direct access to the individual optical channels.

Option 1 : Sinusoidal Electrical Control Signals

The switch and modulator configurations refered to in the multiplex Option 1 above are without further modification suitable for implementation of the demultiplexing function, with the optical signals propagating through the configuration in the reverse direction.

However, the cascade of optical "time windowing" functions of identical shape and width in the multiplexer and demultiplexer may lead to data patterning, as demonstrated in Fig.4.29 for the calculated output 'eye' diagram of one channel after a complete 4:1 - 1:4 multiplexing and demultiplexing operation. Assumed are 2x2 optical switches with V_π amplitude control signals throughout (see Fig.4.25 for the multiplexer output only). The pulse width modulation or patterning results from the NRZ format of the multiplexed optical signal, combined with a sampling function of equal FWHM value. Consequently the end-to-end performance may be improved by employing lower duty cycle optical pulses at the multiplexer output, and/or with lower duty cycle sampling windows in the demultiplexer. The second configuration of the multiplexer Option 1 provides some reduction in the generated output pulse width and consequently improves the situation if employed as demultiplexer, due to the $2 \cdot V_\pi$ electrical drive to the highest speed optical

processing stages. The resulting end-to-end performance of a complete Mux-Demux based on such a configuration is also shown in Fig.4.29, with much reduced data patterning in terms of residual pulse width modulation and interference from adjacent channels.

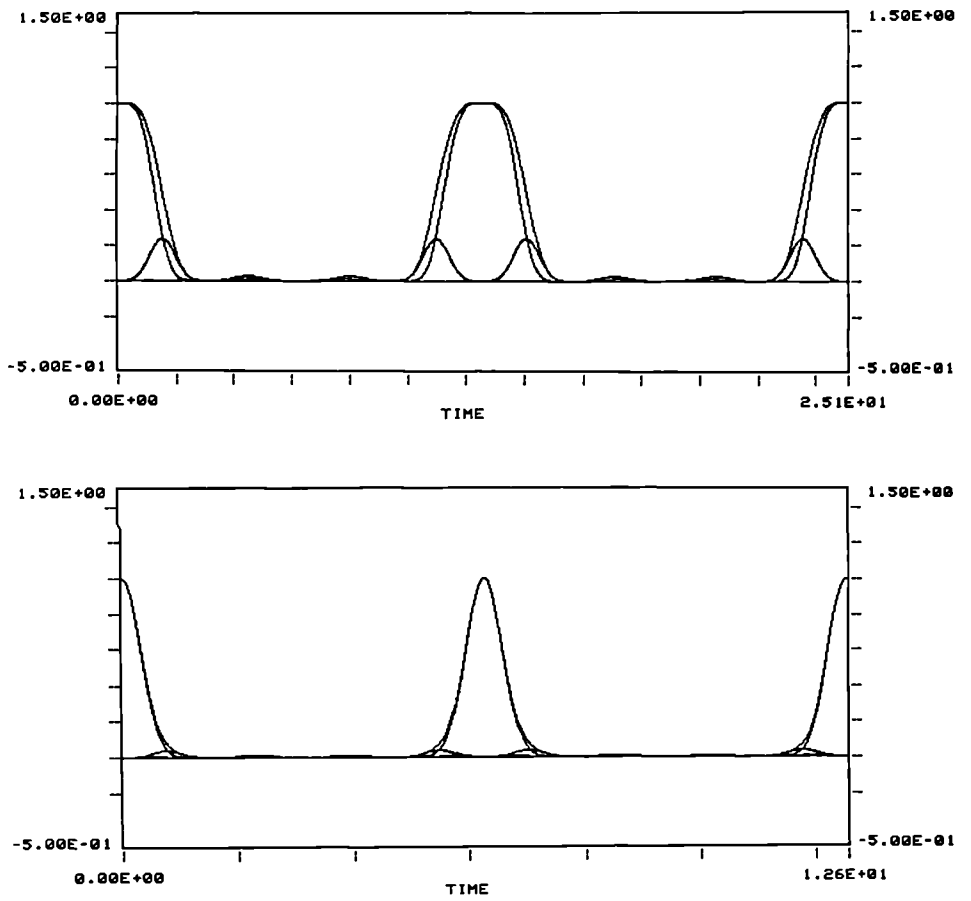

Fig. 4.29 4-Channel Mux-Demux based on 2x2 Optical Switches with V_π Drive (upper), 4-Channel Mux-Demux with minimum Electrical Drive Frequencies (lower).

Experimental verification of the latter demultiplexing approach has been obtained in the context of 20 Gbit/s linear and non-linear fibre transmission system experiments [Wickens, Spirit and Blank, (1) and (2)], in which four 5 Gbit/s RZ optical data channels were multiplexed through passive interleaving and then demultiplexed after fibre propagation with 5 GHz, $2 \cdot V_\pi$ and V_π amplitude sinusoidal electrical drive to the two demultiplexing stages ($LiNbO_3$ travelling wave electro-optic devices), thus ensuring that all electrical data and control signals did not exceed 5 GHz.

Option 2 : Broadband Electrical Control Signals

The main disadvantage of restricting the demodulator electrical control signals to sinusoidal format lies in the limited range of demultiplexing which can be achieved in a single stage. Although $2 \cdot V_\pi$ drive provides a doubling of the speed of operation, both V_π and $2 \cdot V_\pi$ operation result in a 1–to–2 demultiplexing operation per stage, requiring a complex structure of cascaded active stages for higher order multiplexed systems. However, the addition of harmonic frequency terms to the electrical control signal permits variable duty cycle optical processing, and all the approaches and compromises discussed for optical pulse generation (IV.2.2) apply also in this context. This then allows direct access to one out of N OTDM channels in a single processing stage. In particular, demodulation carried out as per Table 4.2 and Fig.4.7 results in selective access to one channel, with the remaining N–1 channels either lost as in the case of a MZ demodulator ("destructive" access to the wanted channel) or emerging on the second output fibre in the case of a 2x2 optical switch (true "channel drop" operation). Similarly, demultiplexer operation with inverted bias (and potentially also reduced drive level) as in Fig.4.9 permits selective "destruction" of one channel in N (e.g. in order to ensure channel privacy in a distribution network), with a minimum requirement in terms of electrical drive frequencies and amplitudes.

In all cases, the relative time domain widths of the optical channel pulses and the demultiplexing windowing function are of prime importance, as demonstrated in Fig.4.29 for single frequency operation. If the requirement is solely for obtaining a sampled version of the data in a particular channel, then a sampling window width less than the bit–interval will ensure that no patterning (pulse width modulation) is obtained. This can always be achieved in the context of "destructive" demultiplexing or sampling. However, if at the same time it is important not to leave behind any optical energy in the demultiplexed time slot, the demultiplexing may need to be carried out in two stages: either "full time slot" demultiplexing followed by "RZ" sampling in the dropped–out channel, or short pulse sampling of the wanted channel followed by a "clean–up" full window selective destruction on the through data path in order to ensure that all

remaining optical energy within the demultiplexed time slot is removed.

In an experimental demonstration of 1-in-16 channel demultiplexing (N=16) with simultaneous local data channel insertion ("Optical Drop-and-Insert") the principle of optical demultiplexing with low duty cycle repetitive electrical modulator/switch control signals has been demonstrated at a line-rate of 2.24 Gbit/s, with optical demultiplexing and channel re-insertion performed at the 140 Mbit/s level. A low duty-cycle electrical drive signal of V_π amplitude was connected to a 2x2 optical switch of 2.24 GHz modulation bandwidth (3 GHz $LiNbO_3$ switch). Fig.4.30 displays the 2.24 Gbit/s line-signal 'eye' diagram after one channel has been extracted and the 'eye' diagram for the extracted channel, demonstrating successful operation with all the signal pulse powers switched into the correct output paths. [Blank and Cox] contains the details of the full drop-and-insert system operation.

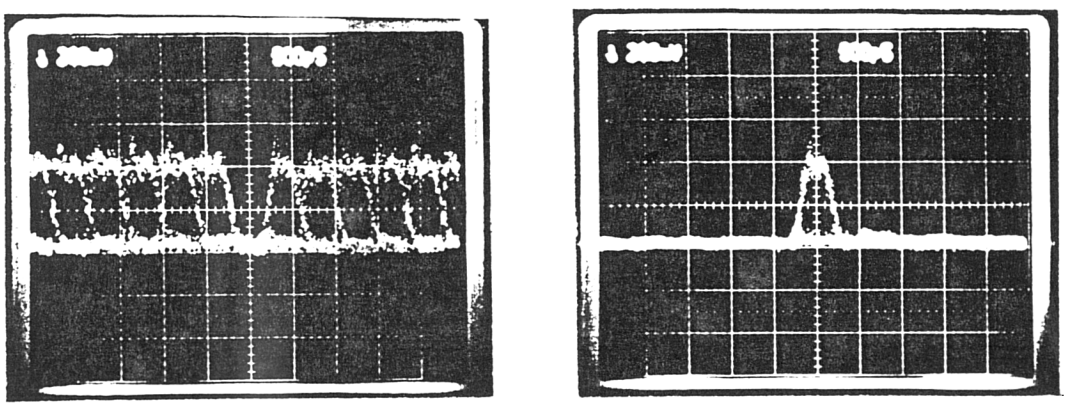

Fig.4.30 Optical Channel Drop at 2.24 Gbit/s System Speed:
Remaining 15 Channels (left), Dropped-out Channel (right).

The disadvantage of such a configuration is the need for an electrical switch drive signal with a fundamental frequency component at the speed of the local channel (e.g. 140 MHz), plus all harmonics upto (N-1)/N times the full line-rate (here upto and including 2.10 GHz). Overall system improvements would be achieved by means of $2 \cdot V_\pi$ electrical drive at a fundamental frequency of half the local line-rate (70 MHz), as described in

IV.2.2, Fig.4.10. The use of a reduced number of harmonic frequency terms together with the fact that the highest component required is at a frequency equal to half the full line-rate allows an optical switch to be employed with only half the electrical bandwidth and consequently with reduced V_{π}, resulting in substantial advantages in electrical drive power requirements.

IV.4.3 Synchronisation and Networking

Optical multiplexing by means of optical interleaving of individual RZ data streams or the active processing of tributary optical data requires optical synchronisation. This may be achieved either through electrical synchronisation of the electrical signals before conversion into the optical domain, or alternatively via the inclusion of variable optical delay lines at the system signal processing points. Whilst a detailed discussion of network synchronisation issues is beyond the scope of this work, reference to two investigations will serve to demonstrate the feasibility of signal synchronisation in future transmission systems and networks containing optical time domain processing.

Of general interest is the configuration of optical time domain multiplexed tributaries which originate from physically separate locations. As a result, unavoidable variations in the propagation delays of the tributary paths will only allow optical time division multiplexing (passive or active) if these variations are compensated for, either at the point of signal multiplexing via variable optical delays, or at the source of the tributary data via electrical or optical delay adjustments. Since such variations are expected to be slow (of the order of seconds), the speed of response is not a major issue. However the measurement of the system alignment is of vital importance. In [Blank, Bryant, Lord, Boggis and Stallard] and [Lord, Blank, Boggis, Bryant and Stallard], an experimental demonstration and theoretical analysis of a control scheme is provided, based on the measurement of a particular electrical frequency component in the electrical spectrum of the multiplexed, photodetected data signal. Optical signal propagation of 1 Gbit/s RZ optical data through 50 km long tributaries, followed by a further 50 km transmission after

optical multiplexing (interleaving) to 2 Gbit/s output line-rate, provided satisfactory system performance when one of the tributaries (the "slave" channel) was electrically phase controlled by means of an error signal derived from the optical receiver output, which in a practical system would be fed back to the slave transmitter via system supervisory channels. The theoretical analysis of the system feedback phase control revealed a satisfactory tolerance to variations in system component characteristics, thus demonstrating its viability.

The second system configuration of general interest consists of a high capacity, time division multiplexed optical transmission channel which is to be accessed optically at some point in order to extract one of the channels and replace it with a local data signal, for onward transmission. Simultaneous optical "drop-and-insert" has been demonstrated in [Blank and Cox] by accessing a 2.24 Gbit/s line signal at the 140 Mbit/s level. For the implementation of local synchronisation only a low frequency operational amplifier was required in addition to the components in place for the optical data processing operations.

Thirdly, synchronisation of local optical time division multiplexing equipment has been demonstrated with electrical timing extraction after signal detection [Wickens, Spirit and Blank (1), (2)] and by means of all-optical timing extraction [Barnsley, Wickens, Wickes and Spirit] to allow optical demultiplexing of ultra-high speed data channels as analysed in IV.4.2 above, after long distance linear and non-linear fibre propagation with associated long and varying propagation delays.

IV.5 SUMMARY

Ultra-high capacity optical multiplexing techniques have been investigated which allow the generation of optically time multiplexed line signals at data rates well beyond the operating speeds of any of the electro-optic signal processing components in the system. While the generation of short optical pulses may be carried out by means of for example gain switching or mode-locking semiconductor lasers as well as through electro-optic

switching, the required processing for optical demultiplexing and selective access to one channel in N may be carried out efficiently with standard processing devices, operating in non–standard configurations. Optimised operating conditions have been derived both for improving the electrical domain signal requirements (minimum electrical power and bandwidth) and for improving substantially the optical domain signal generation (maximum optical data–rate and maximum optical processing flexibility).

We have shown that the conversion of bandwidth–limited three–level electrical data format directly into optical binary format permits substantial improvements to be achieved in terms of broadband electrical signal power requirements, through allowing the use of electro–optic devices with reduced bandwidth and thus reduced V_{π} value. Alternatively, the maximum achievable broadband data modulation rate may be doubled for a given high speed modulator. This is applicable not only for standard data modulation but also in the context of ultra–high speed OTDM systems, allowing optimisation of the tributary data channels in advance of further optical OTDM processing.

The maximum OTDM system capacity for a given highest electrical drive signal frequency is obtained with sinusoidal electrical drive of $2 \cdot V_{\pi}$ amplitude providing upto a factor six improvement in system speed. However, the optical processing (pulse narrowing, channel multiplexing and demultiplexing) is only carried out as 2–to–1 or 1–to–2 multiplexing/demultiplexing, thus leading to complex system architectures.

By employing electrical control signals containing harmonic frequency terms (and electro–optic modulators and switches optimised for such operation), also of $2 \cdot V_{\pi}$ amplitude, channel processing with a lower duty cycle becomes possible at the expense of some reduction in the ratio of maximum line–rate to maximum electrical control frequency. This permits direct access to one of N time interleaved channels, thus for example enabling channel drop–and–insert to be implemented with a minimum of electro–optic and electrical equipment. The ratio of maximum line–rate to highest electrical

control signal frequency compares as follows for the two approaches. Based on the FWHM optical pulse or sampling width values of Table 4.2, $2 \cdot V_{\pi}$ modulator or switch operation with optimised 3rd and 5th harmonic frequency terms leads to a 11% sampling window, permitting upto 9 multiplexed channels. Combined with the frequency doubling of the $2 \cdot V_{\pi}$ drive, this leads to a 18-to-1 processing ratio, relative to the fundamental drive frequency component. Taking into account the fact that upto the 5th harmonic frequency terms are involved, the overall ratio is 18/5 = 3.6. For a more practical 8-channel setup, the ratio becomes 3.2. This compares with a maximum "speed-efficiency" factor of 6 for the more complex multiplexing architectures based on purely sinusoidal electrical control signals, thus demonstrating the trade-off between processing flexibility and fundamental maximum line speed.

In the next chapter first the fibre propagation characteristics will be analysed of optical pulse shapes appropriate for optically time multiplexed configurations. This will then be followed by an analysis of end-to-end system performance.

CHAPTER V

HIGH SPEED SYSTEM PERFORMANCE

V.1 INTRODUCTION

In this chapter the propagation performance of ultra-high speed optical TDM system configurations will be analysed. As a starting point a number of optical pulse shapes will be considered for use in high speed TDM / OTDM applications. Particular examples of practical interest as well as theoretical reference shapes will be investigated, the purpose of considering the latter being that they either represent an approach which can be fairly well approximated with real devices or to provide some benchmark results. The aim is to identify the extent to which the choice of optical pulse shape determines the overall system behaviour, and in particular the system distance capability. Apart from practical aspects, such as the generation and manipulation of the different types of pulses, their exact characteristics determine the maximum system data-rate achievable as well as the maximum fibre propagation distances before fibre chromatic dispersion provides the limiting factor. The starting point will be a comparison of a figure of merit for each pulse shape, namely the optical time-bandwidth product. Derived as the product of the time domain optical pulse width (Full-Width-Half-Maximum) and the optical power spectral width (-3dB power points), it will be shown that this value alone does not provide sufficient information about a given optical pulse. Modified measurements will be introduced which are aimed at providing a better indication of the expected pulse behaviour in the optical fibre system context. The usefulness of these indicators will then be tested through studying the actual propagation behaviour of the various optical pulses, followed by an analysis of the overall system performance for various schemes of practical interest.

V.2 OPTICAL PULSE CHARACTERISTICS

Current optical fibre transmission systems mainly employ binary digital transmission of Non-Return-to-Zero (NRZ) format, in which an isolated "1" is represented by a pulse of light of notionally rectangular shape and of duration equal to the length of the bit-interval. In practice the limited rise and fall times of electronic and opto-electronic devices result in a somewhat reduced bandwidth of the pulse. Nevertheless, this 'ideal' rectangular pulse waveform will initially be used as a reference against which alternative options can be measured.

For use in very high speed TDM systems, the basic NRZ data format may be kept, possibly with a deliberate slowing down of the pulse edges to achieve reduced optical bandwidth, as long as the required system data rate does not exceed the speed capability of the electronic and opto-electronic digital and analogue devices in the transmitter and receiver. An alternative approach may be to use multi-level optical signal formats, which so far have not been employed in high capacity single mode optical fibre transmission systems since the additional processing required has until now made it more (cost-) effective to develop higher speed components and retain the standard NRZ data format. For the same reasons there has been in the past little incentive to explore alternative or tailor-made optical pulse shapes for improved dispersive transmission performance, since new laser designs and the use of low dispersion fibre have extended the dispersive transmission distances beyond the limits imposed by power budget considerations.

However, when considering transform limited optical pulse and data generation and transmission capacities beyond the normally assumed speed limit of practical devices, the OTDM approach not only solves the electronic and opto-electronic device speed problems, but relies on optical processing which provides the functionality required for optical pulse "engineering", independent of whether NRZ or RZ format optical line signals are employed. Consequently, an analysis of the characteristics of a single isolated pulse will allow conclusions to be drawn as to the likely behaviour of the chosen pulse type in a system context, in preparation for a full system study. Here, a total of nine basic optical

pulse shapes will be analysed, all of which represent either a useful "theoretical" benchmark or alternatively a "realistic" pulse shape, which in practice can be obtained or at least closely approximated. In optical transmission systems the electrical pulse characteristics after photodetection, such as pulse width and electrical spectral bandwidth, are of interest as far as electronic processing is concerned, for signal to noise ratio optimisation, regeneration and electronic multiplexing. For an analysis of pulse propagation, however, their characteristics in the optical domain need to be considered. Consequently, the optical time bandwidth product is of interest here, derived as the product of the optical pulse duration, as measured in the optical domain or after photodetection, and the optical pulse spectral width as measured in the optical domain.

For an optical pulse of power waveform P(t) and optical carrier wavelength λ_s, the complex electric field description is:

$$E(t) = [P(t)]^{\frac{1}{2}} \cdot \exp(j2\pi ct/\lambda_s)$$

In the following, a monochromatic source of wavelength λ_s is assumed, followed by a modulation mechanism which provides pure amplitude modulation thus providing transform limited optical pulse generation. The pulse power waveforms under consideration are summarised in Table 5.1, with W representing the time domain FWHM pulse width:

Ref.	Description	P(t)
A	Single sided exponential	$\exp(-0.693147 \cdot t/W)$
B	Rectangular	$\mathrm{Rect}(t/W)$
C	Trapezoidal	$t_r = t_f = t_{top} = W/2$
D	Triangular	$t_r = t_f = W$
E	Sinusoidal	$0.5 \cdot (1+\cos(\mathrm{pi} \cdot t/W))$, $-W < t < W$
F	Gaussian	$\exp(-2.77 \cdot t^2/W^2)$
G	Sech^2	$4 \cdot [\exp(1.76 \cdot t/W)+\exp(-1.76 \cdot t/W)]^{-2}$
H	Sinusoidal drive to MZ modulator	see Section IV.2.2, Fig.4.7
K	F–doubling MZ modulator drive	see Section IV.2.2, Fig.4.8

Table 5.1 Optical Pulse Shapes

Pulses of particular practical interest are shape E (corresponding to electrical drive of triangular shape to a Mach Zehnder modulator), shape G (output from soliton laser [Smith, Armitage, Wyatt, Doran and Kelly]), shape H, and shape K. Pulses of shape K might originate from the optical pulse generation process described in Section IV.2.2, or alternatively they represent an approximation to the optical pulses obtained from a duobinary electrical drive to a Mach-Zehnder optical modulator (Section IV.3.1), biassed for conversion of electrical duobinary data to optical binary format (Fig.4.13).

The time-bandwidth product TBP_{FWHM}, defined as the product of the FWHM pulse width (optical power waveform) and the FWHM optical spectral width (-3dB optical bandwidth), is listed in Table 5.2 for each of the nine cases, as well as their RMS time bandwidth product TBP_{RMS}, obtained by using the respective RMS values in place of the FWHM measurements for both the time and spectral domain signal widths.

Assuming optical pulses of identical FWHM width in the time domain, the time-bandwidth product TBP_{FWHM} provides a correct representation of the relative optical spectral width (FWHM) for each pulse shape, confirming that pulse shape A (exponential) is most bandwidth efficient, followed by shape G ($sech^2$), shape F (gaussian) and shape K (frequency doubling MZ modulator).

The RMS measurements, however, clearly provide a very different picture. In this case the "well contained" optical pulse shapes, i.e. without long tails in the time domain, appear to be far more advantageous (shapes K, F, E and H), with the previously leading options A and G now coming last.

Shape	A	B	C	D	E	F	G	H	K
TBP_{FWHM}	0.11	0.88	0.70	0.54	0.59	0.44	0.32	0.66	0.50
TBP_{RMS}	0.50	0.31	0.12	0.11	0.09	0.08	0.83	0.09	0.08
$WTBP_{-10dB}$	0.37	0.88	0.70	0.54	0.59	0.44	0.33	0.66	0.50
$WTBP_{-15dB}$	0.55	0.88	0.70	0.54	0.59	0.49	0.44	0.66	0.52
$WTBP_{-18.5}$	0.69	0.88	0.70	0.54	0.59	0.54	0.51	0.66	0.56
$WTBP_{-20dB}$	0.73	0.88	0.70	0.54	0.59	0.57	0.54	0.66	0.58

Table 5.2 Optical Time Bandwidth Product for Pulse Shapes of Table 5.1

The fact that the FWHM and RMS values in Table 5.2 provide such a contradictory picture demonstrates that a modified measurement is required to provide a realistic measure of the likely performance of the different pulse shapes in the context of high capacity optical data transmission systems.

In the case of time division multiplexed optical transmission systems the parameters of interest are the optical pulse width and the pulse to pulse inter-symbol interference (ISI). While the pulse width determines the fundamentally maximum achievable bit-rate, the exact pulse shape and the permissible level of inter symbol interference (ISI) at the center of adjacent bit-intervals have to be taken into account. Consequently the TBP_{FWHM} values derived above should be weighted according to how close pulses can be placed, whilst still achieving a predetermined level of ISI (WTBP: Weighted TBP). The weighting factor shall be the time interval between the centres of two adjacent pulses, expressed as a multiple of the FWHM pulse width W. Whilst in this way only interference terms from adjacent pulses are taken into account, this approach is justified for all the signal shapes under consideration here apart from the exponential shape, pulse A, for which the WTBP values would be worse still if interference terms from more distant pulses were included. In the case of rectangular, sinusoidal and other pulses which do not extend by more than their pulsewidth W in either direction from the pulse center, the weighting factor is equal to 1, thus allowing for a system bit-interval T (system bit-rate B=1/T) equal to the pulse width W, i.e. a 100% efficient utilisation in terms of maximum bit-rate for a given pulse width (Fig.5.1). In the case of pulses with tails extending further than W from the pulse centre, the maximum bit-rate or minimum bit-interval may be limited by the allowable level of ISI at the center of neighbouring time slots. Table 5.2 above includes the modified time bandwidth products WTBP for several levels of ISI, namely -10, -15, -18.5 and -20 dB (optical). The table shows how the level of acceptable ISI modifies the relative advantages of the individual types of pulses. As an example, for a maximum ISI level of -18.5 dB (equivalent to -15.5 dB in a systems context, due to ISI from adjacent pulses on both sides of the time slot under consideration), the leading pulse shapes are now $sech^2$, gaussian, triangular and f-doubling MZ, with their WTBP values showing improvements of

between 36% and 42% over the rectangular pulse shape, and between 15% and 23% over shape H, the currently most widespread configuration in advanced experimental high bit-rate systems employing Mach-Zehnder external modulators.

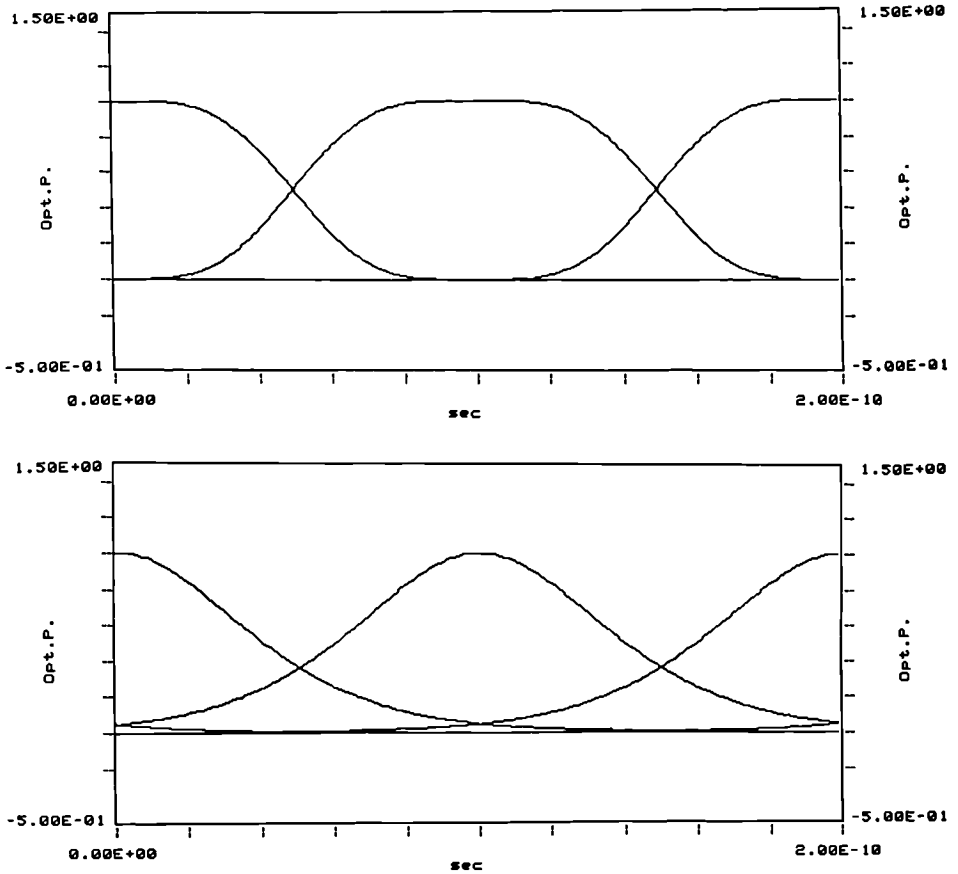

Fig.5.1 Minimum Pulse Spacing Determined by either the Pulse Width (upper) or by the Level of Optical ISI (lower)

Since the time bandwidth product values provide a direct measure of the relative optical bandwidth for a given pulse width (or given bit-rate, in the case of the weighted WTBP measurements), the conclusion could be drawn that optical transmission systems employing linear fibre propagation based on $sech^2$, gaussian, triangular and Mach-Zehnder frequency doubled pulse trains should suffer considerably less from fibre chromatic dispersion than systems employing any of the other pulses considered here. In particular, the improvements over the ideal rectangular and the "rounded rectangular" optical pulse shapes (shapes B and H) might result in a corresponding increase in the maximum achievable dispersion-limited transmission distance. To what extent this conclusion is valid, which is based on

just the pulse width, the basic time-bandwidth product, and a "bit-rate efficiency" weighting process, will be investigated below.

V.3 PULSE PROPAGATION

In order to gain a detailed picture of the propagation behaviour of the optical pulse shapes of interest, their performance will be analysed as a function of the propagation distance for a given fibre chromatic dispersion parameter (i.e. as a function of the total chromatic dispersion). The results will be presented in terms of example pulse widths and propagation distances, with values chosen which are of interest in the context of future generation high capacity transmission systems. Normalisation or mapping of the results onto sets of different starting parameters is straightforward as long as the assumption made here is valid that non-linear fibre propagation effects are insignificant. The following two normalisation values are of particular practical interest :

a) total chromatic dispersion (first order dispersion parameter multiplied by fibre length).
b) ratio of pulse width and square root of total dispersion.

The transmission distances quoted below are representative of a fixed product of the fibre length and the fibre chromatic dispersion parameter, such that twice the distance is available if the fibre chromatic dispersion value is halved, and vice versa. Similarly, for a given pulse shape, doubling (halving) of the pulse width results in halving (doubling) of the optical spectral width, which in turn allows the use of four times (one quarter) of the total dispersion value in order to achieve the same relative pulse distortion. This provides for a constant ratio of pulse width and square root of total dispersion, for a given level of relative distortion due to optical pulse propagation.

As a starting point, the FWHM pulse width, calculated as a function of transmission distance or total chromatic dispersion, provides some insight into the general propagation

behaviour of a particular pulse shape. A summary of full propagation calculations is provided in Fig.5.2 for shapes C to K, for 100 psec FWHM optical transmitter pulse width and 15 ps/(nm·km) fibre chromatic dispersion. Shape B (rectangular) is not included since it represents an unobtainable shape in the context of ultra-high speed transmission, whilst shape H (sinusoidal drive to MZ modulator leading to a "rounded" rectangular shape) provides a practical bench mark figure against which to compare. The upper traces in Fig.5.2 represent the FWHM pulse width as a function of fibre length, the lower traces their respective RMS values.

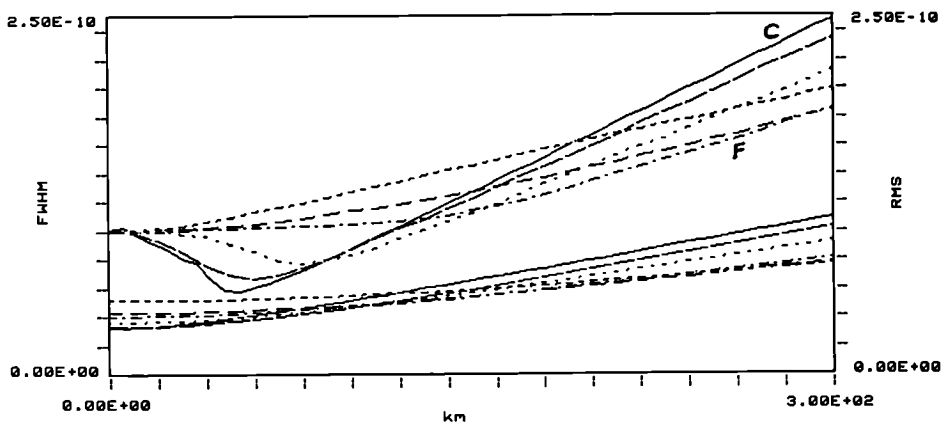

Fig.5.2 Pulse Width Versus Propagation Distance. Upper Group of Traces : FWHM Values. Lower Group: RMS Values. (Identification: at 300 km the shapes are – in order of decreasing FWHM value – C, H, E, G, K and F).

Two general patterns can be observed: shapes C, E and H initially demonstrate a substantial reduction in pulse width, followed by a rapid "recovery" and an asymptotic steady increase at a relatively large rate. On the other hand, shapes F, G and K show a distinctly different behaviour, in that no initial reduction occurs in the FWHM value. Instead, it begins to increase slowly, and then settles to an asymptotic rate of broadening which is substantially smaller than for the first set of shapes. In all cases the RMS values initially rise slowly, later settling down to asymptotic rates of increase of differing magnitudes.

For long transmission distances some clear winners emerge, for example beyond 200 km shapes F and K. The bench mark shape H together with shape C provide the worst performances, as expected from their TBP values. The situation is less straightforward for

applications in NRZ type optical data transmission, where the goal is to keep the optical pulse contained within its allocated time slot. In this case shapes C, E and H seem to provide some advantage by first displaying a reduction in pulse width, followed by an increase back to the launch pulse width after approximately 115 to 130 km, a distance at which shapes F and G (gaussian and $sech^2$) have already broadened considerably and at which shape K (f-doubling MZ) is just beginning to show a noticable increase in its FWHM value.

The differences in the asymptotic rates of pulse broadening after longer distance transmission will be exploited later in a system applications context (V.3.2). First, however, further clarification is required for notional NRZ pulse transmission.

V.3.1 Notional NRZ Signal Format

For NRZ format data the transmitter launch pulse width is normally exactly 100 psec for 10 Gbit/s data transmission. In V.2 above the requirement was identified for adjustments to the optical launch pulse width of certain pulse shapes if particular targets for maximum levels of intersymbol interference have to be met, resulting in effectively an "almost RZ" line format. Full pulse propagation calculations have been carried out, together with an analysis of the level of ISI at 100 psec from the centre of the individual pulse, i.e. at the centre of the adjacent bit-intervals. The results are summarised in Fig.5.3, based on the weighting factors established previously. The FWHM pulse width is again evaluated as a function of propagation distance, with the launch pulse widths adjusted to meet an ISI constraint of -18.5 dB at the transmitter output (upper traces, left-hand y-axis). The lower set of curves represent the levels of ISI at the centre of adjacent bit-intervals, again as a function of distance (right-hand y-axis). Table 5.3 summarises the propagation distances at which the pulse width has broadened to 100 psec (the bit duration at 10 Gbit/s), with the pulse shapes rearranged in order of decreasing propagation performance.

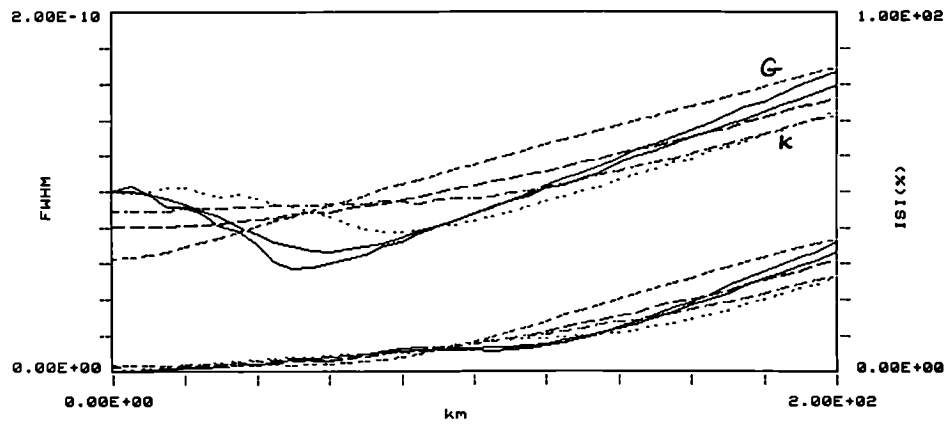

Fig.5.3 FWHM Pulse Width (Upper Group of Traces) and Level of ISI (Lower Group) as a Function of Propagation Distance (Identification: at 200 km the shapes are – in order of decreasing FWHM value – G, C, H, F, E and K).

Pulse Shape	E	H	C	K	F	G	
Broadened to 100 ps:	130.0	118.8	117.0	115.0	92.5	73.6	km

Table 5.3 Maximum Propagation Distances for Pulse Broadening to 100 psec.

One pulse shape now stands out in terms of poor performance : shape G ($sech^2$) suffers considerably from the required reduction in launch pulse width (with the resulting increase in pulse spectral width) in order to meet the –18.5 dB transmitter ISI level, and whilst the ISI performance is among the best upto approximately 90 km pulse broadening limits the maximum transmission distance to only 73.6 km, with all other shapes performing considerably better. In particular, shape E (sinusoidal) with 130 km now out–performs all others in terms of pulse broadening as well as levels of ISI at the neighbouring time slots, with shapes H, C and K following at around 119 to 115 km. Shape F (gaussian) is taking second–worst place. This leads to a situation which is in marked contrast to the results of Table 5.2, which suggested from the $WTBP_{FWHM}$ values (–18.5 dB ISI) the leading pulse shape to be G, followed by F and K. Only shape K has remained roughly in the expected relative position in terms of transmission performance. Worth noting is that the poor performance of shape G could be improved upon to some extent by allowing an

increased level of ISI at the transmitter, since a demand for -18.5 dB transmitter ISI may be unwarranted if after maximum transmission distances ISI values of typically -10 dB are obtained. Thus those pulse shapes which suffer from the transmitter ISI restriction (shape G most strongly, then F and K) woud benefit accordingly. This, however, does not change the fact that for notional NRZ format pulse transmission the time bandwidth product and weighted time bandwidth product do not provide a representative measure of the pulse performance after dispersive pulse propagation. Consequently, a full system analysis based on test data patterns and including the effects of bandwidth limited optical receiver operation will be required in order to establish the correct transmission performance of the various optical pulse shapes for dispersive high capacity data transmission.

V.3.2 RZ Signal Format

Whilst for NRZ format data transmission the analysis carried out in the section above has demonstrated that the optical time bandwidth product does not give a correct indication of the performance of a given pulse shape, Fig.5.2 also indicates that this is likely to be due to the varying "transient" behaviour of the various pulse shapes during the inital propagation in a dispersive medium. After further propagation (e.g. beyond 200 km in this particular example) the rate of pulse broadening settles towards asymptotic values which appear to be in line with the performance predictions based on the optical time bandwidth products. This may therefore be applicable to transmission based on a Return-to-Zero (RZ) launch signal format, with optical pulse broadening permitted up to the width of the bit-interval. Operation with RZ pulse widths equal to 50% and 25% of the bit-interval has been analysed. In these cases the transmitter level of ISI does not represent a limiting factor, and for all pulse shapes the same transmitter FWHM pulse width may be employed.

In the case of 50 % RZ format the transmitter optical bandwidth is being doubled compared with Fig.5.2, whilst the target output pulse width remains at 100 psec. Consequently, as an approximate guide and neglecting the effects of the initial "transient"

in the pulse width development, the achievable transmission distances can be expected to be reduced from $\leqslant$ 150 km to approximately 75 km. Details of the computed FWHM pulse width as a function of distance as well as the levels of ISI as a function of distance are summarised in Fig.5.4. The transmission distance is in all cases limited by the pulse width reaching the 100 psec level, with corresponding ISI values in the region of −15 dB to −12 dB. Table 5.4 summarises the distances at which pulse broadening to 100 psec has occurred.

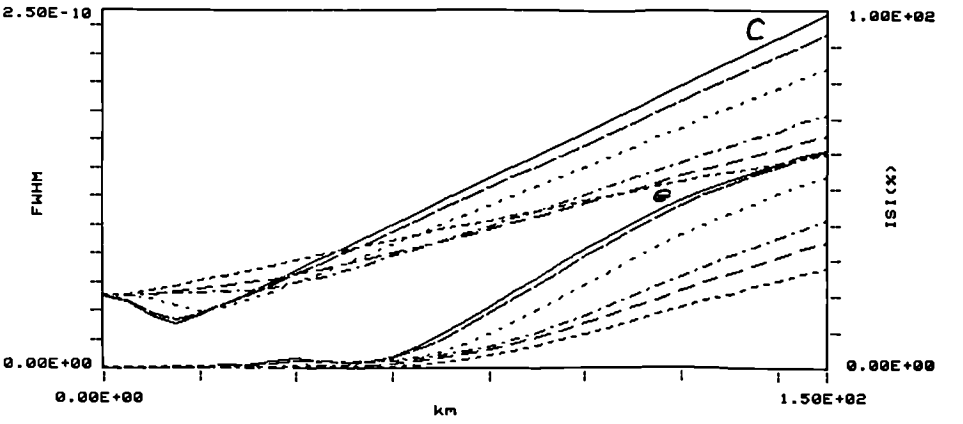

Fig.5.4 FWHM Pulse Widths as a Function of Propagation Distance, 50 % RZ Tx Format (in order of decreasing FWHM at 300 km the shapes are C, H, E, K, F and G).

Pulse Shape	F	K	G	E	H	C	
Broadened to 100 ps:	83.9	81.4	76.4	70.4	63.4	60.3	km

Table 5.4 Maximum Propagation Distances for Pulse Broadening from 50 psec to 100 psec

Apart from shape G still under-performing somewhat the ranking is now almost according to the TBP predictions. And an analysis of the pulse widths after 150 km in Fig.5.4 reveals that finally the performances are in the expected order. For 50 % RZ format transmission systems, a gaussian pulse shape, frequency doubled MZ pulses or a $sech^2$ pulse provide for an improvement of 20 % to 32 % in achievable dispersive transmission compared with the reference shape of sinusoidal drive to a MZ intensity modulator. In addition relatively low levels of ISI are obtained, and the limit is given by the broadening of the FWHM pulse width.

By reducing the transmitter pulse width further to 25 psec or 25 % RZ format, the target 100 psec width is obtained in all cases after the rate of pulse broadening has stabilised, as shown in Fig.5.5.

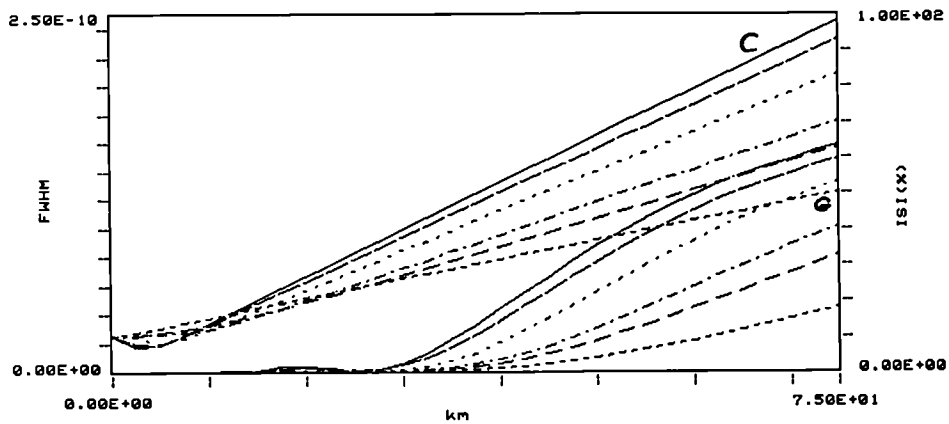

Fig.5.5 Pulse Broadening as a Function of Distance for 25 % RZ Transmitter Format (in order of decreasing FWHM at 75 km the shapes are C, H, E, K, F and G).

Pulse Shape	G	F	K	E	H	C	
Broadened to 100 ps:	56.3	46.9	42.3	35.8	32.1	30.4	km
FWHM at 75km:	125.0	157.0	175.5	209.0	233.0	245.5	psec
Improvement @ 75 km:	46.4	32.6	24.7	10.3	-/-	- 5.4	%

Table 5.5 Maximum Propagation Distances for 25 % RZ Transmitter Format, and Comparison of FWHM pulse Widths after 75 km.

Not only are the results in the expected order, but the relative pulse widths after 75 km are within 0.5 % of the values which would be expected from the TBP_{FWHM} values. Only shape G is still "under-performing" by 5 % (Table 5.5). This confirms that for dispersive propagation, allowing sufficient pulse broadening to several times the initial FWHM value, the optical time-bandwidth-product does provide an accurate description of the relative performance of the various pulse shapes of interest.

In the next section the investigation will now concentrate on how this behaviour of the various types of single pulses translates into system performance of data modulated pulse streams.

V.4 SYSTEM PERFORMANCE ANALYSIS

In the previous section the analysis of pulse widths and levels of ISI as a function of dispersive propagation distance for a single optical pulse provided an indication of the relative performance of the various pulse shapes in a full systems context. However, the knowledge of pulse width versus distance and ISI versus distance does not straightforwardly translate into system performance, and therefore a full calculation of the behaviour of the complete system configuration is required. This extends the analysis from single pulses to pseudo-random data streams, and also introduces the so far neglected effect of a (bandwidth limited) optical receiver. In addition, the potential benefit will be investigated of employing a duobinary signal format at various places in the overall transmission system: at the transmitter input (electrical domain), transmitter output (optical domain), fibre output (optical domain) and receiver output (electrical domain). It will be shown here that substantial benefits may be obtained for dispersive ultra-high bit-rate TDM data transmission, in terms of practical device requirements as well as for ultimate system performance. An analysis of the system performance as a function of transmission distance (or total propagation path dispersion) is obtained by means of full propagation calculations as described in Section II.7. A number of pulse shapes and transmission and detection signal formats of practical interest are analysed below, starting with notional NRZ transmission based on maximum allowable transmitter pulse width for a given line-rate (V.4.1), followed by system operation based on RZ transmitter signal formats (V.4.2). A comparison is then carried out (V.4.3) between the results of these full system calculations, the system performance estimations derived from the pulse width versus propagation distance calculations in Section V.3, and simple system estimations based on only the pulse time bandwidth product (TBP or WTBP). Further improvements in dispersive propagation distances are then identified by means of an analysis of three-level or duobinary detection of binary optical transmitter output data, both of NRZ and RZ format (V.4.4), followed by a summary of the obtainable system performance with duobinary signal detection of duobinary optical transmitter signals (V.4.5).

V.4.1 NRZ Optical Data Transmission

This section will be concerned with the analysis of optical system performance, based on optical pulse shapes as in V.3.1, i.e. employing a maximum optical pulse width for a given line-rate. Additionally, a further system configuration of practical interest will be examined based on duobinary electrical data drive to a MZ modulator, with modulator bias

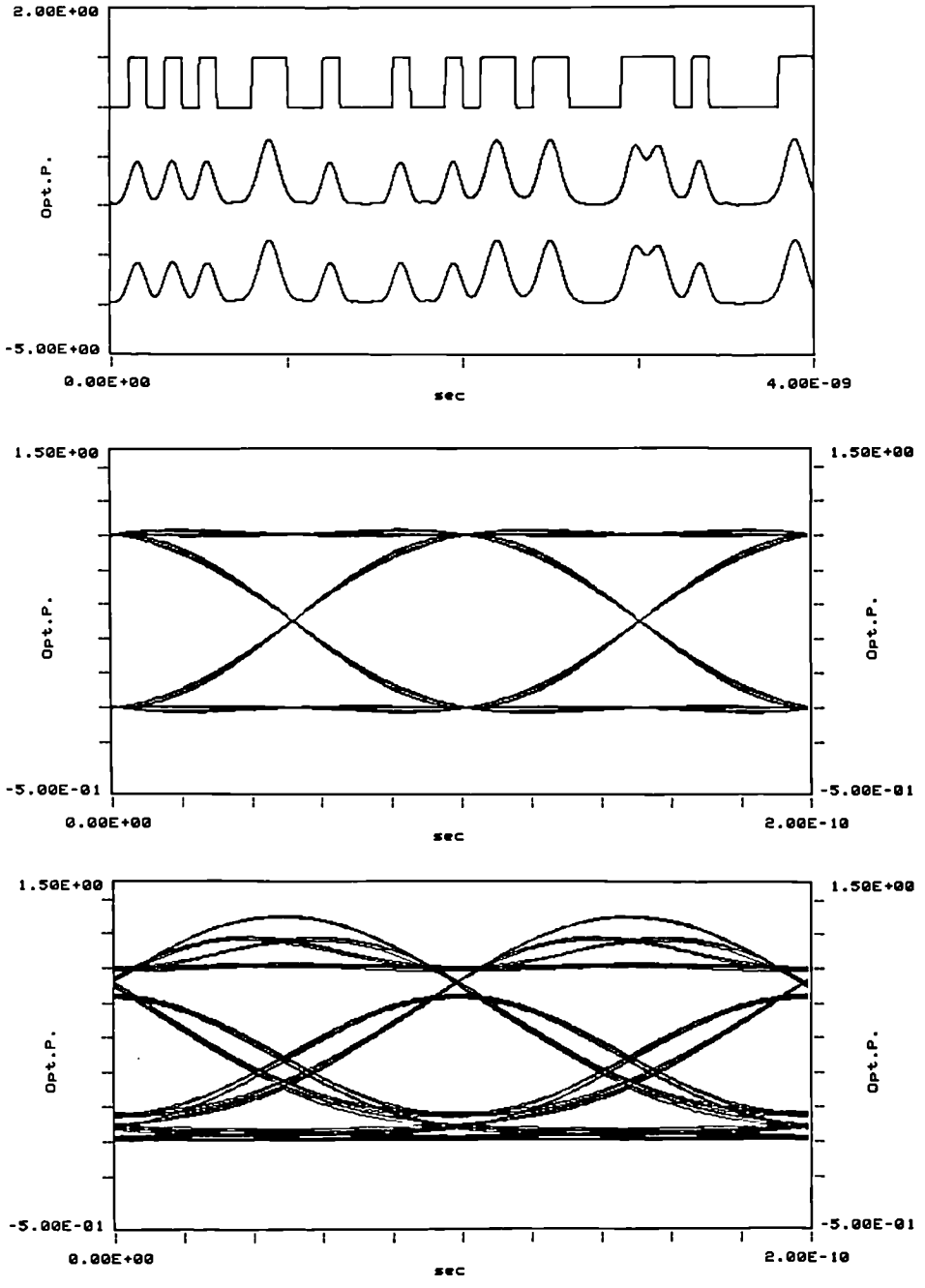

Fig.5.6 Top: Pulse Trains for Rect. I/P : Tx Output, Fibre and Rx Output; Centre: Receiver 'Eye' after 0 km; Bottom: 'Eye' after 90 km.

conditions chosen such that the electrical data signal is converted directly into NRZ optical format. An example of the signals of interest is provided in Fig.5.6, showing a section of a 2^6–1 PRBS data sequence optical pulse train, the fibre output power waveform after propagation through 90 km of fibre and the subsequent receiver output signal, with the latter two showing major waveform distortions. Fig.5.6 also displays the receiver output 'eye' diagram for 0 km fibre propagation and after 90 km when the receiver 'eye' opening has deteriorated by approximately 1.8 dB (optical), indicating that the maximum achievable transmission span is limited to less than 100 km.

A summary of the system performance of seven pulse shapes is provided in Fig.5.7. For each shape the transmitter pulse width is chosen to meet the −18.5 dB ISI criterion as discussed in Sections V.2 and V.3. The results are presented in terms of 'eye' closure (i.e. system penalty) in units of optical dB as a function of transmission distance at a system line−rate of 10 Gbit/s.

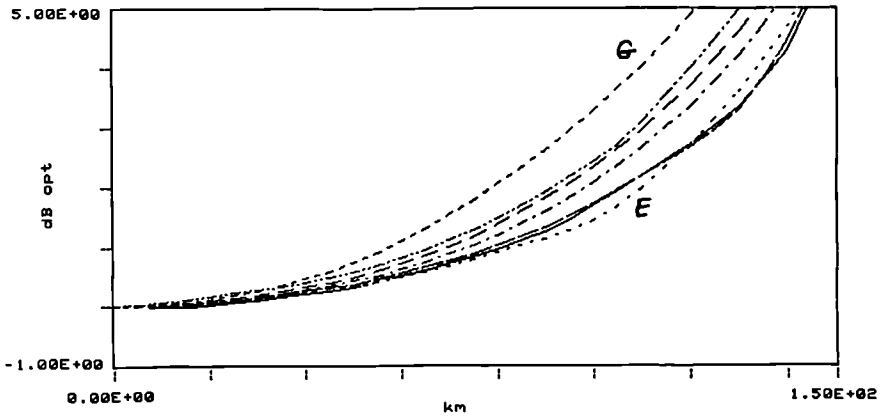

Fig.5.7 10 Gbit/s System Penalty (optical dB) vs Transmission Distance (see following text for curve identification).

At the −1 dB and −2 dB penalty levels the ranking, best to worst, is as follows: shape E (sinusoidal), then C (trapezoidal) and H (sinusoidal MZ drive), followed by K (f−doubling MZ), F (Gaussian), B (Rectangular), then G ($sech^2$). Table 5.6 summarises the achievable transmission distances for 1 dB and 2 dB system penalties, demonstrating clearly the advantage of the sinusoidal MZ drive over a rectangular optical pulse shape (e.g. MZ drive with large electrical bandwidth). However, it also confirms the previous results from

the pulse width analysis in V.3 which demonstrated that for notional NRZ data transmission optical pulse shapes with superior optical time-bandwidth product such as gaussian or $sech^2$ do not necessarily provide improved system performance. In particular the $sech^2$ pulse shape provides the worst performance in Fig.5.7 and Table 5.6, due to its relatively narrow transmitter pulse width as a result of the ISI requirements. Even a reduction in the ISI criterion from -18.5 dB to -12.5 dB only results in moving the system penalty curve for $sech^2$ pulses towards the results of all the other shapes (not shown in Fig.5.7), thus still not providing any system advantage in spite of having the lowest weighted optical time-bandwidth product. Similarly, the results for shapes K and F could also be improved upon somewhat by increasing the level of allowable ISI at the transmitter output.

Shape	Description	-1 dB Distance (km)	-2 dB Distance (km)
E	Sinusoidal	84.9	110.4
C	Trapezoidal	82.1	106.6
H	Sin.MZ drive	79.9	106.4
K	F-Doubling.MZ	75.0	98.9
F	Gaussian	70.2	94.0
B	Rectangular	66.9	92.1
G	$Sech^2$ (-12.5 dB ISI)	65.6	88.8
G	$Sech^2$ (-18.5 dB ISI)	57.7	79.4

Table 5.6 Maximum Transmission Distances for 1 dB and 2 dB System 'Eye' Closure

Worth noting is that the maximum distances are considerably less than the limits identified in V.3, which were based on the simple assumption of allowing the FWHM pulse width to increase upto the width of the bit-interval time slot.

Duobinary Electrical Data Drive to a MZ Modulator :

Whilst the results above indicate that there is limited scope for improving the maximum transmission distance beyond that available with straightforward sinusoidally shaped electrical drive to a MZ modulator (Shape H), a variation of the frequency doubling pulse generation scheme (Shape K) can be shown to be of some benefit. The frequency-doubling sinusoidal MZ drive configuration itself would in reality be very difficult to implement, since the actual hardware configuration employed for the generation of such pulses results in a pulse stream with fixed duty cycle, thus not allowing an optimised pulse spacing (e.g. based on ISI requirements) as assumed in the above calculations. However, the principle of frequency doubling of the drive signal was being made use of in Section IV.3.1 in the context of demodulation of an electrical duobinary signal into binary format optical data. Whilst the resulting pulse shapes are similar to the waveforms obtained from the single frequency electrical drive / frequency-doubling scheme, the main advantage lies in the fact that good ISI performance is automatically obtained, i.e. the signal shape does not suffer from extended pulse tails. Consequently, an analysis of the transmission performance of such electrical duobinary-to-optical binary converted signals will be of particular interest, since the transmitter configuration only requires half the modulator bandwidth of conventional external modulation, with a resulting reduction in the modulator V_π value and thus the electrical drive power.

Below, four modulator operating conditions will be compared, since the choice of bias point and electrical data signal amplitude has considerable effect on the optical pulse shapes generated. The mean modulator bias point may be chosen to be either fully on or fully off. The duobinary data amplitude may be a full $2 \cdot V_\pi$ or a standard V_π. Table 5.7 summarises the operational advantages and disadvantages of the four combinations. The 3rd option is of greatest interest, since it combines low electrical drive power (standard V_π drive to a modulator of half the normal bandwidth) with good optical extinction. The disadvantage of a 3 dB optical "excess" insertion loss of the modulator is due to the fact that with the modulator biassed in the "off" position, an electrical modulation of amplitude

V_π will only switch the modulator half-way towards the "on" position. However, the availability of high performance optical amplification means that such a 3 dB excess insertion loss would be of little importance if in addition to the advantageous electrical drive conditions satisfactory dispersive fibre propagation performance was also to be obtained.

Option No	MZ Bias	Data Ampl.	Advantage	Disadvantage
I	0	V_π	-	Limited on-off ratio (2:1)
II	0	$2 \cdot V_\pi$	High on-off ratio	High electrical drive level
III	V_π	V_π	High on-off ratio	3 dB optical excess loss
IV	V_π	$2 \cdot V_\pi$	High on-off ratio	High electrical drive level

Table 5.7 Modulator Bias and Electrical Drive Options

Since in all four cases the resulting optical signals have differing shapes, only a full analysis of the system performance after dispersive pulse propagation can reveal whether any of the above bias and drive conditions offer particular advantages. For comparison, duobinary transmitter filtering employing both raised cosine frequency domain shaping and sinusoidal time domain pulse shaping have been analysed for their respective effect on transmission performance. It was found that at high system penalties (i.e. worse than -2 dB) the maximum achievable transmission distances were very similar for the same bias and drive conditions when comparing raised cosine and sinusoidal electrical drive filters. However, at the values of practical interest of -1 dB to -2 dB, the sinusoidal electrical drive configurations achieve between 5 and 15 % improvement over raised cosine filtered duobinary transmitter drive signals. Consequently the performance values quoted below are for duobinary electrical input data, filtered to achieve sinusoidal time domain signal shapes.

The resulting system penalty curves are shown in Fig.5.8, with the achievable distances for 1 dB and 2 dB 'eye' closures summarised in Table 5.8.

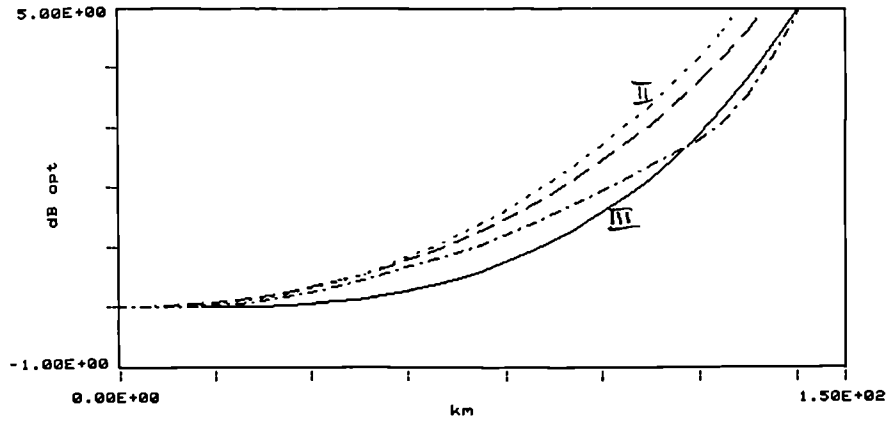

Fig.5.8 System Penalty as a Function of Distance for Electrical Duobinary/ Optical Binary Signal Generation. Options II, I, IV and III (in order of increasing performance at the −1 dB penalty level, see Table 5.8 below).

Option No	MZ Bias	Data Amplitude	−1 dB Distance (km)	−2 dB Distance (km)
I	0	V_π	67.5	91.9
II	0	$2 \cdot V_\pi$	65.4	87.9
III	V_π	V_π	87.1	107.7
IV	V_π	$2 \cdot V_\pi$	74.0	101.8

Table 5.8 Transmission Distances for Duobinary Electrical / Binary Optical Signals

The performance achieved by the third configuration equals the best result of Table 5.6, thus indicating that the advantage of reduced electrical modulator drive amplitude is obtainable at the expense of only a 3 dB excess optical insertion loss, without loss of dispersive fibre propagation system performance. In addition, the required sinusoidal electrical pulse shaping filter is likely to be easier to implement than the generation of sinusoidal optical pulses.

V.4.2 RZ Optical Data Transmission

The broader optical bandwidth of RZ-format line signals leads to a considerable reduction in the maximum transmission distance in a dispersive propagation medium. The results of Section V.3.2 suggested that a 50 % RZ signal format results in a 35 %

reduction for the highest performing pulse shape compared with the best NRZ result, and in a 57 % reduction for a 25 % RZ format. The main advantage of the 50 % RZ signal format is the existence of a strong clock component at the transmission line-rate in the signal power spectrum, facilitating clock extraction either in the optical domain [Barnsley, Wickes, Wickens and Spirit] or after photodetection [e.g. Blank and Cox]. With a 25 % RZ format the clock component is also present, but a further advantage is the low duty cycle allowing for Optical Time Division Multiplexing, i.e. the time interleaving of several independent optical channels. Whilst the performance of complete OTDM system configurations will be analysed in Section V.5 below, in the following the signal propagation will be studied for an individual low duty cycle optical data signal. The aim is once again to achieve maximum transmission distances, and to this extent dispersive fibre pulse broadening will be allowed upto the full bit-period, thus requiring a full bandwidth optical receiver rather than a receiver which would convert a RZ optical signal into NRZ electrical format.

Fig.5.9 summarises the results of calculations of system penalty versus fibre distance for five pulse shapes. All launch pulse widths are 25 psec or 25 % of the bit-interval.

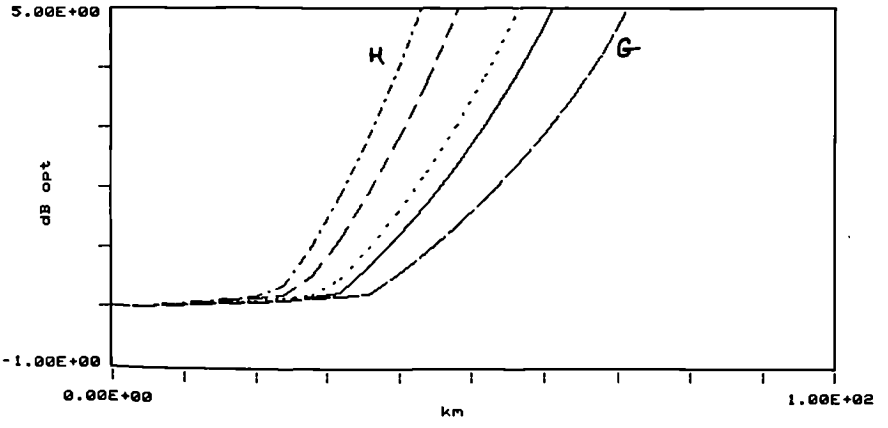

Fig.5.9 System Penalty vs Distance for 25 % Duty Cycle Optical Pulses for Shapes H, E, K, F and G (in order of increasing performance).

In all cases the system penalty increases initially at a slow rate, as a result of all the (slightly dispersed) pulse energy still being contained within the original time slot. When optical energy begins to enter adjacent time slots a "threshold" effect is visible in the

penalty curves, with subsequent rapid system deterioration. The resulting maximum transmission distances for 1 and 2 dB system penalty are summarised in Table 5.9 for all pulse shapes together with the relative advantage over shape H at the 2 dB penalty level.

Shape	Description	-1 dB Distance (km)	-2 dB Distance (km)	Improvement over H (%)
G	$Sech^2$	44.6	53.3	64.0
F	Gaussian	38.4	45.6	40.3
K	F-Doubling MZ	35.9	42.4	30.5
E	Sinusoidal	31.0	36.3	11.7
H	Sinus. MZ drive	27.9	32.5	-/-

Table 5.9 Transmission Distances for Binary Detection of 25 % Duty Cycle Optical Pulses

The ranking in terms of maximum distances is now as could be expected from the optical TBP values for the individual pulse shapes. In particular, shape H shows the worst performance, unlike in the case of NRZ signalling. However, the relative distances are not quite in the inverse ratio of the respective TBP values due to the differences in the transient pulse propagation behaviour during the first few kilometers of dispersive propagation.

Worth noting is that the best distance achieved by shape G with 53.0 km for 2 dB penalty is approximately half the value for the best NRZ data transmission configurations (shape E with 110.4 km, duobinary electrical/binary optical modulation with 107.7 km), although the launch pulse width of 25 % of the bit-interval means approximately a fourfold increase in optical bandwidth. Whilst the large bandwidth is reflected in the large rate of increase above the penalty "threshold" in Fig.5.9, the initial propagation during which the pulses broaden within their respective bit-intervals results in the comparatively high performance in terms of maximum distances.

V.4.3 Comparison of Performance Analysis Techniques

In this chapter three techniques have been employed for the estimation of absolute or relative performances of a range of optical pulse shapes or system configurations: firstly a comparison of different optical pulse shapes based only on the optical pulse time bandwidth product TBP (or a derivative in the form of the weighted TBP), secondly an estimation of achievable propagation distances based on the pulse broadening behaviour of individual pulses during dispersive fibre propagation, and thirdly detailed system modelling with test data sequences and a full system output 'eye' diagram analysis. Whilst the third approach results in an accurate description of system behaviour it requires complex computer modelling, with both large model sizes and long run times. Consequently, it is of interest to identify how closely the full system model results may be approximated by simpler techniques in order to facilitate system design for a variety of practical applications without having to resort to the detailed model.

The second approach of estimating system limits via an analysis of the propagation characteristics of a single optical pulse of suitable shape has the advantage that the computational effort required is substantially reduced. No test data are to be assembled and processed (e.g. 2^N–1 data sequence, plus filtering of the electrical signal), no optical receiver filtering and no 'eye' diagram analysis is required. A comparison of the contents of Tables 5.3 and 5.5 (single pulse analysis) with the results of Tables 5.6 and 5.9 (full system models) indicates that the predictions of the single pulse propagation model are similar to the 2 dB system penalty results of the full model. The simpler model therefore tends to provide a best case over–estimate for the maximum system length, since chromatic dispersion penalties would normally be required to be less than 2 dB optical. Closer inspection of the results reveals that the discrepancies between the two models show some distinct patterns. In the case of NRZ format transmission, the single pulse model over–estimates the achievable distance by between 9% and 18 % for the four leading pulse shapes (E, C, H and K) whilst it provides accurate results for shapes F and G (gaussian and $sech^2$). In the case of RZ format transmission, the accuracy of the pulse

propagation model is somewhat higher, giving a 5.6 % over-estimation of the -2 dB distance for $sech^2$ pulses, with all other results within 3 % of the distances obtained from the full model. Consequently, for many system design applications the simpler pulse propagation model may be employed for estimating the maximum transmission distances available for a given optical pulse shape, signal format and bit-rate.

Whilst the single pulse model provides good approximations it still relies on numerical evaluation of the behaviour of optical signals in a dispersive medium. Of interest is therefore to what extent the simplest of the three approaches may provide realistic estimations, through a system performance evaluation based on only the optical pulse time bandwidth product. As already discussed in Section V.3 the relative performances of different pulse shapes may be estimated directly from the optical pulse time bandwidth product values, but only in the case of low duty-cycle RZ transmitter signal formats. This results from the fact that with RZ formats the pulses are allowed to go through their transient behaviour during initial dispersive propagation, followed by broadening to well beyond their initial pulse width when the rate of broadening is determined by the optical bandwidth for a given pulse width, as expressed in the time bandwidth product. With the relative system performances determined accurately by only the optical time bandwidth product, the question arises to what extent absolute distance values may also be derived without numerical modeling. The following example demonstrates this for $sech^2$ pulses:

Pulse Width ($sech^2$; TBP = 0.32) :	τ	= 25 ps,	
Optical Bandwidth (TBP$\cdot 1/\tau$) :	B	= 12.8 GHz;	
At 1.55 μm wavelength :	$\Delta\lambda$	= 0.1024 nm;	(with 1nm $\triangleq$ 125 GHz)
Resulting Dispersion :	$D\cdot\Delta\lambda$	= 1.536 ps/km;	

If the 25 ps pulse is to broaden by 75 ps to 100 ps, i.e. to the duration of the bit-interval of the 10 Gbit/s line-rate assumed in the examples of V.3, then the maximum fibre distance xl becomes :

xl = 75 ps / (1.536ps/km) = 48.8 km.

This value is approximately 10 % larger than the 1 dB penalty distance and 10 % smaller than the 2 dB penalty distance identified in Table 5.9 for this configuration. Consequently, for low duty-cycle RZ optical signal format, the optical time bandwidth product not only predicts accurately the relative performance of different pulse shapes, but also allows a good approximation of the absolute distances to be obtained by means of simple arithmetic calculations. For NRZ signals the initial transient behaviour is dominating the propagation, with the result that the optical time bandwidth product does not provide a correct indication of even the relative propagation performances and can therefore not be used for simple system calculations.

In the remainder of Section V.4 the full system model will be employed to explore possibilities for further increases in the fibre dispersion limited maximum transmission distances by means of multi-level optical signalling.

V.4.4 Duobinary Detection of Binary Transmitter Signals

A technique well known for providing improved transmission performance under conditions of bandwidth limited pulse propagation is the use of multi-level signalling. One example is the duobinary signal format which results in the signal occupying half the transmission bandwidth for the same digital line capacity. In Chapter IV the issue of utilising electrical domain duobinary signals in conjunction with external modulators has been discussed, for efficient generation of optical binary data as well as for the generation of duobinary optical line signals. Now the performance is analysed of optical duobinary signals in the context of dispersive monomode optical fibre transmission which may be viewed as a bandwidth limited propagation process as in the case of coaxial cable electrical signal transmission. The main differences, however, are that optical signals are unipolar with all signal values expressed in terms of positive optical powers, and that effective channel bandwidth limitations do not result from frequency dependent path attenuation but from signal group delay distortions. As a consequence, dispersive fibre propagation leads to time domain signal distortions which in general are not symmetrical

around the mean signal value, leading to particular problems with multi-level signalling. Initially the investigations will concentrate on the use of standard NRZ or RZ transmitter signal formats as described in Chapter IV and in this chapter, followed by fibre propagation beyond the distance limits identified above. The aim is to investigate to what extent fibre propagation may result in controlled bandwidth limiting of the two-level optical data signal such that when binary decisions may no longer be made photo-detection of the distorted optical signal will allow the output to be treated as a three-level signal, with full duobinary electrical signal processing to recover the original data. The use of both NRZ and RZ transmitter signals will be investigated.

System operation with three-level optical transmitter signal formats followed by three-level detection will be analysed below in Section V.4.5.

NRZ Transmitter Signal Format :

In Fig.5.10 the optical receiver output 'eye' diagrams are displayed for system operation based on transmitter pulse shape H, i.e. for a sinusoidal electrical drive waveform to a MZ optical modulator. The upper trace represents the case of zero optical path chromatic dispersion, the lower trace is for the equivalent of 85 km of fibre at 15 psec/(nm·km) dispersion. In the analysis of the previous sections the opening of the main two-level 'eye' has been the measure of system performance (decision time at t = 50 psec in Fig. 5.10). Now the behaviour of the three-level 'eye' around the decision time of t = 100 psec will be investigated. The main differences compared with two-level detection are firstly the requirement for two threshold detection processes ("lower eye" and "upper eye") with differing behaviour as a function of propagation distance, and secondly the fundamental reduction in the individual 'eye' opening at 0 km by at least 3 dB optical compared with the standard two level 'eye' diagram, as visible in Fig.5.10, upper trace.

The lower trace (after 85 km propagation) demonstrates how the system output 'eye' diagram after dispersive fibre propagation leads in the general case to considerable differences between the openings of the two halves of the three-level 'eye'. The lower

'eye' has been closed considerably more than the upper 'eye', thus providing the limiting factor in the overall system performance analysis. In the particular cases of rectangular or "rounded" rectangular optical pulse shapes, the deterioration in the lower 'eye' occurs more rapidly as a function of distance than the system penalty for standard two level detection. This is clearly visible in Fig.5.10, where the binary 'eye' opening (at t = 50 psec) has been reduced after 85 km by just over 1 dB (optical), whilst the reduction in the effective three-level 'eye' opening (i.e. lower part) is almost 2 dB. Fig.5.11 displays the penalty curves for the two halves of the three-level 'eye' (referenced to the initial opening at L = 0 km). The 1 dB and 2 dB system penalty distances are 58.3 km and 85.5 km, considerably worse than the maximum propagation distances for two-level detection (79.9 km and 106.4 km, Table 5.6). As already outlined in II.7 this approach to system performance evaluation is only correct for negligible signal dependent noise. Especially with three level signalling, signal dependent noise dominating the system performance would change the balance between the two halves of the three-level 'eye'

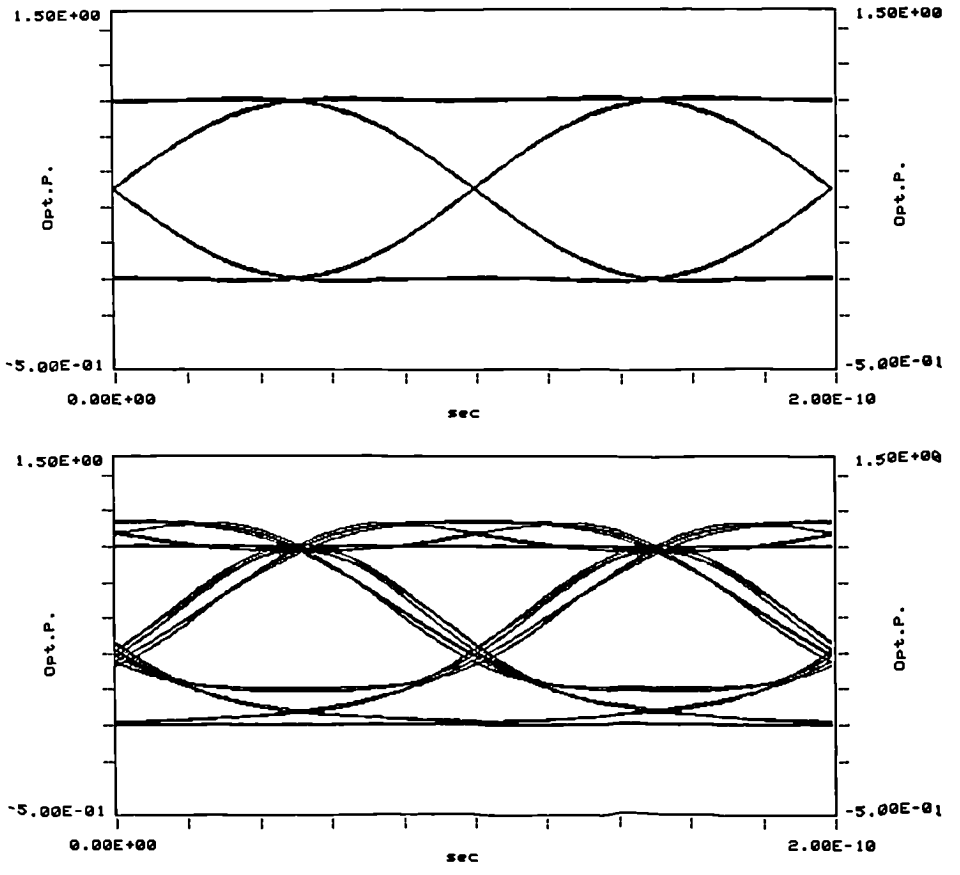

Fig.5.10 3-Level Receiver 'Eye' Diagrams for 0 km (upper) and 85 km (lower), Shape H

diagram, thus necessitating a different overall system optimisation. For the purpose of this study, however, thermal noise dominated receiver performance is assumed. The results and conclusions of the following investigations will therefore provide an indication of the general system behaviour and merit further study for applications with large signal dependent noise.

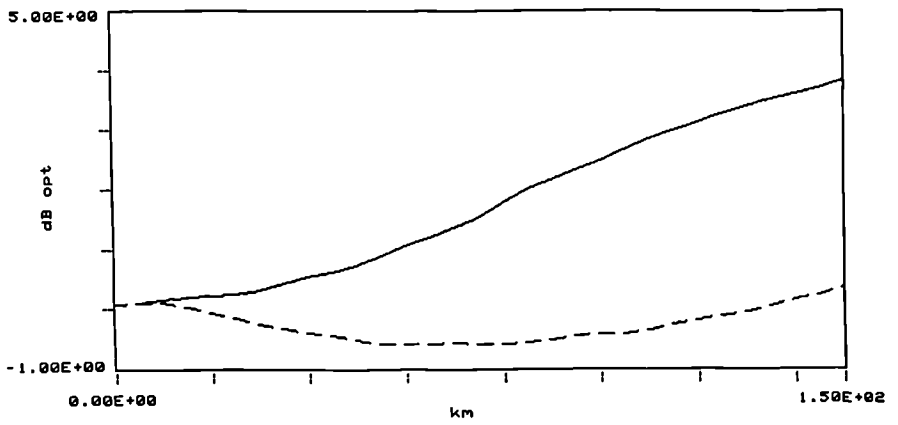

Fig.5.11 Penalty vs Distance for Lower/Upper 'Eye' (solid and broken respectively)

These results for the optical pulse shape H would appear to indicate that three-level detection of binary optical data after dispersive fibre propagation cannot provide any system improvement. However, the particular disadvantage of this and similar pulse shapes is the existence of excessive high frequency terms in the spectrum of the generated data (i.e. large TBP values), combined with a relatively narrow temporal width of the three-level 'eye' opening. This results in the rapid closure of the lower part of the three-level 'eye' after dispersive fibre propagation. Consequently, optical launch pulse shapes which provide for a wider lower 'eye' and a reduced TBP value might be expected to perform better. In Fig.5.12 the system penalty curves are presented for several pulse shapes of interest: shape H for reference (left most curve), followed by shape F (gaussian), shape K (frequency-doubled MZ) and finally shape G (-12.5 dB ISI version). In all cases only the result for the worse, i.e. lower half of the three-level 'eye' is presented. The maximum distances for 1 and 2 dB system penalties are summarised in Table 5.10, including the respective relative advantages over the equivalent binary detection distances of Fig.5.7 and Table 5.6. For shapes F, K and G the results demonstrate a

clear advantage, in the region of 40 % to 90 %. Thus considerable increases in maximum transmission distances are achievable by means of three-level detection of two-level transmitter output signals, after dispersive fibre propagation. However, since the system performance is in all cases limited by the deterioration of the lower half of the three-level 'eye' diagram, there is likely to be some potential for further improvement if the deterioration in the lower and upper halves of the three-level 'eye' diagram could be better balanced.

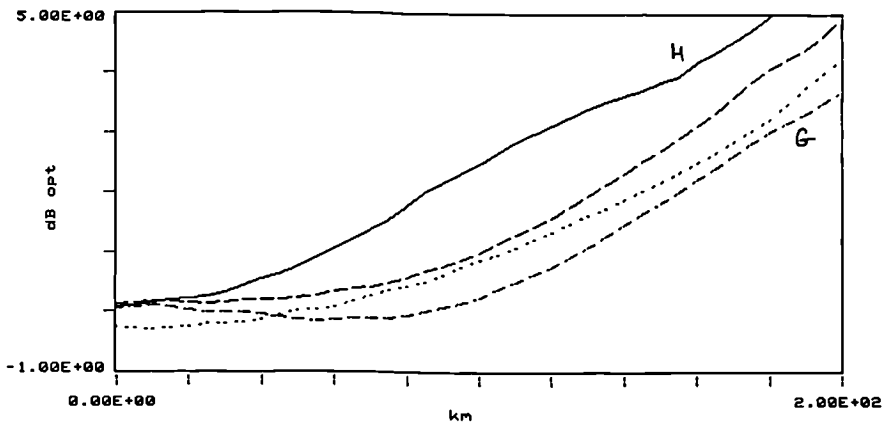

Fig.5.12 System Penalty for Duobinary Detection of NRZ Transmitter Signals (left to right/worst to best: shapes H, F, K and G)

Shape	Description	-1 dB Distance (km)	-2 dB Distance (km)	Improvement re binary(%)
G	$Sech^2$	127.4	154.6	94.2 / 74.1
K	F-Doubling MZ	106.4	143.9	41.9 / 45.5
F	Gaussian	100.3	131.3	42.9 / 39.7
H	Sinus. MZ drive	58.3	85.5	-27.0 /-19.6

Table 5.10 Duobinary Detection of NRZ Launch Pulses

The transmitter modulation scheme of Section IV.3.1 of duobinary electrical data converted into binary optical output was analysed in Section V.4.1 for its performance in the context of binary optical detection. It is also well suited for the improvement of the three-level detection system performances of Table 5.10 above, since as in the case of binary optical detection the choice of modulator bias and electrical data drive amplitude allows for

variations in the exact shape of the (binary) optical pulse train generated, as well as for deliberate reductions in the extinction ratio of the transmitter output signal.

For binary detection, the highest system performance was obtained with V_π peak-to-peak electrical data amplitude and a mean modulator bias of also V_π, resulting in minimum electrical bandwidth and drive power requirements together with a high optical extinction ratio at the transmitter output. If the same transmitter configuration is employed for three-level signal detection after dispersive propagation, the maximum transmission distances are found to be 76.4 km and 120.9 km for 1 dB and 2 dB 'eye' closures respectively, substantially worse than the best results of Table 5.10 above. Although the longer distance of 120.9 km is somewhat better than the equivalent binary detection distance of 107.7 km in Table 5.8, the 1 dB distance is worse at 76.4 km compared with 87.1 km for binary detection. This suggests that no real advantage is being gained as a result of three-level detection after dispersive fibre propagation. The reason is once again that dispersive fibre propagation leads to non-uniform optical signal distortions, with the lower 'eye' of the three-level signal closing more rapidly.

However, the use of a MZ external modulator provides the option to pre-distort the transmitter optical signal through adjustments to the electrical bias and the signal drive amplitude. By this means the optical extinction ratio of the launch signal may be adjusted as well as the asymmetry in the transmitter output 'eye' diagram. A detailed analysis has been carried out of the system performances with various combinations of electrical bias and drive levels, and the system output signal shown in Fig.5.13 for back-to-back

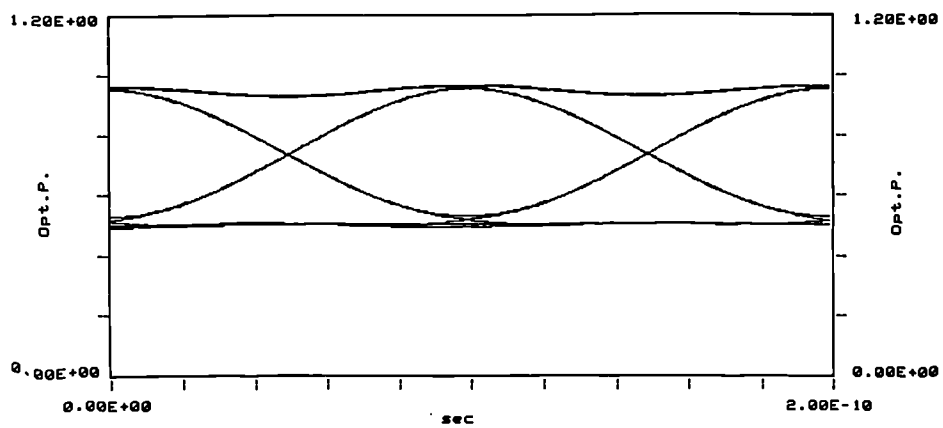

Fig.5.13 System Output 'Eye' Diagram, Without Fibre Dispersion

operation was found to lead to the largest improvements in dispersion limited transmission distances (modulator bias in the "on" position, peak-to-peak drive amplitude of V_π).

The system penalty curves for both the upper and lower 'eye' of the three-level signal are shown in Fig.5.14, demonstrating how some pre-distortion of the transmitter

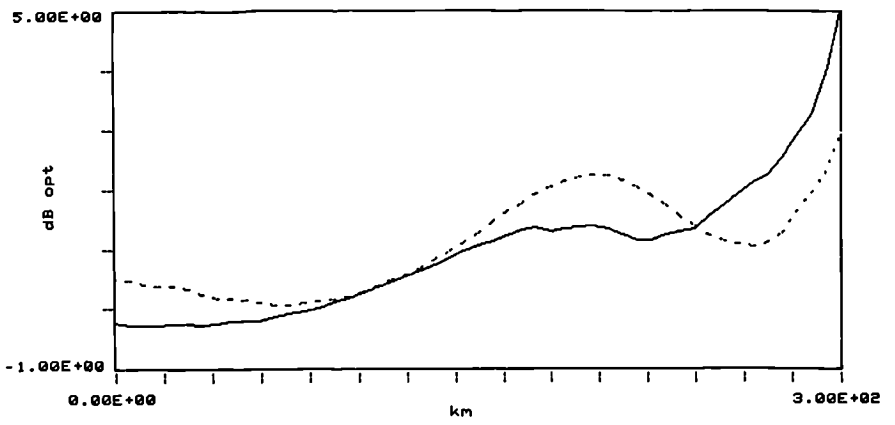

Fig.5.14 System Penalty versus Distance, upper (dashed) and lower (solid) half.

signal may result in a considerable increase in the maximum dispersive propagation distance through balancing the deterioration in both halves of the three-level 'eye' diagram after photodetection. The fibre dispersion limited transmission distances are now 139.2 km for 1 dB and 218.0 km for 2 dB penalty. Moreover, after a brief rise of the penalty curve to beyond 2 dB it decreases again, resulting in a secondary 2 dB distance of 260.3 km. The consequence is an overall improvement of 105 % and 148 % over the best 2 dB penalty distance obtained previously for any of the practical binary system configurations analysed, namely the 106.4 km for binary detection of standard sinusoidal electrical MZ drive in Table 5.6. The results also represent a 41 % and 68 % improvement respectively over the highest performance of any of the basic duobinary detection schemes of binary transmitter data as summarised in Table 5.10.

RZ Transmitter Signal Format :

As demonstrated in Section V.4. for binary detection, substantial differences exist in the system behaviour of RZ format transmitter signals compared with NRZ optical data. In the case of RZ format signals the individual pulses will have gone through their transient

phase during initial dispersive propagation before any interaction with adjacent pulses becomes an issue.

As an example, Fig.5.15 depicts the receiver output 'eye' diagram for 25 psec launch pulses of shape H (sinusoidal drive to MZ) for back-to-back system operation and after 55 km of fibre, for the case of a 10 Gbit/s standard optical receiver designed to provide a raised cosine electrical signal spectrum for NRZ optical input data. Without dispersive fibre propagation, the standard optical receiver has too large a bandwidth. Whilst the central 'eye' is wide open, the two triangles of the three-level 'eye', at 50 psec offset from the normal sampling time for two-level operation, are much reduced compared with

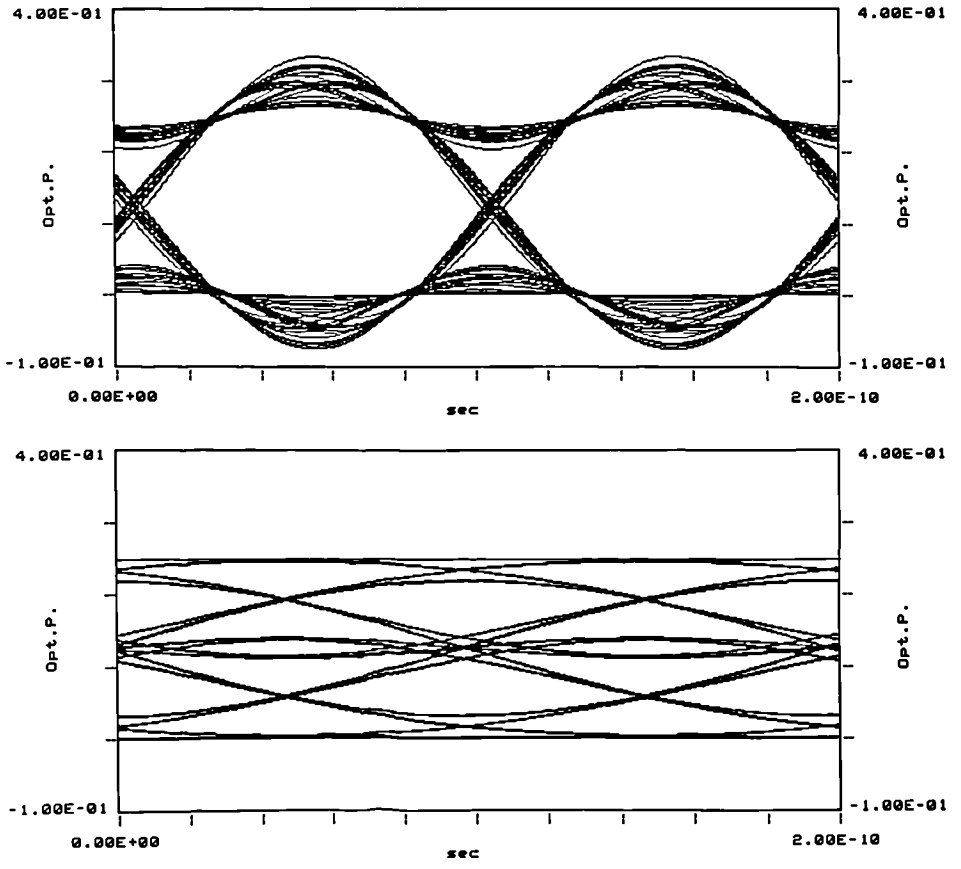

Fig.5.15 System Output 'Eye' for 25 psec Transmitter Pulses with no Transmission Fibre (upper), and after 55 km of Fibre (lower).

a standard 'eye' diagram. After 55 km of fibre, however, a distance at which normal two-level detection has led to system failure with a penalty of 11 dB, the three-level 'eye' is now clearly defined. The system measurement of interest is the opening of the

worse of the two halves (upper and lower) of the three level 'eye' relative to a reference opening. The three level 'eye' opening at 0 km is unsuitable as a reference for the reasons described above, and consequently the reference value has been chosen to be one half of the opening of the binary 'eye' diagram at 0 km.

The results of full system calculations in the form of the three-level 'eye' openings as a function of transmission distance are summarised in Fig.5.16. The five pulse shapes analysed are the same as employed in the study of RZ signal fibre propagation with binary detection in Section V.4.2 above.

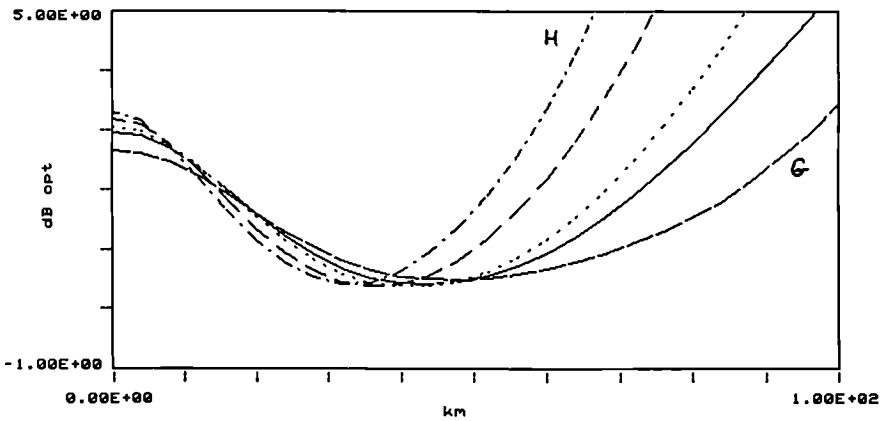

Fig.5.16 System Penalty as a Function of Distance for Three-level Detection of 25 % RZ Transmitter Signals (Shapes H, E, K, F and G in order of increasing performance).

For back-to-back operation a considerable penalty of approximately 3 dB is obtained for all pulse shapes in addition to the fundamental 3 dB reduction in 'eye' opening, as a result of the combination of RZ optical signal format and the receiver transfer function appropriate for NRZ signalling. The situation improves with propagation distance, and after 40 to 50 km the penalty is reduced to no more than 0.5 dB as a three-level signal of standard shape emerges. At longer transmission distances, the fibre dispersion effects become excessive and the penalty curves begin to rise again. Worth noting is that from the point of minimum penalty onwards the penalties rise slowly and in a controlled manner without the "penalty threshold" effect of the RZ signal propagation results with binary detection (Section V.4.2). To demonstrate the differences Fig.5.17 displays both the binary and duobinary detection results for the three leading pulse shapes, namely $Sech^2$,

Gaussian and F-doubling MZ. Since for longer distances the rate of increase in system penalty is also reduced for duobinary detection, the duobinary approach does provide a stable system configuration in which the system penalties develop in a controlled manner as required for practical system operation.

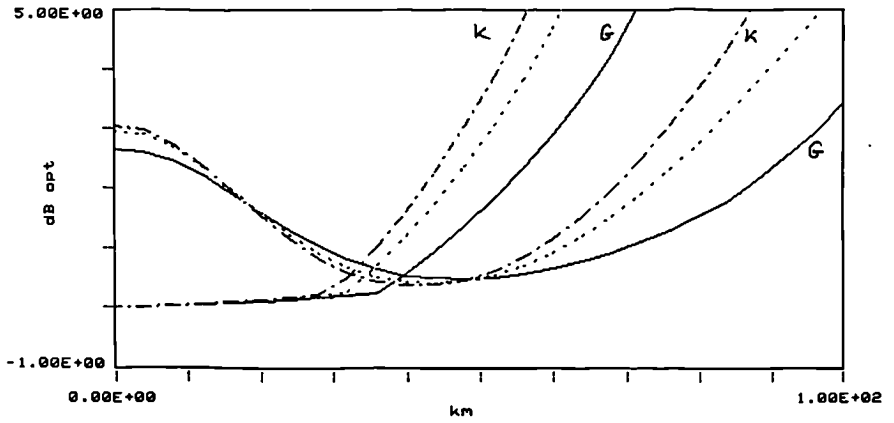

Fig.5.17 Comparison of System Penalties for Binary and Three-Level Detection for Shapes K, F and G (in order of increasing performance).

Details of the maximum distances for 1 and 2 dB system penalty are summarised in Table 5.11 for the five pulse shapes, together with the relative improvement over straight RZ data transmission with binary detection.

Shape	Description	-1 dB Distance (km)	-2 dB Distance (km)	Improvements re binary (%)
G	$Sech^2$	69.8	86.5	56.5 / 62.3
F	Gaussian	61.1	73.0	59.1 / 60.1
K	F-Doubling MZ	58.1	68.2	61.8 / 60.8
E	Sinusoidal	50.1	58.8	61.6 / 62.0
H	Sinus. MZ drive	44.7	52.6	60.2 / 61.8

Table 5.11 System Lengths for Three-Level Detection of 25 psec, 10 Gbit/s Signals

The results demonstrate that by allowing a 3 dB penalty in the effective 'eye' opening through changing from binary to duobinary detection, the maximum dispersion limited transmission distances for 25 % RZ data transmission may be extended by approximately

60 % compared with standard binary detection for all the five optical pulse shapes investigated. The resulting −1 dB and −2 dB distances of 69 km and 86 km for the highest performing pulse shape ($Sech^2$) represent only a ≈ 20 % reduction on the best NRZ transmission configuration of Table 5.6, inspite of the 25 % RZ pulse format with its associated increase in optical signal bandwidth.

V.4.5 Duobinary Transmitter Signals

Since three−level detection has been shown to provide under certain circumstances a substantial improvements in the overall system performance for standard binary signalling of NRZ or RZ format, the potential needs to be analysed for further improvements through full three−level optical transmission.

Firstly three−level optical data generation is required. Secondly, the optical detection bandwidth is to remain as for binary NRZ line signals in order to limit the amount of ISI introduced on the three−level signal and after dispersive fibre propagation. The system penalty after long distance fibre propagation will then be due to distortions in the received three−level signal. However, as a result of the unipolar nature of the optical power signal the distortions will in general be different in the two halves of the overall three−level 'eye' diagram. In the following, several system configurations are analysed in order to establish whether under these conditions three−level signal detection of three−level transmitter launch signals may provide any advantage in the context of dispersive fibre propagation at multi−Gbit/s system line−rates. Improvements in the overall system performance could be expected due to the signal baseband bandwidth as well as the optical domain bandwidths being reduced considerably compared with binary transmission, suggesting much increased tolerance to path dispersion. On the other hand, a three−level unipolar signal might suffer excessively from asymmetric signal distortions, leading to large discrepancies between the upper and lower halves of the signal 'eye' diagram.

The generation of an optical three−level signal may be carried out by applying a bandwidth limited version of the original electrical binary signal directly to the modulator.

This approach has already been presented in Section IV.3, both for conversion of electrical duobinary to optical binary format (Figs.4.13 and 4.14) and for electrical duobinary to optical duobinary format (Fig.4.11). In the latter case, a peak-to-peak electrical signal amplitude of V_π and a modulator mean bias point of $V_\pi/2$ result in an optical three-level signal of maximum peak level and high optical extinction ratio.

However, as in the case of electrical duobinary to optical binary signal conversion a number of combinations of bias levels and signal amplitudes are possible with each resulting in particular modifications to the generated optical three-level signal shapes. The basic configuration of Fig.4.11 can be expected to suffer from the problem of asymmetric signal distortion after fibre propagation, with the upper part of the three-level 'eye' remaining open, initially maybe even increasing in size as optical power from the adjacent full height pulses disperses, and the lower part of the 'eye' closing relatively quickly. This has been confirmed through full system calculations, and unless otherwise stated, in the following the penalty curves are given for the worse affected half of the three-level 'eye'.

In order to counter the asymmetric pulse distortion, changes in the electrical modulator bias and drive levels may be employed, for example with a peak-to-peak amplitude of $V_\pi/2$ instead of V_π. Due to the non-linear modulator transfer function this leads to no more than a $\approx$ 30 % reduction in the modulated optical signal peak-to-peak amplitude, accompanied by a reduction in optical extinction ratio down to approximately 5.7 to 1. The result of this modification, however, is considerable in terms of dispersive propagation performance, as demonstrated with the system penalty results for both drive amplitudes in Fig.5.18. The 1 dB and 2 dB penalty distances are 123.6 km and 167.7 km respectively for full V_π electrical drive, but are increased to 153.1 km and 199.6 km for $V_\pi/2$ electrical modulation amplitude. In both cases the lower part of the three-level 'eye' limits the performance after dispersive signal propagation as discussed above for unipolar signal values in the case of a symmetrical transmitter output signal. In order to compensate for this asymmetry the transmitter bias point may be adjusted such that the three-level optical launch 'eye' becomes asymmetric, in order to predistort the optical signal by providing an enlarged lower and reduced upper opening of the 'eye' diagram.

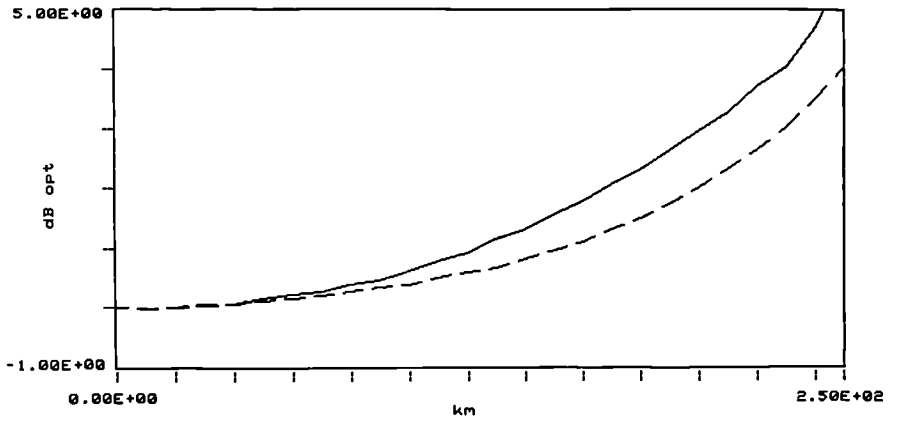

Fig.5.18 System Penalty for V_π (solid) and $V_\pi/2$ (broken) Modulator Drive Amplitudes

Fig.5.19 displays the back-to-back system output 'eye' for a modulator bias point of $0.4 \cdot V_\pi$ and an electrical signal peak-to-peak amplitude of $0.5 \cdot V_\pi$. Due to the reduction in electrical drive level combined with the chosen modulator bias point reduced peak-to-peak optical modulation is obtained as well as a limited optical extinction ratio of just below 3 to 1. The system penalty curves as a function of fibre length for both halves of the 'eye' diagram have been normalised to the mean value of the lower and upper 'eye' openings for 0 km (Fig.5.20). The maximum distances are now 173.7 km and 211.7 km for 1 dB and 2 dB penalty respectively. Minor improvements in these values may be obtained through additional bias point and drive level adjustments, at the expense of a larger starting penalty in the initially worse half of the 'eye'. As an example, a further increase in the mean optical signal level by means of an electrical modulator bias of $0.35 \cdot V_\pi$ leads to the initial penalty increasing to around 1 dB rather than the 0.5 dB

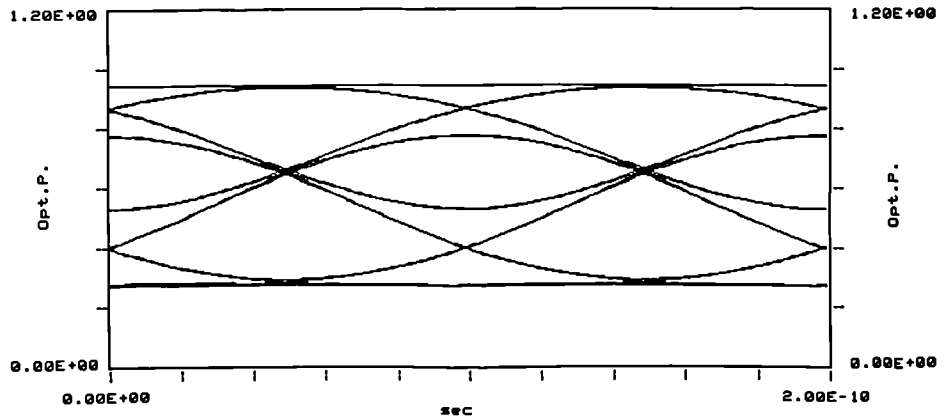

Fig.5.19 System 'Eye' Diagram for Pre-Distorted Transmitter Output

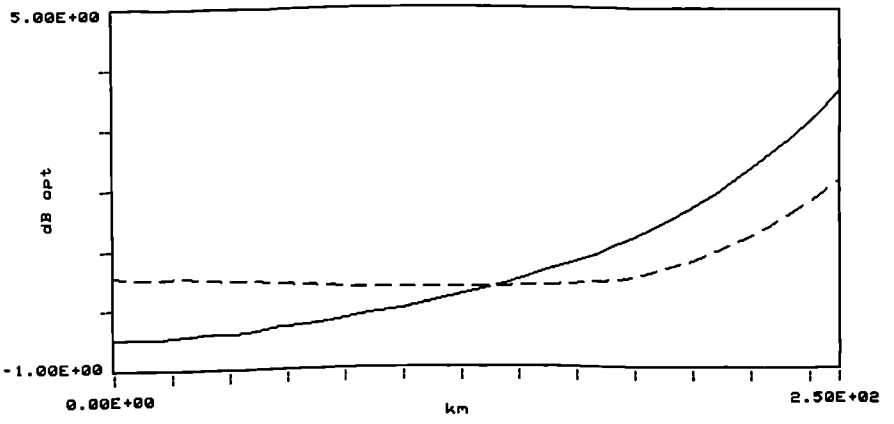

Fig.5.20 System Penalties for the Upper (dashed) and Lower (solid) half of the Three-Level 'Eye'Diagram, for a Modulator Bias of $0.4 \cdot V_{\pi}$, and a Drive Amplitude of $0.5 \cdot V_{\pi}$

shown in Fig.5.20 for the worse half of the 0km three-level system 'eye' diagram. However, some "recovery" takes place such that a 1 dB penalty distance may still be computed. The 1 dB and 2 dB system penalty distances then increase to 180.7 km and 216.4 km, respectively.

Consequently, the highest overall system performance in terms of 1 and 2 dB system penalty distances is generally obtained with a three-level optical transmitter signal and three-level optical detection. Three-level detection of suitably pre-distorted binary optical transmitter signals may result in maximum dispersive fibre transmission distances of similar magnitude at the 2 dB penalty level, with some particular system configurations out-performing three-level detection of three-level launch signals as described in V.4.4 above. However, full three-level optical signal transmission has the overall advantage of requiring lower bandwidth transmitter components and providing a substantially longer propagation distance over which low system penalties below 1 dB are achieved, as demonstrated in the above examples with 174 km (Fig.5.20) for full three-level signalling compared with 139 km (Fig.5.14) for three-level detection of binary launch signals.

V.5 OTDM SYSTEM PERFORMANCE

In Chapter IV several techniques have been presented for the implementation of OTDM multiplexing and demultiplexing of optical data streams in order to facilitate the generation and processing of ultra-high capacity time domain signals without the need for corresponding processing speeds in the electronic domain. In this chapter the system performance investigations have so far been based on the basic optical signal shapes and formats of interest, without reference to the method of optical data generation employed. Also, the calculations of system dispersion penalties and limits have been based on optical detection at the receiver being carried out at the full line-rate. Consequently, it is now appropriate to address the overall system performance issues for full OTDM configurations employing optical demultiplexing prior to optical detection.

Three basic configurations will be analysed:

- A point-to-point transmission system of given line capacity. The main issue is the extent to which the end-to-end system performance depends on whether full line-rate optical detection is carried out first followed by electrical processing, or optical processing precedes optical detection.

- The inclusion of optical line processing elements in order to provide simple line regeneration for extended range high speed transmission. Any limitation in the end-to-end power budget is assumed to be taken care of by means of optical amplification, thus permitting system optimisation purely in terms of reducing fibre chromatic dispersion effects.

- Full OTDM network operation. This includes long distance fibre propagation in the individual low speed tributary input channels before optical multiplexing, fibre propagation of the full line-rate OTDM signal, and further propagation of the optically demultiplexed output signals.

V.5.1 Optical Sampling ahead of Photo Detection

At ultra-high bit-rates a point-to-point transmission system based on optical time division multiplexing as discussed in Chapter IV employs optical processing for the purpose of facilitating ultra-high speed optical data manipulation without the need for electronic signals beyond the frequency of the line-rate of the individual input and output data channels. The demultiplexing operation represents an optical sampling process on the full line-rate optical data stream. After dispersive fibre propagation the choice of a particular sampling scheme will have consequences beyond the issues of data pattering discussed in Chapter IV. In particular, a sampling window of duration equal to the line signal bit-interval results in both the wanted pulse energy and all the dispersed energy from adjacent time slots to be passed onto the optical receiver, whilst an optical sampling window substantially narrower than the bit-interval results in a true optical time sample to be taken. Since after dispersive fibre propagation the level of optical interference may vary across the bit-interval (e.g. energy from adjacent time slots present near the time slot boundaries but not at the centre), optimally-timed optical sampling prior to optical detection, followed by electrical threshold detection, might allow improvements in the end-to-end system performance.

In the context of OTDM signal processing a choice is automatically required regarding the relative duration of the sampling window in the demultiplexer. The same principle may be applied to standard transmission with full line-rate optical detection where the introduction of an optical sampling gate prior to photodetection may be beneficial in the context of dispersive fibre propagation. It is this basic system configuration which will now be analysed to establish the magnitude of achievable system performance improvement.

In order to allow a direct comparison with the standard detection results of Section V.4.1 optical transmission will be considered at the same data rate of 10 Gbit/s over dispersive fibre. The numerical system model has been enhanced such that after standard data generation and dispersive propagation optical sampling is carried out with adjustable sampling pulse shape, pulse width and sampling time, followed by standard optical

detection and analysis of the system output 'eye' diagram. Computation of the 'eye' opening for a sufficient number of distance values finally results in the plot of system penalty as a function of transmission distance. As in the case of OTDM demultiplexing, a variety of optical sampling pulse shapes are available, and for the purpose of this study two shapes of practical interest have been analysed, namely the gating shape obtained from standard sinusoidal electrical drive to a MZ modulator (shape H), and the shape obtained with $2 \cdot V_{\pi}$ electrical drive to a MZ modulator (shape K). The relative sampling window width has been varied from 50 % to 10 % of the bit-interval in order to investigate the dependence of the overall system performance on the sampling pulse characteristics. Fig.5.21 summarises the results for 10 Gbit/s NRZ transmitter operation (pulse shape H), for a sampling shape of type K. Also included is for comparison the system penalty curve for standard detection without optical sampling.

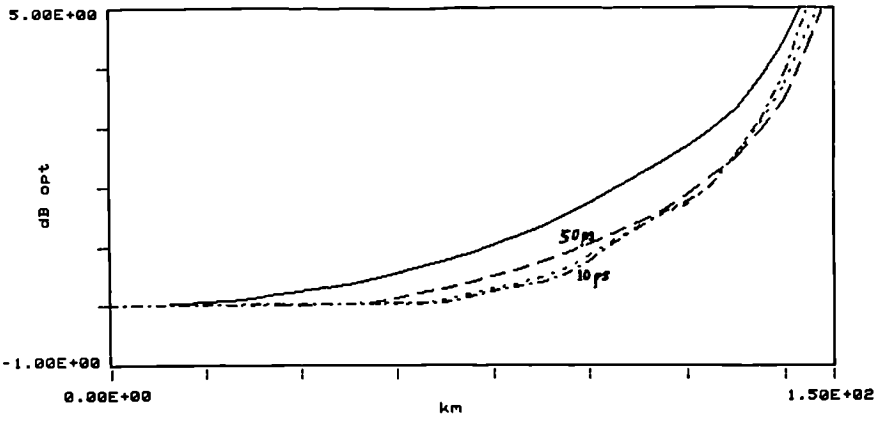

Fig.5.21 System Penalty versus Transmission Distance at 10 Gbit/s with Optical Sampling before Detection, in the order of increasing performance: no sampling; 50 psec sampling; 25 psec sampling; 10 psec sampling.

For all three values of sampling pulse width some system improvement is obtained, such that the −1 dB distance of 80 km for standard detection improves to 99km, 103 km and 104 km for 50 %, 25 % and 10 % optical sampling widths, respectively. The reason for this considerable improvement in maximum distances of 24 % to 30 % lies in the difference between the optical signal shape at the receiver input and electrical signal shape after detection. For small values of fibre dispersion, energy from adjacent time slots has dispersed to some extent into the interval under consideration, without though reaching its

centre. Whilst optical sampling at this point therefore results in a low level of effective ISI, optical detection and low-pass filtering without prior optical sampling leads to all optical ISI present across the whole bit-interval to be passed on to the electrical domain, followed by spreading of the interfering signals due to bandwidth limiting in the receiver. For high levels of fibre dispersion, however, optical interference occurs across the whole bit-interval. As a result, little advantage can be gained from optical sampling prior to detection once the system penalty without optical sampling has risen beyond 4 to 5 dB.

For the same reasons, the system improvements are identical for all three sampling window widths in the case of limited fibre dispersion (e.g. up to approximately 60 km in Fig.5.21). At higher dispersion values reductions in sampling width below 25 % of the bit-interval show a rapidly diminishing return in terms of system performance improvements, due to the relative sampling width beginning to represent a good approximation to a sampling impulse. The particular shape of the sampling window should for the same reasons be of limited importance in the case of narrow sampling windows, whilst for relatively wide sampling there may be some effect. Recalculation of the above results for a sampling shape of type H rather than K revealed that even for 50 % relative sampling width only minor changes were obtained in the overall system penalty curves, with no discernable differences for 25 % and below. This confirms that the relative sampling window duration rather than the exact shape is determining the system performance.

These results demonstrate that optical sampling with sampling widths of 10% to 50% of the bit-interval may be employed prior to photodetection in order to achieve improvements in the maximum dispersion limited transmission distances of up to 30 %. In principle the same improvements could be obtained without optical sampling, by means of substantial increases in the optical receiver detection bandwidth, combined with ultra-high speed electrical sampling and threshold detection. However, apart from the difficulties of the electronic processing speeds required, the large optical detection bandwidth required would result in a substantial reduction in receiver sensitivity, thus not allowing practically required system power budgets to be achieved.

For an OTDM environment in which optical sampling already takes place the above results indicate that subject to overall system power budget constraints an optical demultiplexing process based on short optical sampling windows will improve the dispersive propagation system behaviour, especially in the low system penalty regime in which optical transmission systems normally operate.

V.5.2 Optical Line Signal Regeneration

As identified in Section V.4.2 above the propagation of low duty-cycle RZ optical pulses leads to a particular characteristic in the system penalty versus propagation distance curve, with the penalty increasing slowly during initial propagation when all the pulse energy is still contained within the original bit-interval, followed by a sudden and steep rise when pulse energy begins to spill over into adjacent time slots. This particular behaviour may be exploited in the context of repeatered systems by introducing optical sampling at regular intervals in order to reduce the optical pulse width back to its original value, just before the pulse broadening extends to beyond the bit-interval. Since the optical RZ format data stream contains a strong clock component, timing extraction, whether of traditional electrical nature after photodetection of some of the signal or based on novel optical techniques [Jinno and Matsumoto], [Barnsley, Wickes, Wickens and Spirit]) can easily provide the required clock signal to drive a local sampling gate. As a result, further dispersive signal propagation is possible, leading to total transmission distances well beyond the chromatic dispersion limits analysed above. The principle is illustrated in Fig.5.22. The fibre span between the RZ format signal source (e.g. OTDM demultiplexer output) and the optical receiver is replaced with a series of fibre spans and optical sampling gates, with optical amplification stages compensating for fibre span and sampling losses. The optimum position of the optical gain stage depends on the system application, however a good system noise performance will usually be obtained with the configuration of Fig.5.22. If each fibre span is limited in length such that dispersive pulse broadening does not extend beyond the limits of the bit-interval, the system penalty after

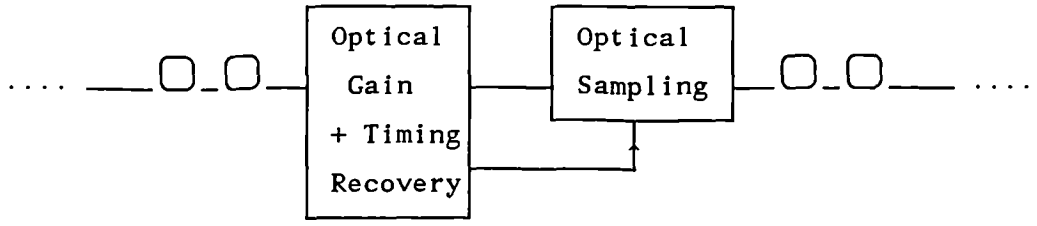

Fig.5.22 Optical Sampling Gates as In-Line Repeaters

each processing stage can be expected to return to approximately the same value as at the beginning of the previous span, thus allowing large numbers of stages to be cascaded subject to a satisfactory optical signal-to-noise ratio being maintained. The results of some example system calculations for 10 Gbit/s RZ format data are summarised in Fig.5.23 and Fig.5.24. The optical pulse shape at the transmitter output is chosen to be of type K, as is the shape of the optical sampling gates. After each regeneration stage the signal amplitudes are adjusted such that the mean signal power is restored, since a considerable percentage of the pulse energy is lost in the sampling process. This could be implemented straightforwardly by means of doped fibre amplifiers with a minimum level of amplifier control complexity. Fig.5.23 displays the resulting system penalty in terms of 'eye' closure as a function of distance for a launch pulse of 25 % duty cycle (25 psec at 10 Gbit/s) and for a sampling width of also 25 %. Processing takes place at 20 km, 40 km and 60 km total transmission distances. Fig.5.24 presents the equivalent result for a 10 % RZ transmitter format (10 psec pulses), also with 10 psec wide processing. The increase in optical bandwidth due to the shorter optical pulses necessitates more frequent optical

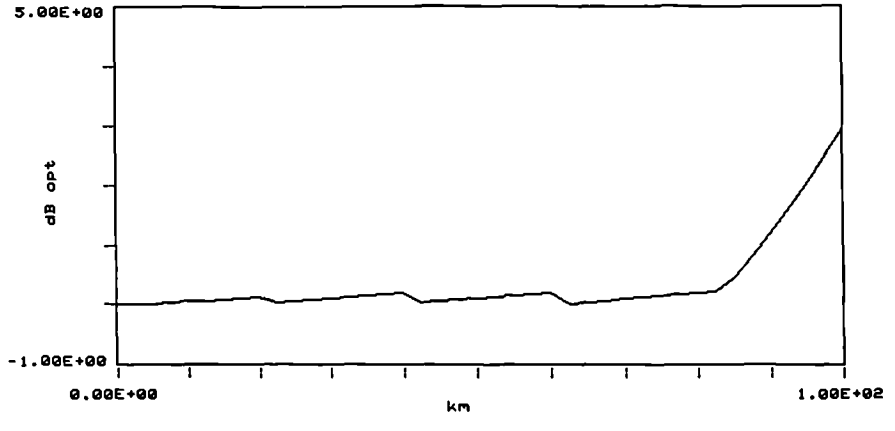

Fig.5.23 System Penalty for 25% RZ Format Data and 20 km Sampling Intervals

processing, implemented at 10 km intervals up to the last stage at 80 km. The penalty curves demonstrate that although a shorter pulse width requires shorter distances between reshaping stages, system operation is possible with dispersive system penalties not exceeding 1 dB, even after a large number of optical sampling stages.

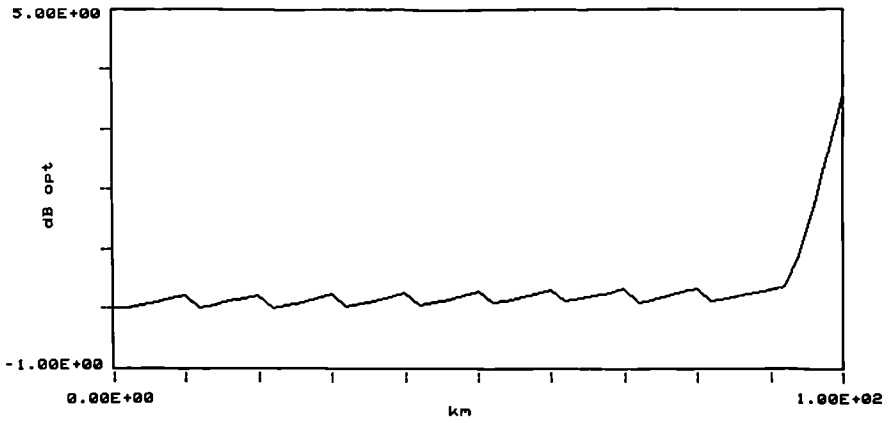

Fig. 5.24 System Penalty for 10 % RZ Format Data and 10 km Sampling Intervals

If the fibre propagation distances between reshaping stages become too large, the system penalty builds up substantially during each span. Fig.5.25 demonstrates this with a result for the 10 % RZ format data system of Fig.5.24, but with the individual spans extended from 10 km to 15 km. This allows in each fibre span dispersive propagation to just beyond the penalty threshold point in the basic performance curve described in Section V.4.2, Fig.5.9. As a result, the overall system penalty increases from span to span, allowing only a limited number of cascaded stages before the end-to-end system penalty reaches values too large for satisfactory system operation.

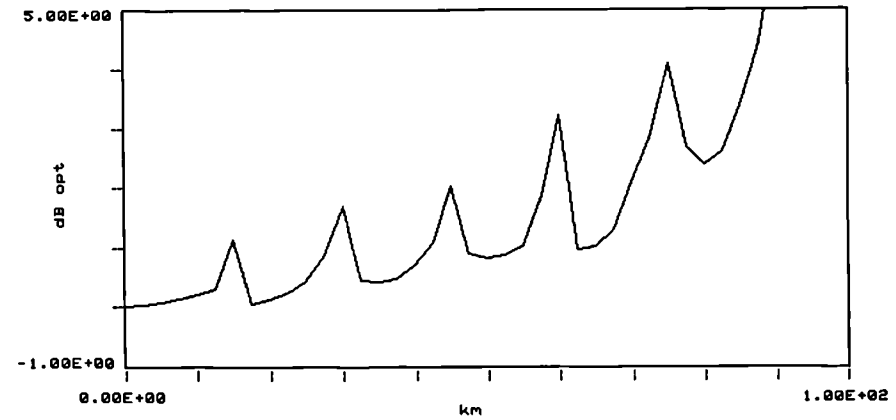

Fig. 5.25 System Penalty for 10 % RZ Format Data and 15 km Sampling Intervals

The results of Fig.5.23 and Fig.5.24 demonstrate how substantial increases are achievable in the overall transmission distance by means of relatively simple signal reconditioning, through optical sampling gates driven by a clock signal extracted from the line signal itself. The importance of this approach lies in the fact that only processing elements are required which operate at the clock frequency of the tributary data channels (single frequency or with a limited number of harmonic terms), just as identified in Chapter IV for efficient low frequency OTDM data processing.

V.5.3 OTDM Networks

If the concept of a point-to-point OTDM system is extended to optical time domain networking through the inclusion of fibre transmission spans before the optical multiplexer as well as after the demultiplexer (Fig.5.26), consideration needs to be given to the resulting overall end-to-end system performance. The propagation in the tributaries and along the centre span are in general not independent of each other. In the following, only the limits imposed by fibre chromatic dispersion will be discussed, networking issues such as for example the time domain synchronisation of the tributary channels at the multiplexer input are beyond the scope of this study. However, for the case of a two-channel system, an analysis has been presented [Lord, Blank, Boggis, Bryant and Stallard] which addresses the problems due to variations in the group delay of the physically separate thus independent tributary fibres, together with experimental results demonstrating the feasibility of closed loop control.

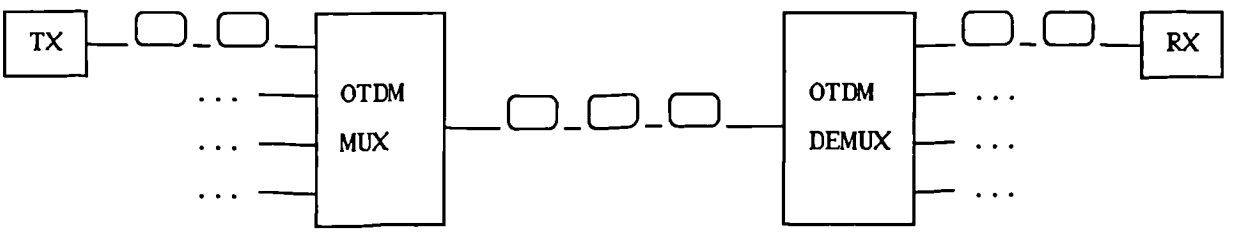

Fig.5.26 An OTDM Transmission Network

The basic situation is unchanged as far as the ultra-high line-rate transmission in the centre transmission span between the multiplexer and demultiplexer is concerned. However, the additional requirement is now that the effects of any chromatic dispersion before the multiplexer and after the demultiplexer must also be taken into account to ensure satisfactory end-to-end performance.

On the multiplexer side, two system configurations are of interest as discussed previously in Chapter IV, namely NRZ format data on the input fibres which requires an active multiplexer, or RZ format optical data with optical pulse widths suitable for passive interleaving at the multiplexing point. In the first case, the optical pulse broadening in the tributaries must remain sufficiently small such that it does not extend too close to the centre of adjacent time slots where the narrow-width optical sampling of the incoming data will be performed. Consequently, the maximum permissible distances are equal to the propagation distances of a standard NRZ transmission system at the same line-rate which employs optical sampling ahead of photodetection, as discussed in V.5.1 above. In the case of an RZ optical signal format on the input tributaries, the multiplexer may then take the form of a passive optical combiner, in which case the whole transmission span from the tributary transmitters to the input of the demultiplexer becomes effectively one single propagation system, with the dispersion limit determined by the total distance. If an active multiplexer is to be employed, RZ transmitter pulses would not provide any advantage over NRZ format signals, since RZ optical pulse propagation in the tributaries only limits the dispersion limited maximum tributary lengths. If however RZ signal format were to be used, the active multiplexer would play the same role as an optical gating regeneration stage described in V.5.2 above, leading to the same requirements on maximum propagation distance in order to avoid end-to-end system penalties.

The situation is somewhat simpler after the demultiplexer output where each output fibre contains an optical data pulse train of RZ format. Consequently, the analyses of RZ format data propagation and detection apply as presented in Sections V.4.2 and V.4.4 above for the identification of maximum fibre spans between the demultiplexer output and the optical receivers. In order to maximise the achievable transmission distances up to the

optical receiver it will therefore be a major advantage if the optical demultiplexing process results in one of the better performing optical pulse shapes, such as $sech^2$, gaussian, frequency-doubling MZ (shape K), or a similar pulse shape of low optical time-bandwidth product. In addition, optical processing may be employed at specific points along the transmission path in order to reshape the propagating signals, as detailed in V.5.3 above.

For any particular overall system configuration of interest, a full performance analysis may then be carried out by means of modelled signal propagation through the cascaded sequences of processing devices and fibre spans, such that an overall system penalty may be computed relative to a back-to-back system reference point.

V.6 SUMMARY

In this chapter the end-to-end system performance limitations have been identified which result from the effects of fibre chromatic dispersion in ultra-high speed digital optical data transmission systems. After an initial analysis of the expected relative system performance of a variety of optical pulse shapes, based on only their optical time bandwidth products, a detailed numerical analysis of the actual pulse propagation behaviour has been carried out, followed by full system performance calculations based on receiver output signal 'eye' diagram evaluations for pseudo-random digital test data sequences. The modeling has confirmed that for NRZ optical signal formats the optical pulse time bandwidth product does not provide a reliable basis for estimating system performance, whilst for low duty-cycle RZ format optical signals the end-to-end performance may be analysed based on only the knowledge of the pulse time bandwidth product, the pulse width, the bit-interval and the fibre chromatic dispersion parameter.

After identifying the optical pulse shapes which provide the lowest system penalties for a given propagation distance, several methods have been investigated for increasing the maximum chromatic dispersion limited transmission distances. Firstly, three-level optical detection of binary transmitter signals was found to allow substantial increases in system

lengths, with further improvements available by means of optimised three-level optical signal generation in the transmitter combined with three-level receiver detection. Overall improvements in dispersion limited propagation distances compared with standard binary transmission were found to be as high as 100 % in some cases, such that the maximum system length for 10 Gbit/s operation over high dispersion fibre may be increased from approximately 100 km to as much as 200 km, with one particular configuration providing a result of 260 km for a 2 dB system dispersion penalty.

In the context of transmission systems employing OTDM channel processing as discussed in detail in Chapter IV, the resulting ultra-high speed line signals of RZ and possible also NRZ format lead to substantially reduced maximum transmission spans. The final part of the chapter therefore has been concerned with the system improvements which may be obtained through relatively simple processing (2R regeneration), carried out directly in the optical domain without the need for optical detection, electrical processing and signal conversion back to the optical domain, which is normally assumed to be necessary in dispersion limited optical transmission systems. The potential has been demonstrated for considerable increases in the maximum transmission distances of fibre chromatic dispersion limited systems. In standard binary systems optical sampling prior to photodetection may provide up to 30 % increases in transmission spans, and in the context of ultra-high speed OTDM system configurations 2-R line regeneration allows large numbers of fibre spans to be cascaded.

The fact that for ultra-high speed OTDM system operation optical pulses of $sech^2$ or similar shape provide the overall highest system performance is an important result. It means that for linear fibre propagation analysed here, the highest performing pulse shapes are the same as are required for non-linear (soliton) propagation, [Hasegawa and Kodama]. If the step-index fibre assumed in this study is replaced with low dispersion fibre (e.g. dispersion shifted fibre for operation at 1.55 μm signal wavelength) as might well be envisaged for future high capacity back-bone transmission networks, the resulting increases in linear dispersion limited transmission distances lead to non-linear fibre propagation effects accumulating sufficently to begin to dominate the system behaviour.

Especially at ultra-high line-rates it is then important that the optical transmitter pulses are as close as possible to the ideal $sech^2$ waveform for soliton propagation [G.N.Brown, I.W.Marshall and D.M.Spirit]. With the recent practical demonstrations of the feasibility of non-linear system operation at ultra-high line-rates [Wickens, Spirit and Blank (2)], the OTDM multiplexing approaches and optimum signal shapes identified in this work will lend themselves to applications in both notionally linear propagation systems which are dominated by large linear fibre dispersion over relatively short propagation distances thus experiencing negligible non-linear signal distortion, and in long-distance non-linear propagation systems in which the fibre non-linearity is employed to counteract linear dispersive pulse broadening. Thus the same transmitter signal shapes and optical multiplexing and processing stages may be employed for systems based on either linear or non-linear fibre propagation, and also for future OTDM networks which may utilise both linear and non-linear propagation, depending on the transmission spans and individual capacities of the various tributaries and back-bone links.

CHAPTER VI

CONCLUSIONS AND RECOMMENDATIONS FOR FUTURE WORK

CONCLUSIONS

This thesis has investigated the potential for increasing the overall performance of intensity modulated high capacity optical transmission systems based on electronic as well as optical time division multiplexing. Two fundamental system limitations have been considered. Firstly, the maximum operating speed of electronic multiplexing equipment and the bandwidth limitations of opto-electronic devices such as lasers and modulators provide a limit to the achievable data-rate. As a solution, optical time division multiplexing allows substantial increases in the maximum system capacity based on the same opto-electronic devices. Secondly, chromatic dispersion in monomode optical transmission fibre leads to maximum achievable propagation distances which reduce rapidly with increasing optical line-rate. Appropriate choices of optical pulse shapes and signal formats have been found to permit substantial increases in the maximum system length for a given line-rate compared with conventional NRZ signalling.

The starting point for this study has been the development of a series of computer programs to model the end-to-end signal transfer characteristics of a range of optical transmission system configurations. In Chapter II a summary has been provided of the characteristics of the main system components under consideration, followed by a description of the approach taken in this study towards the evaluation of overall system performance. On the transmitter side, the options available for signal conversion from the electronic into the optical domain range from directly modulated Fabry-Perot and Distributed Feedback semiconductor lasers to external amplitude modulators. The choice of transmitter source and modulation approach dominates the overall system behaviour as far

as signal deterioration due to fibre chromatic dispersion is concerned. With the assumption of suitable optical amplification techniques being available to overcome device insertion losses and path propagation losses, it is the fibre dispersion which leads to the overall system limitations.

Chapter III has provided examples of the system limitations for a range of standard configurations, from Fabry-Perot laser sources combined with low dispersion fibre to external modulation over high dispersion fibre. Model results have been validated by means of comparisons with experimental results obtained as part of this work as well as through comparison with results published by other workers. These allow conclusions to be drawn as to the capacity and distance limitations of the system configurations of practical interest. In particular, it has been found that system operation based on Fabry-Perot lasers and low-dispersion fibre may allow impressive performances to be achieved (experimental results of 2 Gbit/s over 100 km and 5 Gbit/s over 50 km), if sufficient control is available over the laser and fibre spectral characteristics. On the other end of the performance scale, the advantages of ideal external modulation may under certain circumstances be matched by direct optical phase or frequency modulation of a semiconductor DFB laser, allowing both approaches to achieve 10 Gbit/s data transmission over at least 60 to 70 km of standard step-index monomode fibre at 1.55 μm operating wavelength. Higher system speeds, however, present a major problem, not only due to the difficulties of electronic multiplexing but also as a result of the limitations in the intrinsic direct laser modulation response. Direct intensity modulation in particular is limited by the slow laser response during optical turn-off.

In Chapter IV techniques have been presented for the generation and processing of ultra-high speed optical TDM line signals. These are based mainly on opto-electronic devices with the same characteristics as discussed for standard system operation in the previous chapters. For the implementation of OTDM system configurations Mach-Zehnder external modulators in particular (independent of the device technology employed such as Lithium Niobate, Polymer, or Semiconductor) have been found to be able to satisfy the three main requirements for signal processing, namely short pulse generation, efficient data

modulation and optical pulse selection or demultiplexing.

The generation of optical pulse trains with appropriate pulse durations and repetition rates is known to be achievable in several ways, through direct laser modulation (gain switching or mode-locking), and laser PSK or FSK modulation with optical demodulation, all of which are highly sensitive to small variations in the operating point of the laser device employed. In this work external modulation techniques have been analysed which allow the separation of the generation of the optical carrier signal and the actual pulse creation or shaping process, thus providing for stability and reproducibility.

After the generation of suitable optical pulse trains at the pulse repetition rate of the tributary channels data modulation is required, preferably with minimised drive bandwidth and power requirements to reduce system complexity. Various configurations have been analysed with the following main results:

i) The electrical domain modulator bandwidth may be reduced to approximately one quarter of the tributary line clock frequency whilst still allowing correct binary data modulation in the optical domain. This is achieved via conversion to three-level electrical signals before the modulator, with appropriate modulator operating conditions selected to perform automatic decoding back to a two-level modulated optical signal. Suitable electrical data precoding may be employed to achieve correct conversion of the original binary electrical data to binary optical signals.

ii) The optical modulator may be employed to perform a conversion of directly modulated laser data in optical NRZ format to optical RZ format, suitable for subsequent OTDM interleaving. From a systems point of view optical excess bandwidth associated with direct laser modulation (wavelength chirp) is removed in the process, thus permitting standard components to be employed for achieving ultra-high system operation with ideal signal characteristics.

iii) Alternatively, particular combinations of the modulator bias point and electrical data precoding and filtering allow direct conversion of an electrical NRZ data format to optical RZ format, suitable for subsequent OTDM signal interleaving.

iv) A study has been carried out into the interactions between the pulse generation and data modulation techniques in order to achieve data pattern independent modulation of the optical pulse train.

v) Whilst optical demultiplexing requires optical switching to be carried out on the full line-rate data signal, processing techniques have been identified which minimise the electrical control signal frequency and also the switch drive powers. An analysis of complete OTDM multiplexing and demultiplexing operations has then identified suitable overall system configurations which minimise cross-channel interference and data patterning effects.

Having identified OTDM techniques as a suitable means for achieving substantial increases in the optical signal line-rate for a given set of opto-electronic components, Chapter V then has addressed the second main system issue of dispersive propagation distance limitations. Firstly, a comparison of the propagation performance has been carried out of a range of optical pulse shapes in terms of RMS and FWHM pulse widths as a function of fibre distances. The results demonstrate that for NRZ format optical signalling the basic pulse optical time-bandwidth product cannot be employed to predict the likely system performance, whilst for RZ format signalling the time-bandwidth product does provide a good indication of dispersive propagation pulse behaviour. The comprehensive system models employed to investigate the applicability of simple analytical evaluations of the expected system performance based on time domain pulse width and frequency domain spectral width have then been extended to an analysis of system operation over distances beyond the standard dispersion limits. In particular, the following results have been obtained :

vi) Three-level detection of binary optical transmitter signals may be employed to extend the dispersion limited propagation distances (2 dB penalty distances) by upto $\approx$ 100 % for NRZ transmitter formats ($\approx$ 150 % in one particular configuration) and by approximately 60 % for 25 % RZ data signals.

vii) Three-level detection of symmetric three-level optical transmitter signals, obtained through bandwidth limited electrical data drive to a standard external modulator, also results in substantial increases in the maximum transmission distances over basic binary transmission. Additionally, predistortion of the three-level optical transmitter signal may be employed to counteract to some extent the non-uniform deterioration in the three-level signal 'eye' diagram after dispersive fibre propagation. As a result, the increases in the maximum system distances are similar to the best results obtained with three-level detection of binary transmitter data, when the comparison is carried out at the 2 dB system penalty level. However, the maximum distances for a 1 dB penalty are substantially better with the three-level transmitter format (≈ 120 % improvement compared with ≈ 75 %), thus providing a much longer transmission distance over which the system dispersion penalty remains small.

When OTDM signal processing is employed in the context of ultra-high capacity fibre transmission, the optical sampling processes developed for the multiplexer and demultiplexer may also play a useful role in the context of increasing the dispersion limited transmission distance. Firstly, the sampling process in the optical demultiplexer of an OTDM system may be carried out either with a sampling pulse width equal to the bit-interval of the full-rate line signal or with a sampling window considerably shortened. A short sampling window relaxes the transmitter requirements regarding levels of interference from adjacent time slots and was also found to permit higher levels of path dispersion for a given level of acceptable system dispersion penalty. Secondly, at the very high line-rates considered here the dispersion limited propagation distances are considerably reduced. Accordingly optical 2R signal regeneration by means of optical sampling has been investigated (Retiming and Reshaping). Applicable both to RZ format optically multiplexed signals at the full system line-rate and to the RZ format tributary line signals, optical sampling driven by a clock signal extracted from the incoming line signal (retiming) has been shown to allow repeated optical regeneration as long as the individual propagation distances remain below the characteristic distance at which the RZ system penalty reaches its

threshold. Consequently the findings relating to OTDM signal propagation and system dispersion limitations are as follows:

viii) For dispersive fibre propagation, the achievable transmission distances may be increased by as much as 35% by means of optical sampling prior to photodetection, both in standard system configurations and in OTDM systems.

ix) Optical 2R regeneration by means of a timing extraction device driving an optical sampling gate allows successful signal regeneration of RZ format data as long as the individual fibre spans are shorter than some characteristic distance. The maximum number of regeneration stages will then be limited only by system signal-to-noise ratio considerations and will thus be dependent on the amount of optical gain and its associated noise figure in each of the regeneration stages.

In summary, techniques have been presented which allow ultra-high speed system operation based on bandwidth limited devices appropriate for standard system configurations. The potential has been identified for substantial improvements in dispersive propagation distances, both in systems employing NRZ optical signal formats and for RZ format OTDM transmission configurations, demonstrating the considerable potential of optical processing techniques for improving overall system and network capacities.

RECOMMENDATIONS FOR FUTURE WORK

In this work the end-to-end system performance calculations have been based on raised cosine frequency response optical receiver transfer functions of appropriate bandwidth for the particular applications under investigation. In the context of dispersion limited optical data transmission, optical receiver optimisation may be carried out to provide additional system margins which may be employed to increase the overall system performance or to provide robustness with respect to component tolerances.

The system performance analyses have been based on receiver 'eye' diagram closures relative to the signal obtained without dispersive propagation. Optimisation of receiver bandwidth and frequency response will also alter the receiver output signal-to-noise ratio, whether it is dominated by receiver thermal noise or optical signal-spontaneous or spontaneous-spontaneous beat noise terms as a result of optical amplification stages in the system. Consequently, further investigations could be aimed at identifying whether receiver optimisation would in some system configurations give rise to noticable differences in the end-to-end system performance compared with the results obtained in this work. In particular, if signal-dependent noise dominates the detection process this may need to be taken into account in the overall system optimisation.

The pulse propagation and overall system performance analyses of Chapter V have assumed optical pulse generation with minimum, i.e. transform-limited optical time-bandwidth products for all the pulse shapes under study. As mentioned in III.5 optical prechirping may be employed to increase the maximum fibre transmission distance for standard NRZ or RZ system operation if both the sign and amplitude of the optical carrier wavelength variations are chosen appropriately. Further studies could be aimed at investigating the extent to which the high performance system configurations identified in this study might be improved further with the addition of pre-chirping of the optical carrier.

Finally, this work has been targeted at high capacity systems operating in the low-loss 1.55 μm wavelength window over the widely available and installed step-index monomode fibre, resulting in high chromatic fibre dispersion at the operating wavelength. It is straightforward to estimate the system limits due to linear dispersion through simple scaling of the maximum distances in proportion to the inverse of the fibre dispersion value, until higher order dispersion terms become significant in the close proximity of the fibre dispersion-zero wavelength. However, the resulting distances rapidly become long enough to make non-linear fibre propagation effects non-negligible, especially at todays optical power levels of several mW as are easily available from fibre amplifiers. Whilst non-linear transmission systems (soliton systems) have been analysed in some detail for

Gbit/s operation over trans–oceanic distances, ultra–high capacity systems of several tens of Gbit/s will be limited to somewhat shorter distances of a few hundred km to one or two thousand km as part of national backbone telecommunication networks [Brown, Marshall and Spirit]. Further studies are required for these applications where, especially in an optical networking environment, ideal soliton propagation may not be achievable and compromises between ultimate distances and network flexibility may be required. The fact that the highest performing optical pulse shapes for linear transmission of RZ format OTDM signals are known to be suitable for non–linear soliton propagation may allow network operation with signals alternating between linear propagation on shorter spans and non–linear propagation along backbone transmission links.

In conclusion, a number of techniques have been identified for the implementation of ultra–high speed Optical Time Division Multiplexed transmission systems and networks, followed by an analysis of methods for increasing fibre chromatic dispersion limited transmission distances. The significance of the multiplexing approaches lies in the ability to employ limited bandwidth opto–electronic components, whilst the transmission studies have identified major improvements in the achievable dispersion limited linear propagation distances.

APPENDICES

A2-1 BASIC RATE EQUATIONS

In the laser cavity a change in electronic carrier concentration results from the injection of new carriers and the loss of carriers due to carrier recombination and stimulated emission. For the case of spatially uniform carrier and photon concentrations the resulting differential equation relates the carrier concentration n and photon density S as follows :

$$\frac{dn}{dt} = \frac{j}{e \cdot d} - \frac{n}{\tau} - \Gamma \cdot A \cdot (n - n_t) \cdot S \qquad (A2.1)$$

(e: electronic charge, d: active layer thickness)

Similarly, a change in photon density is caused either by stimulated gain or by photon losses, expressed by the photon lifetime, and through spontaneous emission, characterised by the spontaneous emission factor β_{spon} and carrier density and carrier life time:

$$\frac{dS}{dt} = \Gamma \cdot A \cdot (n - n_t) \cdot S - \frac{S}{\tau_{ph}} + \beta_{spon} \cdot \frac{n}{\tau} \qquad (A2.2)$$

For the case of strong lasing action, i.e. operation well above lasing threshold, this non-linear system in the carrier concentration n and photon density S simplifies for CW operation as follows :

with

$$\frac{1}{\tau_{ph}} = \Gamma \cdot A \cdot (n_{bias} - n_t) \approx \Gamma \cdot A \cdot (n_{th} - n_t)$$

the current density and photon density are related by

$$\frac{j_{bias}}{e \cdot d} = \frac{n_{th}}{\tau_{sp}} + \frac{S_{bias}}{\tau_{ph}} \qquad (A2.3)$$

and the threshold carrier density becomes

$$n_{th} = n_t + \frac{1}{\Gamma \cdot A \cdot \tau_{ph}} \qquad (A2.4)$$

For the special cases of operation below lasing threshold and well above lasing threshold, some insight into the laser behaviour can be gained as follows:

Below threshold and for a change of bias current from a given value to zero, the first and third terms of equation (A2.1) can be neglected, thus providing the simple result

$$\frac{dn}{dt} = -\frac{n}{\tau} \qquad \text{(A2.5)}$$

with solutions for n of the form $e^{-t/\tau}$ i.e. exponential decay of carrier density, governed by the carrier life time τ. Similarly, any increase in bias level below lasing threshold leads to an exponential carrier density rise also governed by τ.

For small signal laser operation well above threshold, linearisation of the rate equations around an operating point leads to an analysis of the small signal laser frequency response.

With the injection current density, the carrier density and the photon density all represented in the form $X = X_{bias} + X^*$, the linearised rate eqations become:

$$\frac{dn^*}{dt} = \frac{j^*}{e \cdot d} - \Gamma \cdot A \cdot (n_{th} - n_t) \cdot S^* - \frac{n^*}{\tau} - \Gamma \cdot A \cdot S_{bias} \cdot n^*$$

$$\frac{dS^*}{dt} = \Gamma \cdot A \cdot (n_{th} - n_t) \cdot S^* - \frac{S^*}{\tau_{ph}} + \beta_{spon} \cdot \frac{n^*}{\tau} + \Gamma \cdot A \cdot S_{bias} \cdot n^* \qquad \text{(A2.6)}$$

This represents a second order system, with the resonant frequency ω_0 and damping factor β_0 given by :

$$\omega_0^2 = \frac{j - j_{th}}{j_{th} - j_t} \cdot \frac{1}{\tau_{ph} \cdot \tau}$$

$$\beta_0 = \frac{j - j_t}{j_{th} - j_t} \cdot \frac{1}{\tau} \qquad \text{(A2.7)}$$

From these results it becomes apparent that in order to obtain a fast laser, a compromise is required for the relative levels of transparency current density and threshold current density (since their difference enters into the expression for ω_0 directly as well as indirectly through the photon life time), and the photon and carrier lifetimes should be as

small as possible (i.e. good optical confinement), whilst a laser bias as high above threshold as possible is required.

However:

Some text books give a solution somewhat different to the one shown in equations (A2.7), namely:

$$\omega_0^2 = \frac{j - j_{th}}{j_{th}} \cdot \frac{1}{\tau_{ph} \cdot \tau}$$

$$\beta_0 = \frac{j}{j_{th}} \cdot \frac{1}{\tau} \qquad \text{(A2.8)}$$

If equations (A2.8) are used for calculating the resonant frequency and damping coefficient for a particular set of laser parameters and bias level, the values obtained do not match up with experimental observations. The reason for the discrepancies lies in the approximations made in the derivation of eq.(A2.8) : For early lasers operating in the 800 nm wavelength window the threshold current densities and carrier densities were substantially higher than their respective transparency values. As a result, in both formulae the terms $j_{th}-j_t$ were simply approximated by j_{th}, without too great an error. In todays 1.3 and 1.55 μm lasers however, the threshold values are within 10 to 20 % of the material gain transparency values, thus making this approximation absolutely invalid. Unfortunately, the (in this context invalid) modified expressions for ω_0 and β_0 continue to be reported, without having necessarily attached to them the conditions under which they are appropriate.

Solutions to the system of simultaneous non-linear differential equations (A2.1) and (A2.2) are obtained numerically by means of the Runge-Kutta method. As in the real world, the system is driven by the time-varying laser injection current, represented here by the variable j(t).

A2-2 RATE EQUATIONS WITH CARRIER DIFFUSION

Inclusion of carrier diffusion across the laser active layer leads to modified rate equations as follows:

$$\frac{dn(x)}{dt} = \frac{j}{e \cdot d} - \frac{n(x)}{\tau} - \Gamma \cdot A \cdot (n(x) - n_t) \cdot S(x) + D_c \cdot \frac{d^2 n(x)}{dx^2}$$

$$\frac{dS(x)}{dt} = \Gamma \cdot A \cdot (n(x) - n_t) \cdot S(x) - \frac{S(x)}{\tau_{ph}} + \beta_{spon} \cdot \frac{n(x)}{\tau} \qquad \text{(A2.9)}$$

where D_c is the carrier diffusion parameter.

For carrier and photon distribution profiles of :

$$S(x) = 2 \cdot S_0 \cdot \cos^2(\pi x / W)$$

and

$$n(x) = n_0 + n_1 \cdot \cos(2\pi x / W)$$

and with some rearrangement of terms, the following new set of three simultaneous differential equations is obtained [Bickers and Westbrook]:

$$\frac{dn_0}{dt} = \frac{j}{e \cdot d} - \frac{n_0}{\tau} - \Gamma \cdot A \cdot (n_0 + \frac{n_1}{2} - n_t) \cdot S_0$$

$$\frac{dn_1}{dt} = - \frac{n_2}{\tau} \cdot (1 + 4 \pi^2 D_c \cdot \frac{\tau}{W^2}) - \Gamma \cdot A \cdot (n_0 + n_2 - n_t) \cdot S_0$$

$$\frac{dS_0}{dt} = \Gamma \cdot A \cdot (n_0 + \frac{n_1}{2} - n_t) \cdot S_0 - \frac{S_0}{\tau_{ph}} + \beta_{spon} \cdot \frac{n_0}{\tau} \qquad \text{(A2.10)}$$

Here n_0 represents the mean carrier concentration, averaged across the laser thickness, and n_1 is the deviation from this mean value.

Throughout the laser and system modeling employed in this work the three rate-equation model is used.

A2-3 Model Flow Chart: Direct Laser Modulation

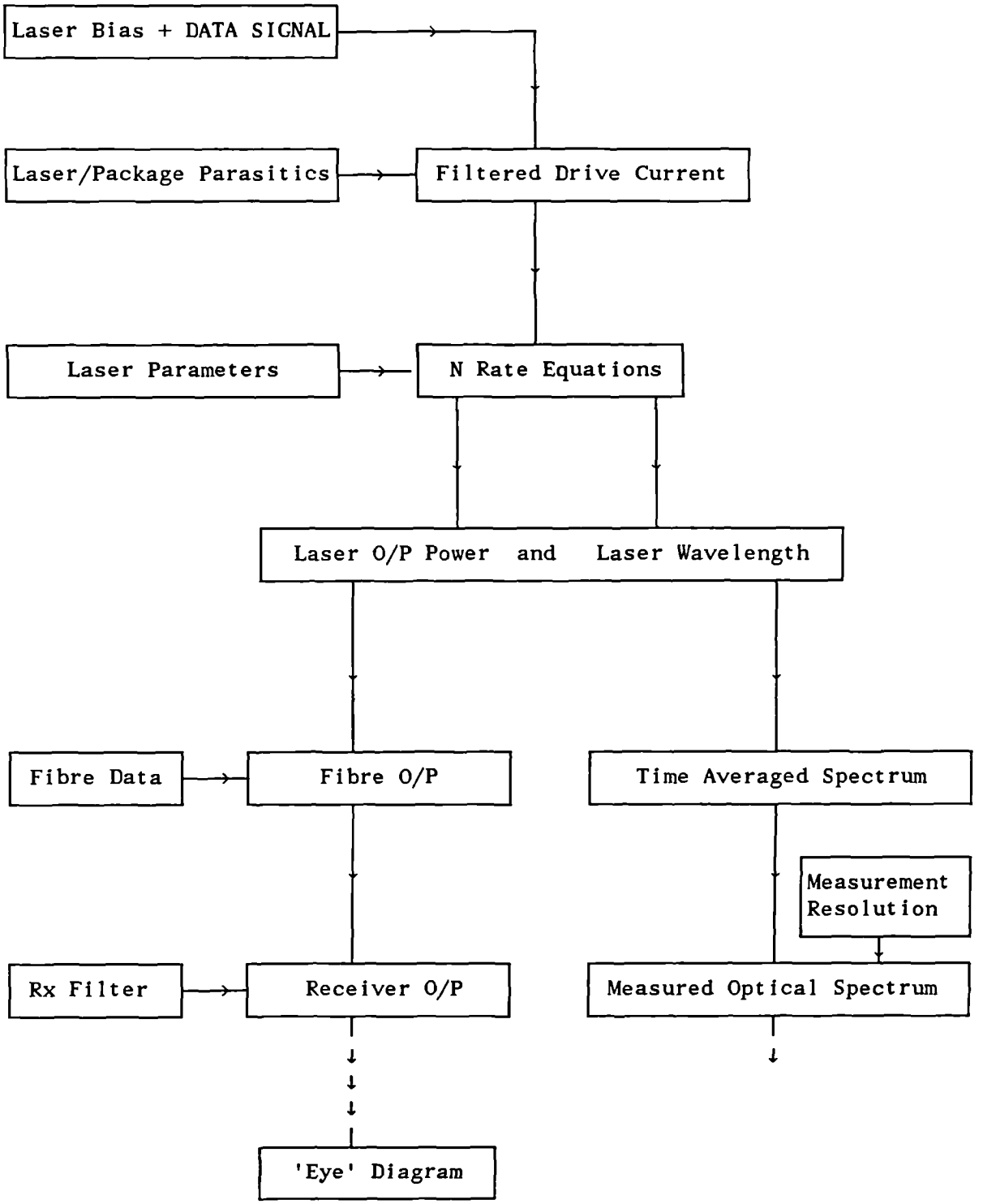

A2-4 Model Flow Chart: External Modulation

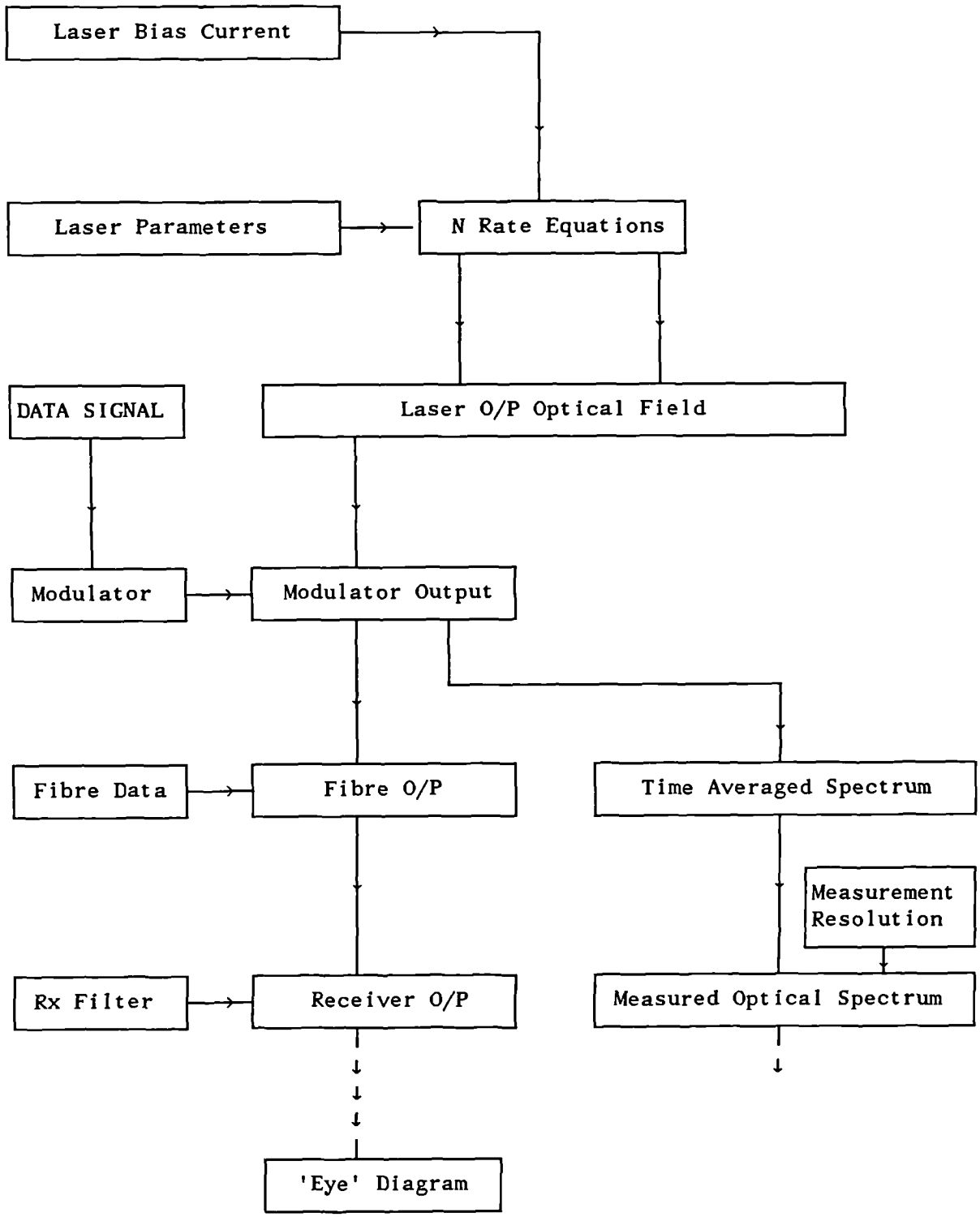

A2-5 Model Flow Chart: Evaluation of System Penalty Versus Fibre Length

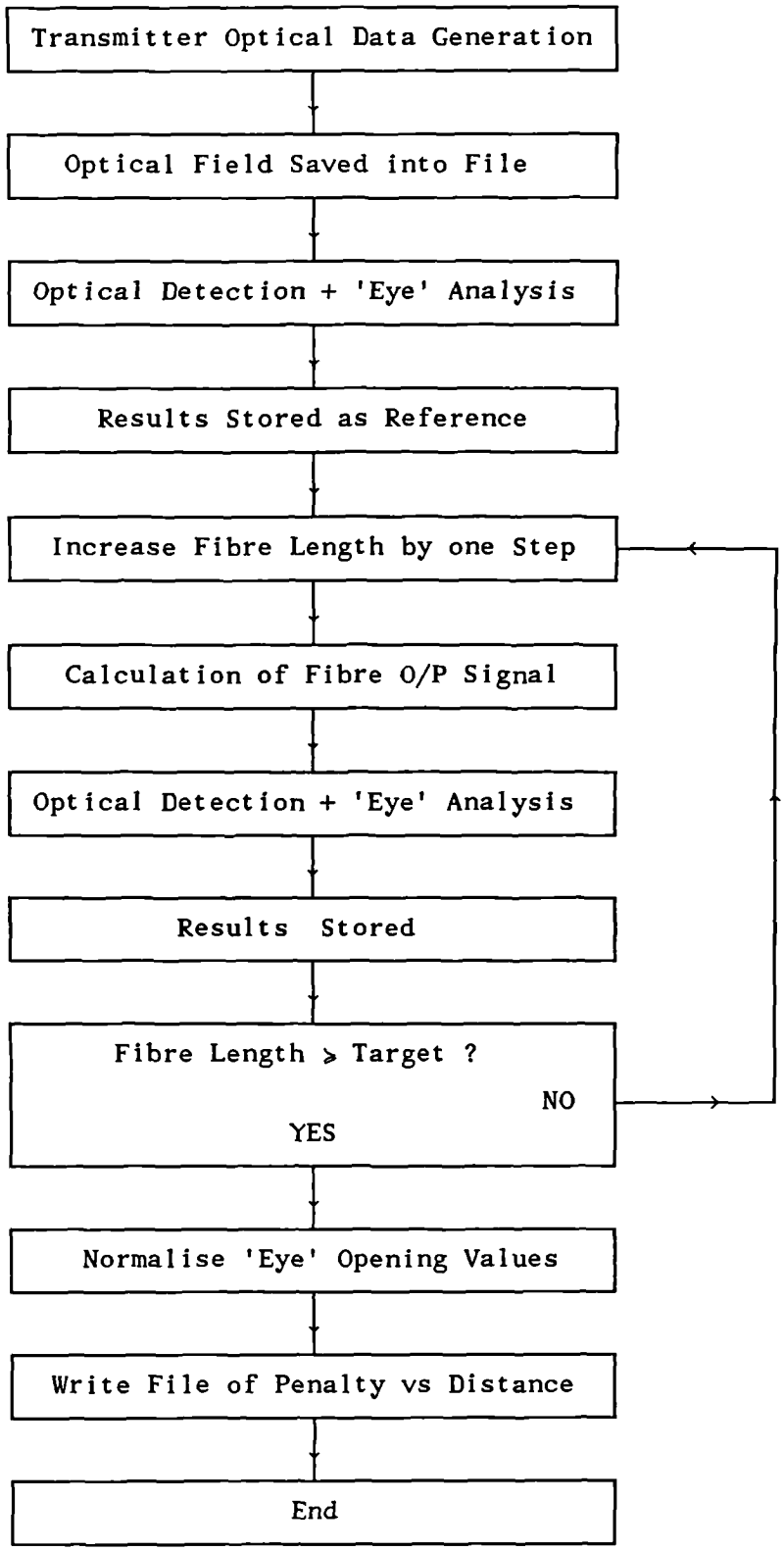

REFERENCES

R.C.Alferness, "Guided-Wave Devices for Optical Communications", IEEE Jnl.Quantum Electron., Vol.QE-17, No.6, June 1981, pp.946-959.

A.Alping, T.Anderson, R.Tell and S.T.Eng, "20 Gbit/s Optical Time Multiplexing With TJS GaAlAs Lasers", Electron.Lett., Vol.18, No.10, May 1982, pp.422-423.

P.E.Barnsley, H.J.Wickes, G.E.Wickens and D.M.Spirit, "All-Optical Clock Recovery From 5 Gb/s RZ Data Using a Self-Pulsating 1.56μm Laser Diode", IEEE Photon.Technol.Lett, Vol.3, No.10, October 1991, pp.942-945.

P.E.Barnsley, G.E.Wickens, H.J.Wickes and D.M.Spirit, "A4x5 Gb/s Transmission System with All-Optical Clock Recovery", IEEE Photon.Technol.Lett., Vol.4, No.1, January 1992, pp.83-86.

L.Bickers and L.D.Westbrook, "Reduction of Laser Chirp in 1.5 μm DFB Lasers by Modulation Pulse Shaping", Electron.Lett., Vol.21, January 1985, pp.103-104.

L.C.Blank, "Multi-Gbit/s Optical Time Division Multiplexing Employing $LiNbO_3$ Switches with Low-Frequency Sinewave Drive", Electron.Lett., Vol.24, No.25, December 1988, pp.1543-1544.

L.C.Blank, L.Bickers and S.D.Walker, "Long Span Optical Transmission Experiments at 34 and 140 Mbit/s", IEEE Jnl. of Lightwave Technology, Vol.3, No.5, October 1985, pp.1017-1026.

L.C.Blank, E.G.Bryant, A.Lord, J.M.Boggis and W.A.Stallard, "150 km Optical Fibre Transmission Network Experiment with 2 Gbit/s Throughput", Electron. Lett., Vol.23, No.19, September 1987, pp.977-978.

L.C.Blank and J.D.Cox, "Demonstration of Optical Drop-and-Insert for Accessing 2.24 Gbit/s Optical Transmission Systems Directly at the 140 Mbit/s Level", IEE Conference Publication No.292, Part 1, pp.463-466 (European Conference on Optical Communication, ECOC, 1988).

L.C.Blank, R.A.Garnham and S.D.Walker (1), "2 Gbit/s and 2.4 Gbit/s Optical Transmission Field Trial Over A 32 km Installed Route", Electron.Lett., 1986, Vol.22, No.1, January 1986, pp.33-35.

L.C.Blank, R.A.Garnham and S.D.Walker (2), "Experimental Optical Transmission Systems at 2.4 Gbit/s", Conference Proceedings EFOC/LAN 86, 23-27 June 1986, Amsterdam, pp.35-39.

J.E.Bowers, "Millimetre-Wave Response of InGaAsP Lasers", Electron.Lett., Vol.21, No.25/26, December 1985, pp.1195-1197.

J.E.Bowers, B.R.Hemenway, T.J.Bridges and E.G.Burkhardt, "26.5 GHz Bandwidth InGaAsP Lasers with Tight Optical Confinement", Electron.Lett., Vol.21, No.23, November 1985, pp.1090-1091.

G.N.Brown, I.W.Marshall, D.M.Spirit, "Computer Simulation of Ultra-High Capacity Non-Linear Lightwave Transmission Systems", 3rd IEE Telecommunications Conference, March 1991, Edinburgh.

A.Bruce Carlson, *Communication Systems*, 3rd Edition, 1986, McGraw-Hill, pp.413-417.

E.G.Bryant, S.F.Carter, R.B.J.Lewis, D.M.Spirit, T.Widdowson and J.V.Wright, "A 2.488 Gbit/s FSK Field Demonstration Over 132 km Submarine Cable Employing An Erbium Power Amplifier", IEE Colloquium on Microwave Optoelectronics, London, 26 October 1990, Digest No.1990/139, Paper No.15.

J.Buus, "Principles of Semiconductor laser Modelling", IEE Proceedings, Vol.132, Pt.J, No.1, February 1985, pp.42-51.

T.E.Darcie, M.E.Dixon, B.L.Kasper and C.A.Burrus, "Lightwave System Using Microwave Subcarrier Multiplexing", Electron.Lett., Vol.22, No.15, July 1986, pp.774-775.

M.De Oliveira Duarte, "The Application of Decision Feedback Techniques to Digital and Optical Communications", PhD Thesis, May 1984, Department of Electrical Engineering Science, University of Essex, U.K.

A.D.Ellis, S.J.Pycock, D.A.Cleland and C.H.F.Sturrock, "Dispersion Compensation in 450 km Transmission System Employing Standard Fibre", Electron.Lett., Vol.28, No.10, May 1992, pp.954-955.

A.F.Elrefaie, R.S.Vodhanel, R.E.Wagner, D.Atlas and D.G.Daut, "10-20 Gbit/s Modulation Performance of 1.55 μm DFB Lasers for FSK Systems", Technical Digest Topical Meeting on Optical Fibre Communications OFC'89 (Opt.Soc.America, Washington), 1989, paper WN3.

S.Fujita, M.Kitamura, T.Torikai, N.Henmi, H.Yamada, T.Suzaki, I.Takano and M.Shimada, "10 Gbit/s, 100 km Optical Fibre Transmission Experiment Using High-Speed MQW DFB-LD and Back-Illuminated GaInAs APD", Electron.Lett., Vol.25, No.11, May 1989, pp.702-703.

R.A.Garnham and L.C.Blank, "100 dB Optical Path Loss Transmission System Experiment Employing Two Linear Optoelectronic Repeaters", Electron.Lett., 1989, Vol.25, No.3, pp.179-180.

A.H.Gnauck, C.A.Burrus, S.-J.Wang and N.K.Dutta, "16 Gbit/s Transmission over 53 km of Fibre using Directly Modulated 1.3 μm DFB Laser", Electron.Lett., Vol.25, No.20, September 1989, pp.1356-1358.

K.Hagimoto, Y.Miyamoto, T.Kataoka, K.Kawano and M.Ohhata, "A 17 Gb/s Long-Span Fibre Transmission Experiment using a Low-Noise Broadband Receiver with Optical Amplification and Equalisation", Topical Meeting on Optical Amplifiers, Monterey, C.A., USA, 1990.

A.Hasegawa and Y.Kodama, "Signal Transmission by Optical Solitons in Monomode Fibre", Proc.IEEE, 1981, Vol.69, pp.1145-1150.

H.A.Haus, S.T.Kirsch, K.Mathyssek and F.J.Leonberger, "Picosecond Optical Sampling", IEEE Jnl. Quantum Electronics, Vol.QE-16, No.8, August 1980, pp.870-874.

R.Heidemann, "Investigations on the Dominant Dispersion Penalties Occuring in Multigigabit Direct Detection Systems", IEEE Jnl.Lightwave Technology, Vol.6, No.11, November 1988, pp.1693-1697.

N.Henmi, T.Saitoh, S.Fujita, M.Yamaguchi, H.Asano, I.Mito and M.Shikada, "Dispersion Compensation by Prechirp Technique in Multigigabit Optical Amplifier Repeater Systems", Proceedings OSA Topical Meeting on Optical Amplifiers, Monterey, C.A., USA, 1990.

M.Jinno and T.Matsumoto, "All-Optical Timing Extraction Using a 1.5 μm Self Pulsating Multielectrode DFB LD", Electron.Lett., Vol.24, No.23, November 1988, pp.1426-1427.

R.L.Jungerman, C.A.Johnson, D.W.Dolfi and M.Nazarathy, "Coded Phase-Reversal $LiNbO_3$ Modulator With Bandwidth Greater Than 20 GHz at 1.3 μm", Electron.Lett., Vol.23, No.4, February 1987, pp.172-174.

P.Kaiser, S.Nagel, S.Shimada, N.Olsson, D.Payne, "Optical Amplifiers and Their Applications", Proceedings of OSA Topical Meeting on Optical Amplifiers, Monterey, C.A., USA, 1990.

T.L.Koch and R.C.Alferness, "Dispersion Compensation by Active Predistorted Signal Synthesis", IEEE Jnl.Lightwave Technol., Vol.LT-3, No.4, August 1985, pp.800-805.

T.L.Koch and J.E.Bowers, "Nature of Wavelength Chirping in Directly Modulated Semiconductor Lasers", Electron.Lett., Vol.20, No.25/26, December 1984, pp.1038-1039.

T.L.Koch and P.J.Corvini, "Semiconductor Laser Chirping-Induced Dispersive Distortion In High-Bit-Rate Optical Fibre Communication Systems", Proceedings ICC'88, Paper 19.4, pp.584-587.

T.L.Koch and R.A.Linke, "Effect of Nonlinear Gain Reduction on Semiconductor Laser Wavelength Chirping", Appl.Physics Letters,Vol.10,March 1986,pp.613-615.

F.Koyama and K.Iga, "Frequency Chirping of External Modulation and Its Reduction", Electron.Lett., Vol.21, No.23, November 1985, pp.1065-1066.

F.Koyama and Y.Suematsu, "Analysis of Dynamic Spectral Width of Dynamic-Single-Mode (DSM) Lasers and Related Transmission Bandwidth of Single-Mode Fibres", IEEE Jnl.Quantum Electron., Vol.QE-21, No.4, April 1985, pp.292-297.

R.A.Linke, "Transient Chirping in Single-Frequency Lasers: Lightwave Systems Consequences", Electron.Lett., Vol.20, No.11, May 1984, pp.472-474.

A.Lord, L.C.Blank, J.M.Boggis, E.G.Bryant and W.A.Stallard, "Theory of Control Mechanism for an Optically Time-Division-Multiplexed System", Electron. Lett, Vol.24, No.1, January 1988, pp.29-31.

A.J.Lowery and I.W.Marshall, "Numerical Simulations of 1.5 μm Actively Mode-Locked Semiconductor Lasers including Dispersive Elements and Chirp", Jnl.Quantum Electronics, Vol. QE-27, August 1991, pp.1981-1989.

A.J.Lowery, N.Onodera and R.S.Tucker, "Stability and Spectral Behaviour of Grating-Controlled Actively Mode-Locked Lasers", Jnl.Quantum Electronics, Vol. QE-27, November 1991, pp.2422-2430.

M.J.O'Mahony (1), "Semiconductor Laser Optical Amplifiers for Use in Future Fibre Systems", Jnl.Lightwave Technology, 1988, No.6, pp.531-544.

M.J.O'Mahony (2), "Duobinary Transmission with PIN-Fet Optical Receivers", Electron.Lett., Vol.16, 1980, p.752.

M.J.O'Mahony (3), "Laser Partition Noise and its Effects on System Performance", British Telecom Research Laboratories Research Memorandum No.81R5/8.

M.J.O'Mahony (4), "Signal Design for Optical Communications", in *Mathematical Topics in Telecommunications, Vol.I Optimisation Methods in Electronics and Communications*, Pentech Press, 1984.

D.J.Malyon, L.C.Blank, R.E.Hobbs, D.J.Elton, A.J.Cockburn and W.A.Stallard, "Long-Span High Capacity Transmission System Experiments Employing Two Near-Travelling-Wave Laser Amplifiers", IEE Conf.Publication No. 292 Part 1 (European Conference on Optical Communication ECOC'88).

D.J.Malyon and W.A.Stallard, "565 Mbit/s FSK Direct Detection System Operating with Four Cascaded Photonic Amplifiers", Electron.Lett., Vol.25, No.8, 1989, pp.495-497.

D.Marcuse and C.Lin, "Low Dispersion Single-Mode Fibre Transmission - The Question of Practical versus Theoretical Maximum Transmission Bandwidth", IEEE Jnl.Quantum Electronics, Vol.QE-17, No.6, June 1981, pp.869-878.

D.Morris, P.J.Legg, C.W.Ford and P.A.Rosher, "A Lithium Niobate Bandpass Modulator for Optical Subcarrier Transmission Systems", IEE Colloquium on Microwave Optoelectronics, London, 26 October 1990, Digest No.1990/139, Paper No.3.

M.Nakazawa, K.Suzuki and Y.Kimura, "Transform-Limited Pulse Generation in the Gigahertz Region from a Gain-Switched Distributed-Feedback Laser Diode Using Spectral Windowing", Optics Letters, Vol.15, No.12, June 1990, pp.715-717.

Y.Namihira, T.Kawazawa and H.Wakabayashi, "Polarisation Mode Dispersion Measurements in 1520 km EDFA System", Electron.Lett., Vol.28,No.9,1992, pp.881-883.

A.W.Nelson, L.D.Westbrook and P.J.Fiddyment, "Design and Fabrication of 1.5 μm Ridge Waveguide Distributed Feedback Lasers", IEE Proceedings, Vol.132, Pt.J, No.1, February 1985, pp.12-19.

K.Ogawa, "Analysis of Mode Partition Noise in Laser Transmission Systems", Jn.Quantum Electronics, Vol.QE-18, No.5, May 1982, pp.849-855.

K.Ogawa and R.S.Vodhanel, "Measurements of Mode Partition Noise of Laser Diodes", IEEE Jnl.Quantum Electronics, Vol.QE-18, No.7, July 1982, pp.1090-1093.

S.Ogita, M.Yano and H.Imai, "Theoretical Calculation of the Linewidth Enhancement Factor of DFB Lasers", Electron.Lett.,Vol.22,No.11,May 1986,pp.580-581.

S.Ogita, M.Yano, H.Ishikawa and H.Imai, "Linewidth Reduction in DFB Laser by Detuning Effect", Electron.Lett., Vol.23, No.8, April 1987, pp.393-394.

R.Olshansky and D.Feye, "Reduction of Dynamic Linewidth in Single-Frequency Semiconductor Lasers", Electron.Lett., Vol.20, 1984, pp.928-929.

N.A.Olsson, G.P.Agraval and K.W.Wecht, "16 Gbit/s, 70 km Pulse Transmission by Simultaneous Dispersion and Loss Compensation with 1.5 μm Optical Amplifiers", Electron.Lett., Vol.25, No.9, April 1989, pp.603-605.

C.D.Poole, N.S.Bergano, R.E.Wagner and H.J.Schulte, "Polarisation Dispersion in a 147 km Undersea Lightwave Cable", Conf.Proceedings European Conference on Optical Communication (ECOC'87), Helsinki, pp.321-324.

C.D.Poole, "Measurement of Polarisation-Mode Dispersion in Single-Mode Fibres with Random Mode Coupling", Optics Letters, Vol.14, No.10, May 1989, pp.523-525.

J.J.O'Reilly, M.Duarte, L.C.Blank, "On the Application of Quantised Feedback and Partial Response Techniques to High Bit-rate Optical Fibre Communications", 20th Annual Allerton Conf. on Communications, Control and Computing, Univ.of Illinois, Urbana, Ill., USA, Oct.1982, Digest pp.967-974.

S.Saito, Y.Yamamoto and T.Kimura, "Semiconductor Laser FSK Modulation and Optical Direct Discriminator Detection", Electron.Lett., Vol.18, 1982, pp.468-469.

X.Shan, D.Cleland and A.D.Ellis, "Stabilising Er Fibre Soliton Laser with Pulse Phase Locking", Electron.Lett., Vol.28, No.2, January 1992, pp.182-184.

M.Shirasaki, H.Nishimoto, T.Okiyama and T.Touge, "Fibre Transmission Properties of Optical Pulses Produced Through Direct Phase Modulation Of DFB Laser Diode', Electron.Lett., Vol.24, No.8, April 1988, pp.486-488.

M.Shirasaki, I.Yokota and T.Touge, "20 Gbit/s No-Chirp Intensity Modulation by DPSH-IM Method and its Fibre Transmission Through 330 ps/nm Dispersion", Electron.Lett., Vol.26, No.1, January 1990, pp.33-35.

H.J.A. da Silva, J.J.O'Reilly, "System Performance Implications of Laser Chirp for Long Haul High Bit Rate Direct Detection Optical Fibre Communications", Conference Proceedings ICC'88, Paper 19.5, pp.0588-0592.

K.Smith, J.R.Armitage, R.Wyatt, N.J.Doran and S.M.Kelly, "Erbium Fibre Soliton Laser", Electron.Lett., Vol.26, No.15, July 1990, pp.1149-1151.

D.M.Spirit, L.C.Blank, S.T.Davey and D.L.Williams, "System Aspects of Raman Fibre Amplifiers", IEE Proceedings, Vol.137, Pt.J, No.4, August 1990, pp.221-224.

D.M.Spirit, L.C.Blank, D.L.Williams, S.T.Davey and B.J.Ainslie, "5 Gbit/s, +10 dBm Lossless Transmission In 10 km Distributed Erbium Amplifier", Electron.Lett., Vol.26, No.20, July 1990, pp.1659-1660.

D.M.Spirit, G.R.Walker, P.W.France, S.F.Carter, D.Szebesta, "Characterisation of Diode-Pumped Erbium-Doped Fluorozirconate Fibre Optical Amplifier", Electron.Lett., 1990, Vol.26, No.15, pp.1218-1220.

D.M.Spirit, G.E.Wickens, G.E.Walker, D.L.Williams, L.C.Blank, "140-km 20-Gbit/s Repeaterless Transmission Employing Distributed Erbium Amplification", in 'Optical Fibre Communications Conference', Vol.5, 1992 (Optical Society of America, Washington D.C.), Paper TuI5, page 51.

M.Suzuki, Y.Noda, Y.Kushiro and S.Akiba, "Dynamic Spectral Width of an InGaAsP/InP Electroabsorption Light Modulator under High-Frequency Large-Signal Modulation", Electron.Lett., 1986, Vol.22, No.6, pp.312-313.

A.Takada, T.Sugie and M.Saruwatary, "Transform-Limited 5.6 ps Optical Pulse Generation At 12 GHz Repetition Rate From Gain-Switched Distributed Feedback Laser Diode By Employing Pulse Compression Technique", Electron.Lett., Vol.22, No.25, December 1986, pp.1347-1348.

G.H.B.Thompson, *Physics of Semiconductor Laser Devices*, New York, Wiley, 1980.

R.S.Tucker, "High Speed Modulation of Semiconductor Lasers", IEEE Jnl. Lightwave Technology, Vol.LT-3, No.6, December 1985, pp.1180-1192.

R.S.Tucker and D.J.Pope, "Circuit Modeling of the Effect of Diffusion on Damping in a Narrow-Stripe Semiconductor Laser", IEEE Jnl.of Quantum Electronics, Vol.QE-19, No.7, July 1983, pp.1179-1183.

R.S.Tucker, J.M.Wiesenfeld, A.H.Gnauck and J.E.Bowers, "8 Gbit/s Return-to-Zero Modulation of a Semiconductor Laser by Gain-Switching", Electron.Lett., Vol.22, No.25, December 1986, pp.1329-1331.

R.S.Vodhanel, A.F.Elrefaie, M.Z.Iqbal, R.E.Wagner, J.L.Gimlett and S.Tsuji, "Performance of Directly Modulated DFB Lasers in 10-Gb/s ASK, FSK, and DPSK Lightwave Systems", IEEE Jnl. Lightwave Technology, Vol.8, No.9, September 1990, pp.1379-1386.

S.D.Walker, L.C.Blank, R.A.Garnham and J.M.Boggis, "High Electron Mobility Transistor Lightwave Receiver for Broad-Band Optical Transmission System Applications", IEEE Jnl.of Lightwave Technol., Vol.7, No.3, March 1989, pp.454-458.

L.D.Westbrook (1), "Dispersion of Linewidth-Broadening Factor in 1.5 μm Laser Diodes", Electron.Lett., Vol.21, No.22, October 1985, pp.1018-1019.

L.D.Westbrook (2), "Measurements of dg/dN and dn/dN and their Dependance on Photon Energy in λ=1.5μm InGaAsP Laser Diodes", IEE Proceedings, Vol.133, Pt.J, No.2, April 1986, pp.135-142.

G.E.Wickens, D.M.Spirit and L.C.Blank (1), "20 Gbit/s, 205 km Optical Time Division Multiplexed Transmission System", Electron.Lett., Vol.27, No.11, May 1991, pp.973-974.

G.E.Wickens, D.M.Spirit and L.C.Blank (2), "Nonlinear Transmission of 20 Gbit/s Optical Time-Division-Multiplexed Data, Over 205 km of Dispersion Shifted Fibre", Electron.Lett., Vol.28, No.2, January 1992, pp.117-118.

J.Yamada, A.Kawana, T.Miya, H.Nagai and T.Kimura, "Gigabit/s Optical Receiver Sensitivity and Zero-Dispersion Single-Mode Fibre Transmission at 1.55 μm", IEEE Jnl.Quantum Electron., Vol.QE-18, No,10, October 1982, pp.1537-1546.

J.P.Van der Ziel, R.A.Logan, "Generation of Short Optical Pulses in Semiconductor Lasers by Combined dc and Microwave Current Injection", IEEE Jnl. Quantum Electronics, Vol.QE-18, No.9, September 1982, pp.1340-1350.